Resonant single-stage, PWM-Resonant two-stage dc-dc converter for satellite power supply

By

Rajesh Ghosh

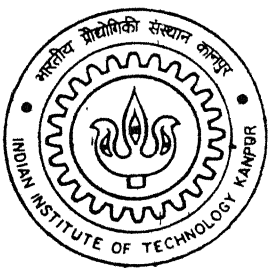

DEPARTMENT OF ELECTRICAL ENGINEERING/ACES

Indian Institute of Technology Kanpur

JANUARY, 2002

Resonant single-stage, PWM-Resonant two-stage dc-dc converter for satellite power supply

A thesis submitted
in partial fulfillment of the requirements
For the degree of

MASTER OF TECHNOLOGY

By

RAJESH GHOSH

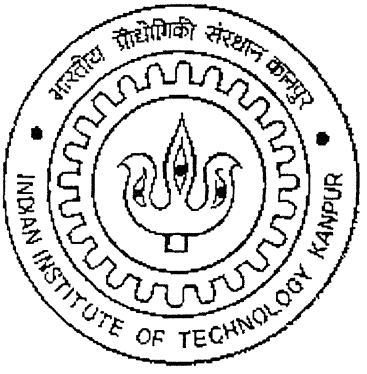

to the

Department of Electrical Engineering /ACES
INDIAN INSTITUTE OF TECHNOLOGY, KANPUR
January 2002

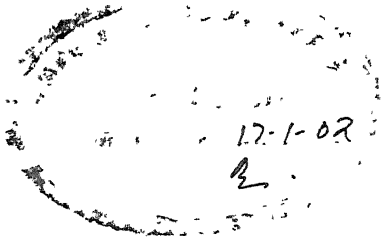

CERTIFICATE

This is certified that the work contained in this thesis entitled

Resonant single-stage, PWM-Resonant two-stage dc-dc converter for satellite power supply

by

Rajesh Ghosh

has been carried out under our supervision and that this work has not been submitted elsewhere for any degree

Dr. S.P.Das
Assistant Professor
Department of Electrical Engineering.
Indian Institute of Technology
Kanpur, India

Dr. S. R. DORADLA
Professor
Department of Electrical Engineering.
Indian Institute of Technology
Kanpur, India

Acknowledgements

I express my deep sense of gratitude and sincere thanks to my supervisor Prof S R Doradla for his invaluable guidance and constant encouragement throughout my study at IIT Kanpur It has been a great experience to get the basic training of research under his rich experience, exemplary patience and exceptional capabilities of reducing complexities to simpler form

I am highly indebted to my supervisor Dr Shyama P. Das, without whose guidance it would have been impossible to accomplish the entire work His way of tackling problems and analyzing from the root has resulted in good understanding of the problem

I want to express my sincere thanks to my teachers Prof. G K Dubey, Prof S C Srivastava, Prof S S Prabhu, Prof A Ghosh whose courses have built the foundation upon which the work is based

I would like to express thank to Prof A Joshi and Prof Sujit K. Biswas (Jadavpur University) without whose help it would have been impossible to accomplish the hardware part of this work

I take this opportunity to thank my senior colleagues Malabika Basu, Ramesh K Tripathi, S Behera and Aswani K Sharma for their indebted support and continuous cooperation throughout this work

I sincerely thank my friends Balaji, Meena, Sanjay, Bikash, Saleem, Shankar, Manoj, Ashesh and many others who made my stay at IIT a memorable thing in my life

The thesis wouldn't have been completed without the active participation of our technical staff In particular I am very much thankful to Mr O. P Arora, Mr Manoj of EE stores, Mr Kaushal, Mr S Pal and many others

I am very much thankful to my parents and other family members for their constant inspiration and encouragement

Finally I would like to express my thanks to all those who helped me directly or indirectly in the progress and completion of this work

Rajesh Ghosh

Dedicated
to my
beloved parents

Abstract

Two possible solutions for Electronic Power Conditioner (EPC) of the Traveling Wave Tube Amplifier (TWTA) used in satellite applications are given. Considering the transformer leakage inductance, inter turn capacitance and output diode bridge rectifiers junction capacitance the first scheme is a single-stage LCLC four element dc-dc resonance power converter. Operation above the resonance reduces the switching loss and also reduces the volume and size of the overall converter Detailed analysis, design and simulation of the four-element resonant converter are given. The second configuration explores the best features of a Series Resonance Converter by operating it at the resonant frequency. The disadvantage of SRC in controlling the output voltage is overcome by a pre-regulator, connected in the front end of the SRC, which is essentially a buck converter. Controlling the duty ratio of the buck converter controls the output voltage across the load. The operation of the SRC at the resonant frequency ensures zero current turn-on and turn-off of the inverter switches which helps in achieving higher switching frequency. The duty ratio control is required to take the input voltage variation into account. Introducing the effect of inherent parasitics of transformer and diode bridge rectifier, a simple two-element SRC is indeed a multi-element topology. A practical prototype of two-stage dc-dc power converter is built and tested for verification of the theoretical results.

Table of Contents Page No.

Lists Of Figures

Nomenclature

a	Ratio L_S/L_P
b	Ratio C_S/C_P
f_O	Resonant frequency (Hz)
f_S	Switching frequency (Hz)
ω_O	Angular Resonant frequency (rad/sec)
ω_S	Angular Switching frequency (rad/sec)
ω_n	Normalized switching frequency
M	Voltage gain of the resonant tank
Q	Quality factor
R_o	Actual load resistance
R	Ac equivalent load resistance
Z_o	Characteristics impedance.
Z_S	Effective input impedance of the resonant tank
V_{in}	Input voltage across the resonant tank
V_{out}	Output voltage of the resonant tank
V_O	Output voltage across the load
V_{dc}	Input dc voltage
V_S	Input voltage to the resonant tank of SRC
V_{LS}, V_{LP}	Voltage across the resonant inductors
V_{CS}, V_{CP}	Voltage across the resonant capacitors
I_{LS}, i_{LP}	Current through resonant inductors
i_P	Primary current of high voltage transformer
i_S	Secondary current of high voltage transformer
I_o	Load current
N_1	Primary number of turns of the high voltage transformer
N_2	Secondary number of turns of the high voltage transformer
D	Duty ratio of the buck converter
I_L	Inductor current of the buck converter.

CHAPTER 1

INTRODUCTION AND LITERATURE SURVEY

1.1 INTRODUCTION

There are certain applications, where a very high voltage dc power is required, with low available dc input voltage. A high voltage power converter is widely used to fulfill that requirement. Some times a multiple output dc voltage is also required. One such application is the Traveling Wave Tube Amplifier (TWTA) for space applications. It has few electrodes, each of which is operated at different high potentials. All these electrodes are to be powered from a common low voltage dc input source. The high voltage power converter should meet the following criteria,

- High efficiency
- Compactness
- Light weight
- Less EMI.

The efficiency the power converter depends on various losses within it. Those are,

- Copper loss and core loss within the high voltage transformer.
- Switching losses in the converter switches.
- Conduction losses within the converter switches.
- Copper losses within the energy storage elements (inductors and capacitors used in the power converter) and in various joints and conductors.

The only controllable losses are the switching losses. The other losses, mentioned above, are more or less uncontrolled, even with the proper design. By applying suitable technique to turn-on

and/or turn-off of the switches, the overall losses can be minimized. The size and weight of the power converter depend inversely on the operating frequency. The only solution to operate the power converter at very high switching frequency is by reducing the switching losses

Resonant dc-dc converters have some advantages over the hard-switched PWM converters. In resonant converters, the switches can be turned on or turned off at instants, when they are carrying no current (zero current transition or ZCT) and/or the voltage across them is zero (zero voltage transition or ZVT). This feature reduces the switching losses and allows the converter to operate at very high switching frequency. The other advantages of resonant converters are less EMI, higher efficiency and sinusoidal operation.

A resonant converter can be operated either below resonance (leading power factor) [1],[2] mode or above resonance (lagging power factor) mode [3],[4]. Operation above the resonance has a number of advantages compared with the operation below the resonance [5], such as,

- No need of di/dt limiting inductors
- No need of lossy snubbers
- Use of internal feedback diodes of MOSFET's
- Reduced size of the resonant elements and high frequency transformers, due to higher operating frequency.
- Current and voltage waveforms are nearly sinusoidal, and the simple sinusoidal steady-state analysis gives reasonably good results.

Basically there are two kinds of resonant converters,

(i) Series Resonant Converter (SRC)

The load is connected in series with the resonant tank. The output voltage is obtained from the resonant tank current.

(ii) Parallel Resonant Converter (PRC)

The load is connected in parallel with the resonant capacitor. The output voltage is obtained from the voltage across the resonant capacitor.

There are three main disadvantages of SRC [6],

(a) The switching frequency varies directly with the load. This results poor cross-regulation in multi-output power supplies.

(b) The ripple current in the filter capacitor is very high This poses a problem in controlling the output ripple voltage over the dc output voltage

(c) The SRC cannot operate at zero load current.

There are two main disadvantages of PRC [6],

(a) A PRC is prone to output short circuit. In case of an output short, the resonant capacitor is shorted, and the resonant inductor only limits the current in the tank circuit. External overload/ short-circuit protection is required.

(b) At light loads, the tank current is independent of the load, and it results in poor efficiency.

In a practical resonant power converter the transformer has magnetizing inductance, leakage inductance and inter-turn capacitance, the output diode bridge rectifier has junction capacitance. These are the parasitic components. At higher switching frequency, their effect cannot be neglected. The simple two element resonant tank of a practical resonant dc-dc power converter (SRC or PRC), is indeed a multi-element complex tank circuit [7]. Including the effect of the parasitics within design, a number of possible three-element and four-element resonant tank topologies were reported in [8], [9]. Although the three-element resonant converter [4], [10] is a better representation of a practical resonant converter, the parasitics of the high frequency output transformer and the output diode bridge lead to a four-element representation of a practical resonant converter. It was reported that several topologies are possible for a four-element resonant converter depending upon how the elements are interconnected [9]. No detailed study of

all these four-element resonant converters is available in the literature as there are many possibilities. One topology of many possible four-element topologies that takes into account leakage inductance and inter-turn capacitance of the output transformer and output diode junction capacitance is considered in chapter-2 for a detailed investigation. This representation leads to the connection of a capacitance in parallel and an inductor in series with the normal series resonant converter. The converter is operated above the resonant frequency. Adjusting the pulse-width of the voltage impressed across the resonant tank input controls the output voltage. The inverter switches of the resonant converter, operating above the resonance frequency, turn 'on' at zero current and zero voltage, but turn 'off ' at finite current and finite voltage Turn-off switching losses are present, which impose limitation on the switching frequency

A Series Resonant Converter (SRC) is the simplest and well-documented configuration. The SRC has high efficiency from full load to part load. An SRC, when operated exactly at the resonant frequency with full pulse-width voltage applied across the input of the resonant tank, all the inverter switches turn-on and turn-off at zero current. This feature reduces the switching losses considerably. The current and voltage stresses of the components and the devices are minimum The converter can be operated at very high switching frequency. Voltage gain of the converter is unity and is independent of the load. Despite of all these advantages, the major disadvantage of SRC is to control the output voltage with change in input voltage. Connecting a pre-regulator with the SRC can control its output voltage for input voltage variations. The pre-regulator can be a low frequency hard-switched PWM converter or a soft resonant switch (Zero Current Switch or a Zero Voltage Switch).

A two-stage dc-dc converter is explained in details in Chapter-3. The first stage is a conventional low frequency buck converter, which is followed by the second stage, an SRC. Controlling the duty ratio of the buck converter controls the output voltage.

1.2 ORGANISATION OF THE THESIS

Chapter-1 describes the introduction and thesis organization. Chapter-2 deals with the problem definition and probable solution techniques. A single stage LCLC dc-dc resonant converter is analyzed, designed and simulated for the high voltage converter of the TWTA. A proposed active filter circuit (for output voltage ripple reduction) is explained with the simulation results Chapter-3 describes the principle of operation, closed-loop control of a two-stage dc-dc power converter for the TWTA. A two-stage topology is analyzed for further study. The chapter-4 deals with the detailed design and simulation study of the proposed two-stage dc-dc power converter for the TWTA. A practical prototype of two-stage converter is implemented in chapter-5. The simulation and implementation results are given for better comparison. Finally the conclusion of the whole work is drawn in chapter-6.

CHAPTER 2

ELECTRONIC POWER CONDITIONER FOR TRAVELING WAVE TUBE AMPLIFIER

2.1 INTRODUCTION

Traveling Wave Tube Amplifier (TWTA) is used in the communication satellite for amplifying the power of any communication signal transmitted through satellite. The TWTA consists of a microwave-amplifying device, known as Traveling Wave Tube (TWT) and an Electronic Power Conditioner (EPC). EPC is providing the DC power necessary for amplifying the signal through TWT. The modern Traveling Wave Tubes (TWTs) used in satellite communication systems are driven by multi output high voltage Electronic Power Conditioners. The modern TWTs used in space applications usually have four collectors, one or two anodes, a cathode (at highest negative voltage) and a helix connected to the reference potential, as shown in Fig. 2.1.The auxiliary power supply required for the TWTA is shown in Fig. 2.2 and the nominal voltages and permissible voltage ripples to the TWTA are shown in Table-1. Electronic Power Conditioner (EPC) is used to generate the required, regulated high voltages, applied between the cathode and various collectors, helix and anodes, with very low output ripples and very high power conversion efficiency. Due to limited DC power and space availability on satellite, the efficiency should be very high and size should be as compact as possible.

2.2 DESCRIPTION AND DESIGN REQUIREMENTS OF THE EPC

The Electronic Power Conditioner consists of power chain for generating the required high voltage outputs with desired regulation, ripples and other electrical specifications as shown in

Table 2.1. The usual power supply connection arrangements to the TWT are shown in Fig. 2.2. The typical block diagram of EPC is shown in Fig. 2.3. The voltages required for cathode and all collectors are generated from the same transformer as shown in Fig 2.4. The rectified and filtered outputs from the different secondaries are connected in series to apply the required high voltages to different collectors and cathode. As shown in Fig. 2.3, the EPC consists of

2 2 1Input EMI Filter

The input EMI filter has been used for preventing the transfer of noise either from converter towards bus or vice versa.

2 2 2 High Voltage Converter

The converter is used to generate the required high voltages to be applied between the cathode to helix, all collectors and both the anodes. This converter should be highly efficient and as compact as possible.

2 2 3 Helix Series Regulator

To meet the extremely stringent regulation requirement by cathode to helix voltage, additional series regulator has been used. Without such an additional circuit practically it is not possible to achieve that stringent regulation requirements. The rectified and filtered secondary output from the high voltage converter is applied to helix electrode through series regulator in the helix current path as shown in Fig. 2.3.

2.2.4 Active Filter For Cathode Voltage

It is not possible to achieve the required low level of RMS and peak ripple for cathode-helix supply with maximum permissible capacitive filter. Incorporating the active filter in the cathode current path reduces the helix cathode supply ripple.

2 2 5 Cathode Current Regulator

In the TWT the control anode voltage determines the amount of current drawn from the cathode. Due to degradation in the physical and chemical properties of cathode with life, the current available from hot cathode has a tendency to decrease over the TWT operating life. The cathode current regulator controls and regulates the voltage applied between cathode and control anode and maintains the cathode current within stringent predetermined range.

2.3 LIMITATIONS

The TWT has limited capability to absorb the energy during turn-on and turn-off. This restricts the maximum amount of energy that can be stored in the output capacitance. As a result, the magnitude of the capacitance connected across the each rectifier segment in the high voltage output is limited to a maximum of 0.022 μF.

2.4 SOLUTIONS

In the present study, the high voltage converter and active filter circuit have been taken up for detailed study. There are many ways that the high voltage converter can be configured. Two configurations are described.

Configuration 1: Single stage dc-dc multi-element resonant converter with simultaneous PWM (Pulse Width Modulation) and FM (Frequency Modulation) control.

Configuration 2: A series connection of pre-regulator and an unregulated dc-dc series resonant converter.

This chapter considers the first configuration for detailed study. The second configuration is explained in Chapter 3. In both methods, the high frequency and high voltage transformer, the

output diode bridge rectifier units, and the filter capacitors are the same. The transformer has a single primary and few secondary windings. In both methods, the turns ratios between the secondary windings remain the same, since the output voltages are the same. Only the turns ratio between primary and secondary may be different depending upon the voltage available across the primary after the inverter and resonant tank. The series connection of the diode bridge rectifier and output capacitor filter arrangement is also the same as shown in Fig. 2 4.

2.5 SELECTED TOPOLOGY

In a power converter, the switches and the output diode bridge rectifier exhibit junction capacitances. The high frequency transformer at the output presents leakage inductance, magnetizing inductance and inter-turn capacitance. These are parasitic components. Their effects can be included by using higher order resonant topology. In the present investigation, the junction capacitance of the diode bridge rectifier and transformer inter-turn capacitance is represented by an equivalent capacitance C_P in parallel. The leakage inductance of the transformer is represented by an equivalent series inductance L_P. The effect of magnetizing inductance has not been included as it is normally very high. The four-element topology as shown in Fig. 2.5 is considered for detailed investigation. It is the same as the conventional series resonant converter (Ls and Cs) with the additional combination of Lp in series and Cp in parallel to take into account the effect of above mentioned parasitics. With two inductors and two capacitors, 17 topologies are possible to realize in a resonant converter with voltage source and voltage sink excitation. The resonant tank topology shown in Fig. 2.5 is one of the 17 possible four-element topologies [9].

2 6 ANALYSIS

The converter is operated at a frequency close to the resonant frequency of the tank circuit Thus, the energy supplied by the source is at the fundamental frequency as the impedance offered by the resonant tank to other higher order harmonics is high. Sinusoidal excitation and response is considered for the purpose of analysis.

2 6 1 Ac Equivalent Load Resistance

Fig. 2.9 shows the equivalent circuit of a four-element resonant dc-dc converter. At the output, a large capacitor is connected across the load resistance R_O. The load voltage is, therefore, considered as a constant voltage with negligible ripple. At the input of the diode bridge rectifier, the output voltage is reflected as a square wave of amplitude V_O. Thus, the amplitude of the fundamental component of the voltage at the output of the resonant tank is

$$V_{out(max)} = \frac{4V_O}{\pi}$$

The current at the input of the diode bridge rectifier is sinusoidal. It is rectified by the diode bridge. The average value of the rectified sine wave is the same as the load current,

$$I_O = \frac{2\,I_{LP(max)}}{\pi}$$

Where $I_{LP(max)}$ represents the peak of the sinusoidal current entering the diode bridge rectifier. The ac equivalent load resistance is given by

$$\frac{V_{out(max)}}{I_{LP(max)}} = R = \frac{8R_O}{\pi^2} \qquad (2.1)$$

2 6 2 Voltage Gain

Under sinusoidal excitation, the voltage gain M of the four-element resonant tank is defined as the ratio of the output voltage to the input voltage.

$$M = \frac{Vout}{V_{in}} = \frac{I_{LP} * R}{I_{LS}(Z_{LS} + Z_{CS}) + I_{LP}(Z_{LP} + R)} = \frac{R}{(Z_{LP} + R) + \frac{I_{LS}}{I_{LP}}(Z_{LS} + Z_{CS})}$$

$$= \frac{R}{(R + Z_{LP}) + (Z_{LS} + Z_{CS})\frac{I_{LS}(Z_{CP} + Z_{LP} + R)}{I_{LS} Z_{CP}}},$$

ω_S = angular switching frequency, $J = \sqrt{-1}$, $Z_{LP} = j\omega_S L_P$,

$$Z_{CP} = \frac{1}{j\omega_S C_P}, \quad Z_{LS} = j\omega_S L_S, \quad Z_{CS} = \frac{1}{j\omega_S C_S}$$

Simplifying the above expression and separating the real and imaginary parts, the expression for voltage gain is

$$M = \frac{1}{-C_P L_S\left[\omega_S^{\,2} - \frac{(C_S + C_P)}{C_S C_P L_S}\right] - \frac{jC_P L_S L_P}{R\omega_S}\left[\omega_S^{\,4} - \left(\frac{1}{C_P L_S} + \frac{1}{L_P C_P} + \frac{1}{L_S C_S}\right)\omega_S^{\,2} + \frac{1}{L_S C_S L_P C_P}\right]}$$

Substituting the following expressions in the expression for the voltage gain, we obtain

$\omega_n = \frac{\omega_S}{\omega_O}$, normalized switching frequency,

$\omega_O = \frac{1}{\sqrt{L_S C_S}}$, Resonance frequency

$R = \frac{8R_O}{\pi^2}$ = is the effective load equivalent ac resistance at the fundamental switching frequency at the output of the resonant tank, R_O is the actual load resistance (dc side) in ohm without considering HV transformer.

$a = \frac{L_S}{L_P}$, $b = \frac{C_S}{C_P}$, Q = Quality factor = $\frac{\omega_O L_S}{R_O}$

$$M = \frac{1}{\frac{1}{b}\left[(1+b)-\omega_n^{\,2}\right] - J\frac{\pi^2 Q}{8ab\omega_n}\left[\omega_n^{\,4} - (1+b+ab)\omega_n^{\,2} + ab\right]} = \frac{1}{A + jB} \qquad (2.2)$$

Where $A = \frac{1}{b}\left[(1+b)-\omega_n^{\,2}\right]$, $B = \frac{8Q}{\pi^2 ab\omega_n}\left[\omega_n^{\,4} - (1+b+ab)\omega_n^{\,2} + ab\right]$

The voltage gain of the resonant tank is a function of ω_n, a, b and Q. With PWM operation, it is necessary to select optimum switching frequency. Suitable values are also to be selected for a and b. Q changes with varying load resistance. To start with, the resonant circuit is studied in detail with various values of a and b. The following quantities are focused in this study

- Current gain I_{LP}/I_{LS}
- Voltage gain V_{out}/V_{in}
- Voltages across resonant elements
- Variation of ω_o with Q
- Pulse width variation to keep the dc output voltage constant as the load resistance is varied.

The desirable features are high current gain, high voltage gain, low voltage stress. The resonant frequency should decrease with increase of load resistance to permit zero-current and zero-voltage turn-on over the entire range of load variation. The range of pulse width variation should be low over the entire range of load variation to keep the output voltage constant. The question is what values are required for a and b in order to achieve these desirable features? Therefore, the simulation is carried out with different sets of a and b. These are (i) a=2, b= 0.5 (ii) a=1, b=1 (iii) a=2, b=2 (iv) a=1, b= 1.5 (v) a=1.5, b=1 (vi) a=1.5, b=1.5 The combination (i) a=2, b=0.5 is found to provide overall optimum performance. The gain M versus normalized frequency ω_n is obtained by (2.2) and is shown in Fig. 2.6(a). The curves with different values of Q converge at two different points A and B. These two points correspond to load independent operation. The

frequencies corresponding to the load independent operation are obtained by equating the second term in the denominator of (2.2) to zero. The frequencies are given by

$$\omega_n = \left[\frac{1}{2}\left\{(1+b+ab) \pm \sqrt{(1+b+ab)^2 - 4ab}\right\}\right]^{\frac{1}{2}} \qquad (2.3)$$

Substituting (2.3) in (2.2), the converter gain at the load independent point is obtained as

$$M = \frac{1}{\frac{1}{2b}\left[(1 \div b - ab) \pm \sqrt{(1+b+ab)^2 - 4ab}\right]} \qquad (2.4)$$

2 6.3 Input Impedance

The effective impedance at the input terminal of the resonant tank is given by

$$Z_S = Z_{LS} + Z_{CS} + \frac{Z_{CP}(Z_{LP} + R)}{(Z_{CP} + Z_{LP} + R)} \qquad (2.5)$$

Substituting for Z_{LS}, Z_{CS}, Z_{LP}, Z_{CP} in terms of switching frequency in (2.5), we have,

$$Z_S = j\omega_S L_S + \frac{1}{j\omega_S C_S} + \frac{R + j\omega_S L_P}{(1 - \omega_S{}^2 L_P C_P) + j\omega_S C_P R}$$

The normalized impedance Z_n is given by

$$Z_n = \frac{Z_S}{Z_O}$$

Substituting the expression for Z_O and simplifying we have

$$Z_n = j\omega_n + \frac{1}{j\omega_n} + \frac{1 + jQ\frac{\omega_n}{a}}{Q\left(1 - \frac{\omega_n{}^2}{ab}\right) + j\frac{8\omega_n}{\pi^2 b}} \qquad (2.6)$$

The frequency response of the normalized impedance Z_n of LCLC topology is shown in Figs. 2.7 and 2.8. These figures show the absolute value and phase angle of Z_n as a function of normalized

frequency ω_n with different values of Q. The resonant frequency is the point where the phase angle curve cuts the X-axis (normalized switching frequency axis). As Q increases, the resonant frequency decreases as shown in Fig. 2 6(b) and with Q > 10, it results in three resonant frequencies. The converter shows the characteristics of PRC in the low frequency region and as the frequency is increased further, the converter operation becomes similar to that of SRC

2 7 PRINCIPLE OF OPERATION

The high voltage four-element dc-dc converter should be able to keep its dc output voltage constant at the reference value for all possible loads and input voltage variation without losing its soft-switching performance. The two control techniques that permit constant output voltage are

(a) PWM (Pulse Width Modulation) control for load variation,

(b) FM (Frequency Modulation) control for input voltage variation.

The principle of PWM control is described in this section while FM control is described in section 2.9. The high voltage four-element dc-dc converter is operated at a switching frequency around 100 kHz To reduce switching losses it is necessary to ensure soft switching for the inverter MOSFET switches. The converter is operated always above the resonant frequency so that the input current to the resonant tank always lags behind the fundamental component of the input voltage to the tank. The dc output voltage across the load is controlled by varying the pulse width of the inverter output voltage to the resonant tank. The soft-switching can be ensured if the rising edge of the modulated pulse leads the zero crossing instant of the tank input current (while going positive). With that condition all the inverter switches will be turned on at zero current and zero voltage but they will turn off at finite current and finite voltage Turn-off losses are however present. The steady state operation of the converter of Fig 2.9 can be explained considering one supply cycle to the resonant tank. For the sake of clarity the high voltage transformer and

multiple rectifier and output filter stages have not been included. All the MOSFETs are gated by a clock signal whose frequency determines the switching frequency ω_S of the converter MOSFETs S_{21} and S_{22} are gated with a controllable time delay (τ) with respect to the gating of S_{11} and S_{12} respectively. The input voltage to the resonant tank is a quasi-square wave as shown in Fig. 2.10 Assuming lagging power factor operation, the waveform of the current i_{LS} is shown in Fig. 2.10. At $t = t_0$, i_{LS} is negative. The diodes DS_{11} and DS_{22} conduct till i_{LS} becomes zero. The period, (t_1-t_0) is referred to as regenerative interval during which the tank circuit returns the energy to the input supply and also supplies the load. At $t = t_1$, the current i_{LS} becomes zero and then goes to positive. Hence, the switch pair S_{11}–S_{22} conduct up to $t = t_2$. The interval $t_2 - t_1$ is called power interval during which the input source supplies the resonant tank and the load. At $t = t_2$, the switch S_{11} is turned off and S_{12} is turned on. The current i_{LS} freewheels through S_{22} resonant tank and DS_{12}. During this interval the voltage applied across the resonant tank is zero This continues up to $t = t_3$ and the interval $t_3 - t_2$ is called free resonant interval. During this interval, the resonant tank supplies energy to the load and no energy is supplied to the input source. Again at $t = t_3$, i_{LS} is positive. The diodes DS_{12} and DS_{21} conduct till i_{LS} becomes zero. The period, (t_4-t_3) is also referred to as regenerative interval during which the tank circuit returns the energy to the input supply and also supplies the load. At $t = t_4$, the current i_{LS} becomes zero and then goes to negative. Hence, the switch pair S_{12}–S_{21} conduct up to $t = t_5$. The interval $t_5 - t_4$ is also called power interval during which the input source supplies the resonant tank and the load. At $t = t_5$, the switch S_{12} is turned off and S_{11} is turned on. The current i_{LS} freewheels through S_{21} resonant tank and DS_{11}. During this interval the voltage applied across the resonant tank is zero. This continues up to $t = t_6$ and the interval $t_6 - t_5$ is also called free resonant interval. During this interval, the resonant tank supplies energy to the load and no energy is supplied to the input source.

Thus there are six distinct intervals in each switching cycle

(a) Two power interval, interval (t_2-t_1) and interval (t_5-t_4)

(b) Two free resonant interval, interval (t_3-t_2) and interval (t_6-t_5)

(c) Two regenerative interval, interval (t_1-t_0) and interval (t_4-t_3).

2.8 DESIGN METHODOLOGY

The high voltage converter is designed with the following specifications.

- DC supply voltage (V_S): 26V-43 V
- Maximum output voltage (V_O): 6300 V (between Anode 1 and Cathode)
- Maximum power output: 270 W
- Tank Specifications: a =2, b= 0 5
- Switching frequency (f_S): 100 kHz

The range of input voltage variation is 26 V to 43 V. However, in order to take various voltage drops (diodes forward voltage drop, resistive drops in various parts of the circuit, conduction drops across switches) into account the minimum input voltage in the worst case is considered to be 22 V. From Fig. 2.6(a) (variation of voltage gain of the resonant tank M with normalized frequency ω_n with Q as parameter), at load independent point ω_n = 1.412, (above the resonant frequency) the voltage gain of the resonant tank M = 1. For minimum input voltage 22 V, the fundamental ac voltage across the input of resonant tank is $\frac{4 \times 22}{\pi}$ = 28 V and the corresponding RMS voltage is 19.8 V. Equivalent ac resistance across the tank output, corresponding to power output of 270 W is

$R = 19.8^2/270 = 1.76\ \Omega$. Assuming Q = 4,

Z_O = characteristics impedance = $QR_o = 4 \times \frac{\pi^2 R_O}{8} = 8.68\ \Omega$.

$L_S = Z_O/\omega_O = 19.38\ \mu H \approx 20\ \mu H$

Where $\omega_O = 2\pi f_S$

f_S = switching frequency = 100 kHz

$C_S = 0.25\ \mu f$.

Hence for a=2 and b=0 5, we have

$L_P = 10\ \mu H$

$C_P = 0.5\ \mu F$.

With these actual values of resonant elements and with 1:1 transformer, the variations of voltage gain and current gain with switching frequency are shown in Figs. 2.11(a) and 2.11(b) respectively. The variation of voltage stresses with actual load resistance is shown in Fig. 2.11(c).

To calculate the turns ratio of the high voltage transformer, initially a single secondary winding with 6300 V at the output of the bridge rectifier is considered. Equating the ac side power and dc side power, turns ratio n = 310 is obtained. However, in the simulation n = 320 is considered to take into account various resistive voltage drops, device finite switching times.

2.9 CLOSED-LOOP CONTROL

The dc-dc converter should be able to maintain constant output voltage for

(a) 10 % to 100 % output load variations,

(b) 26 V to 43 V input voltage variation, without losing soft-switching performance. The simulation study shows that it is possible to obtain soft-switching for the entire load variation while maintaining constant dc output voltage with PWM control. Any attempt to include the effect of higher input voltage would require further reduction in pulse width of the modulated ac voltage across the resonant tank input. As a result, the rising edge of the modulated pulse would

fall behind the zero-crossing instants of the current (while going positive) waveform and inverter switches would lose soft-switching performance. In order to take input voltage variation also into account, it is necessary to introduce additional control technique From the voltage gain curve of the tank, as shown in Fig. 2.6(a), it is clear that voltage gain depends very much on switching frequency around the operating point. A small variation in the switching frequency is sufficient to take input voltage variation into account. Hence, there are two independent controls.

(a) PWM (Pulse Width Modulation) control for load variation,

(b) FM (Frequency Modulation) control for input voltage variation.

The block diagram of close-loop control is shown in Fig. 2.12. For a particular dc input voltage, the converter output voltage is kept constant by varying pulse width of the voltage across the resonant tank input for all possible load variations. The design is such that the converter operates slightly above resonance with full pulse width, impressing a square wave voltage across the input terminals of the resonant tank at full load and at minimum input dc voltage As the load current decreases, the pulse width is decreased by phase shifting the gating pulses G_{21} and G_{22} as shown in Fig. 2.10. It must be noted that gating signals G_{11} and G_{12} are always 180°out of phase with each other This type of gating control decreases the pulse width of the voltage V_{in} impressed across the input of the resonant tank as the load current decreases and if the output voltage is to be held constant. The output voltage is sensed and compared with the reference voltage. The comparator output is fed to the PI controller. The output of the PI controller is applied to the phase shifter circuit through a limiter. The phase shifter takes input pulse from the square wave generator (VCO) and it provides a shifted pulse at its output with respect to the input pulse keeping the frequency and width the same as the input pulse. The degree of phase shift can be controlled from 0-180° by the control voltage to the phase shifter block. The control voltage is obtained from the output voltage of the PI controller through a limiter. The phase shifter provides two complementary pulses to S_{21} and S_{22}, while VCO provides two complementary pulses to S_{11}

and S_{12}. The PWM loop is designed to be much faster than the FM loop. Whenever load and/or input voltage changes, the PWM loop will operate first such that the output voltage is maintained constant. In this process, if the soft-switching gets disturbed, the FM loop will take over and becomes active along with the PWM loop. The output of the FM control drives the VCO The FM loop is designed in such a way that it forces the positive going zero-crossing instants of the input current to the resonant tank to confine with in a narrow band 'A' as shown in Fig 2.10 This narrow band is placed in close proximity to the rising edge of the modulated voltage pulse across the resonant tank input This strategy ensures inverter switches to turn-on at zero current and zero voltage. As the positive going zero crossing of the current falls within the band, the FM control loses its action and maintains a constant frequency at the VCO output. If the positive going zero-crossing instants of the resonant tank input current falls behind the narrow band, FM loop becomes active and starts reducing the output frequency of the VCO (switching frequency). The positive zero-crossing instants of the input current to the resonant tank start moving towards the narrow band. The FM control loop remains active till the zero-crossing of current falls within the band. Similarly, when the positive going zero-crossing instants of the input current to the resonant tank go beyond the narrow band, FM loop increases the switching frequency till they fall back with in the band. When the FM control loop is inactive the output frequency of the VCO is set at some new frequency. In this way soft-switching can always be ensured. FM controller needs two control signals corresponding to the input current and voltage to the resonant tank. Although the input voltage to the resonant tank can be fabricated from the gating pulses of devices, a current sensor is, however, required for obtaining the input current to the resonant tank.

2.10 SABER SIMULATION STUDY

The high voltage converter of the EPC is simulated in the SABER simulator The detailed power circuit is shown in Fig. 2.13. For clarity, the FM and PWM control circuitry are not included. The parameters used are,

$V_S = 22\ V - 43\ V$, $L_S = 20\ \mu H$, $L_P = 10\ \mu H$, $C_S = 0.25\ \mu F$, $C_P = 0\ 5\ \mu F$, $f_S = 99$ kHz-104 kHz

Maximum output power 270 W

Maximum output voltage (between Anode 1 and Cathode) = 6300 V.

The number of turns of primary and different secondary windings of the high voltage transformer are shown in Fig. 2.13. The closed-loop FM and PWM control is designed in such a way that the input current to the resonant tank always lags behind the rising edge of the modulated input voltage to the resonant tank for all pulse widths, load variations and input voltage variations as well. It should be noted that the range of switching frequency variation should be low; otherwise it will be difficult to design the high voltage transformer and output filter capacitors To determine the range of switching frequency variation required for the operation of the converter, the following two cases are considered for SABER simulation.

(a) The switching frequency will be minimum for minimum input voltage and maximum load (100% full load)

(b) The switching frequency will be maximum for maximum input voltage of 43 V and minimum load (10% of full load)

From SABER simulation, corresponding to case(a), the switching frequency at full pulse width is 99 kHz as is shown in Fig. 2.14(a), and in case(b) it is 104.5 kHz as is shown in Fig. 2.14(b). Thus, the range of switching frequency variation required to include FM along with the PWM control is 99 kHz - 104.5 kHz. As the variation in the switching frequency is small, it may not affect the design of high frequency components. The output voltage waveforms at various

terminals of the TWT corresponding to 22 V input, full load, and at switching frequency of 90 kHz are shown in Fig. 2.15(a). The voltage and current stresses in the resonant elements are shown in Fig. 2.15(b). It may be noted that filter capacitors of 0.01 μF are used in the output stages. Using maximum of 0.022 μF may reduce ripples further. Because of some simulation limitation, SABER does not accept a capacitance value more than 0 01 μF. Table-1 shows the nominal voltage and permissible voltage ripple requirements in various voltages to the TWTA From the actual voltage ripples as shown in Fig. 2.15(a), it is clear that all the voltage ripples are within permissible limits except the voltages between electrodes Cathode-Anode1 and Cathode-Control Anode. These two stringent permissible voltage ripples cannot be achieved by capacitive filter of 0.022 μF. It needs an active filter in addition to the capacitive filter. An active filter for controlling output voltage ripple is discussed in the section that follows.

2.11 ACTIVE FILTER

Fig. 2.16 shows an active filter connected in series with the Helix terminal to control the voltage ripple in the Helix-Cathode path. The desired output dc voltage across the Helix-Cathode path is 6100 V with peak-to-peak ripple voltage not to 100 mV. To explain the principle of the active filter, a voltage with ripple is modeled. The actual input dc voltage to the active filter can be thought of an ideal dc voltage (desired output) over which the ripple voltages at various frequencies and offset dc voltage (if any) are superimposed. The idea is to generate a voltage, equal and opposite to the ripple and the offset dc component at each and every instant and add it with the actual voltage. The unwanted component is then cancelled out and ripple-free desired dc voltage is obtained. In Fig. 2 16, V_{CA} is the input voltage to the filter obtained from the output of the high voltage converter of the EPC. This voltage will have large ripple content. Such a voltage is modeled as explained earlier. The active filter is interposed between the load and the rippled

voltage source, which is usually the output of the high voltage power converter. V_{CB} is the voltage across the load (Helix-Cathode) and its ripple content is to be controlled within the specified limit. The active filter essentially consists of a MOSFET switch in series with a resistor R_1 and a capacitor C_1 across the load. The equal and opposite unwanted voltage V_{AB} is generated across the series combination of the MOSFET and resistor R_1. With the help of a potential divider (R_3 and R_2) a control voltage V_{DB} proportional to the actual load voltage is obtained across R_2. Operational amplifier OP-2 is a unity gain buffer to prevent loading of control circuit. The reference control voltage V_{ref} is set at −10 V. The values of R_2 and R_3 are selected such that voltage V_{DB} = −10 V when V_{CB} = -6100 V (desired output voltage). In a digital comparator OP-1, V_{DB} is compared with V_{ref}. Whenever the actual load voltage (V_{CB}) exceeds the reference voltage (6100 V), the MOSFET is turned off and the output filter capacitor across the load starts discharging. The MOSFET is turned on when the actual voltage falls below the reference voltage and the source supplies power to the load and the filter capacitor. The simulation is carried out with the following data.

Reference output voltage = 6100 V

Input voltage $V_{CA} = -[6200e^{-t/\tau} + 15\sin(2\pi f_1) + 10\sin(2\pi f_3) + 5\sin(2\pi f_5)]$ V

Load resistance = R4 = 1.22 MΩ (Helix-Cathode)

τ = Time constant = $(R_5 \times C_2)$ sec.

The input voltage to the filter is modeled by an exponential dc source to account for the gradual rise in voltage at the output of the high voltage converter during start-up. It has a steady state value of 6200 V over which three harmonic voltages at 200 kHz, 600 kHz, and 1000 kHz are superimposed. These correspond to the fundamental, third and fifth harmonics of the ripple voltage. The desired output voltage across the load is 6100 V. In the steady state, average voltage across capacitor C_1 is 6100 V and average input voltage is 6200 V. The average offset dc voltage

of 100 V drops across the series combination of the MOSFET and R1. This dc-offset voltage is required for operation of the active filter to ensure that the minimum instantaneous input voltage is greater than the reference dc output voltage. It may be noted that during start-up the MOSFET remains on till the output voltage crosses the reference value The voltage across the filter capacitor C_1 gradually rises from zero to its final steady-state value as is shown in Fig. 2.17 During this time the voltage drop across the series resistor R_1 is more than its steady-state value. This may damage it due to high power loss. In order to prevent this sort of failure a zener diode is connected across them. During start up it clamps the voltage across them to some safe value The zener diode is selected in such a way that it does not break down in the steady state. Its breakdown voltage is less than the device breakdown voltage as well as voltage rating of R_1. Figures 2.17 to 2 19 show SABER simulation results obtained from the active filter of Fig. 2.16. The build up of voltage across the load during starting as well as in the steady state is shown in Fig. 2.17 without the zener across the series combination of MOSFET and R_1. It may be seen that the difference between input and output voltages during transient state is very high. With the connection of Z_d, the maximum voltage is limited to zener breakdown voltage. The steady state waveforms of input and output voltages are also shown in Fig. 2.17. While the average output voltage is held at 6100 V, the input voltage is held at the average value of 6200 V with a peak-to-peak ripple of 28 V. The voltage across the series combination of MOSFET and R_1, and input ripple voltage are shown in Fig. 2.18. The active filter produces a voltage which is in phase opposition to the input ripple voltage and dc offset voltage. Thus, the ripple is considerably reduced at the output voltage. Fig. 2.19 shows the pulses to the MOSFET and switching behavior of the active filter indicating the final ripple voltage in the output. It is seen that the ripple content in the load voltage is reduced to 25 mV. In order to provide the dc offset voltage for operation of the active filter, slight adjustment of turns in the secondary of the high frequency transformer is required.

2.12 PROBLEMS IN IMPLEMENTATION

(a) The current stresses in the resonant elements are very high. Particularly the current through the parallel capacitor C_P, which is nearly equal to 45 A(peak) It is very difficult to get a high frequency capacitor of such rating

(b) Due to high current stresses the copper losses in various parts of the high voltage converter increase which lowers the efficiency

(c) The inverter MOSFET switches turn on at zero current and zero voltage, but they turn off at finite current and finite voltage. There are turn-off losses, which limits the operating frequency of the inverter.

(d) At light loads the resonant tank input current is quite high compared to actual load current resulting in poor efficiency.

(e) The voltage gain and current gain of the resonant tank are very much susceptible to the parameter variation due to temperature. A small change in the value of the resonant elements from their designed value greatly affects the performance of the converter.

2.13 CONCLUSION

The general description of the Traveling Wave Tube Amplifier (TWTA) used in satellite along with the requirement of various voltages and currents for different electrodes, permissible voltage ripple at different electrodes is given. Two possible solutions for the high voltage converter part of the Electronic Power Conditioner (EPC) are explained. The single stage dc-dc resonant converter is presented in this Chapter. The four-element representation of the resonant tank takes into account various parasitics associated with diode bridge and high frequency transformer. A detailed study of four-element resonant tank by simple fundamental ac circuit analysis shows that there are two load independent operating points. From the standpoint of size and performance of the converter, operation at the higher frequency is preferred. Full pulse width

is applied at minimum input voltage and maximum load. As the load decreases, the pulse width is decreased to maintain constant output voltage. The resonant frequency decreases slightly with increasing load resistance. This feature makes it possible to achieve zero-current and zero-voltage turn-on over the entire range of load variation. As the gain of the converter varies with switching frequency, a large change in the input supply voltage can be accommodated by a small change in the switching frequency without affecting the soft switching performance. The study presented in this chapter reveals that there are two independent controls, namely (a) Frequency Modulation (FM) control for input voltage variation, (b) Pulse width Modulation (PWM) control for load variation. With both FM and PWM control the range of frequency variation required is 99 kHz - 104 kHz . The voltages and the currents in the resonant tank are almost sinusoidal, but the component stresses are quite high. This topology provides inherent short circuit protection capability and continuous conduction even under light load condition. The active filter circuit presented in this chapter successfully reduced the ripple voltage within the permissible limits wherever it is required There are some problems in implementing the high voltage converter part by single stage four-element dc-dc resonant converter. These are addressed in the next chapter by attempting second possible solution for the high voltage converter of EPC. This involves two stages comprising of a pre-regulator (buck converter) and high frequency series resonant converter.

TABLE-1. Permissible voltage ripples in the auxiliary power supply of the TWTA

VOLTAGE	NOMINAL	RIPPLE
Cathode-Collector4	600 V	2 V
Cathode-Collector4	2200 V	7 V
Cathode-Collector4	2800 V	9 V
Cathode-Collector4	3400 V	11 V
Collector4-Helix	1700 V	4 V
Cathode-Helix	6100 V	100 mV
Cathode-Anode1	6300 V	200 mV
Cathode-Control Anode	3400 V	12 V

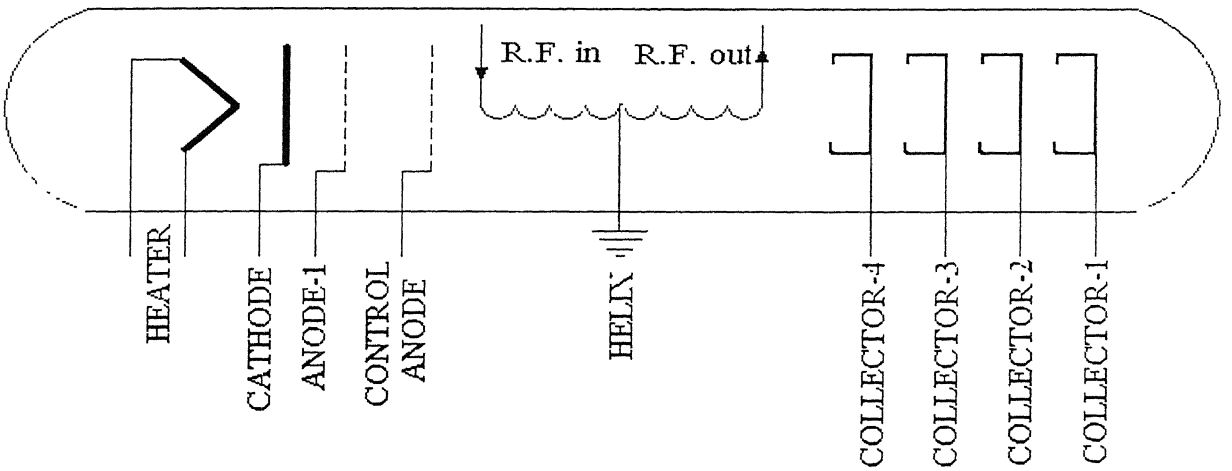

Fig. 2.1. Traveling wave tube amplifier (TWTA).

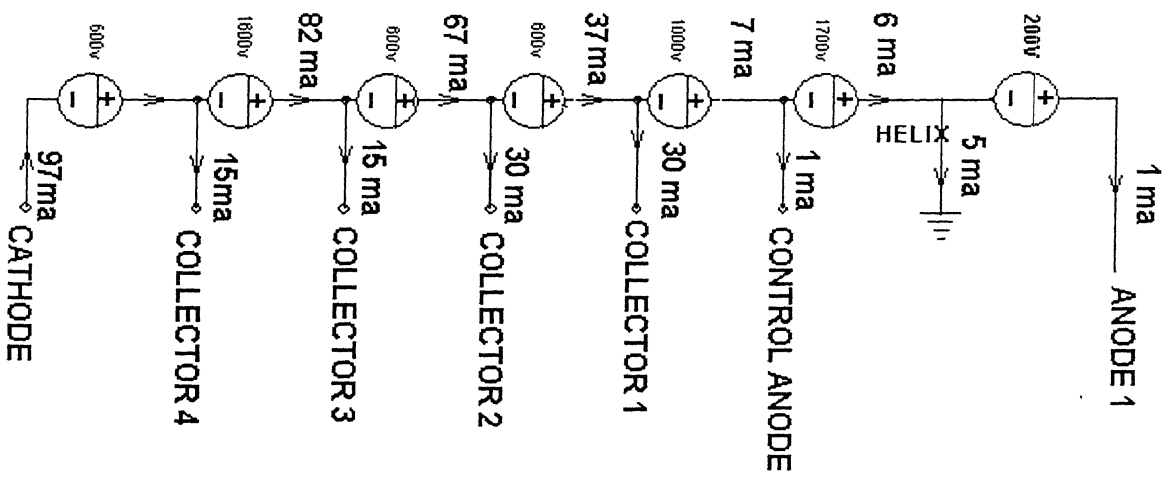

Fig. 2.2 Auxiliary power supplies arrangement for TWT amplifier.

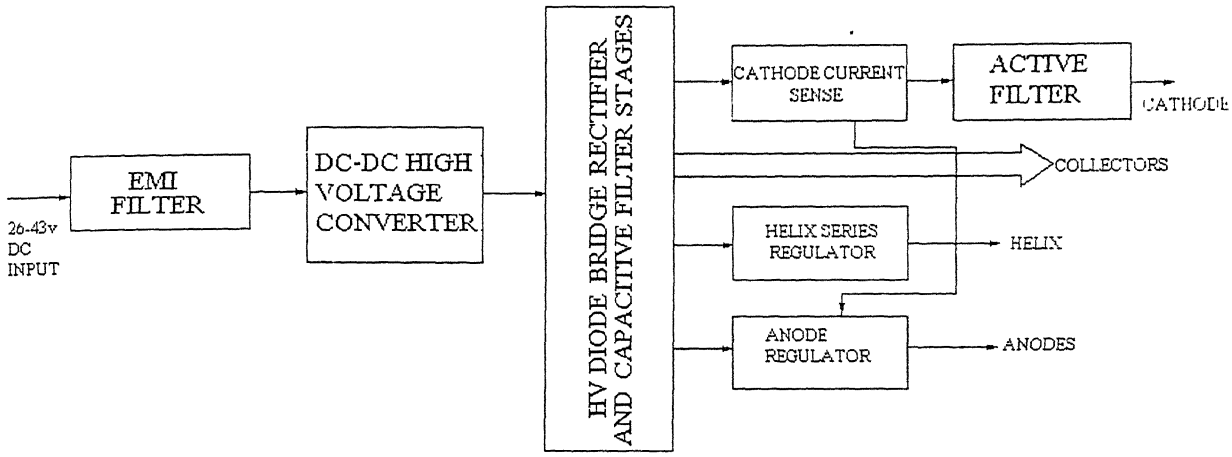

Fig. 2.3. Block diagram of Electronic Power Conditioner.

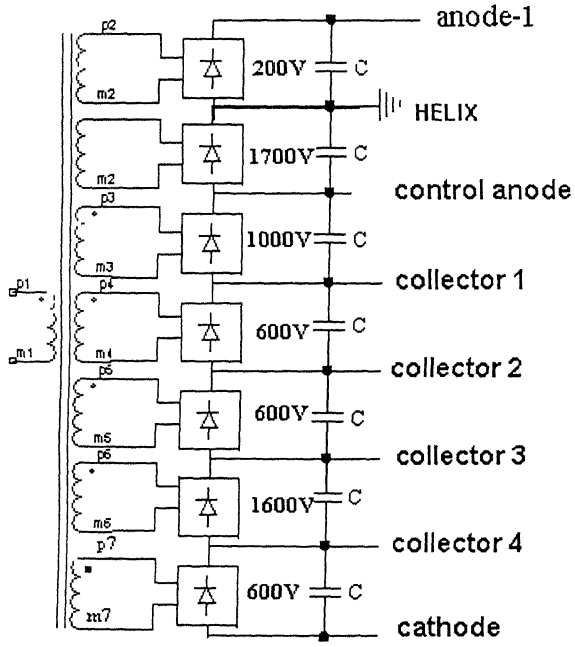

Fig 2 4 High voltage transformer and diode bridge rectifier and capacitor filter stages.

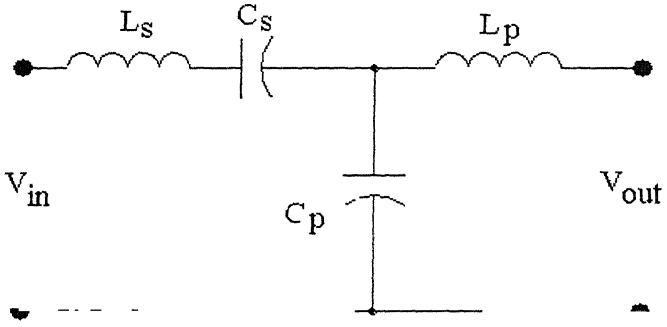

Fig. 2.5 Four element resonant network

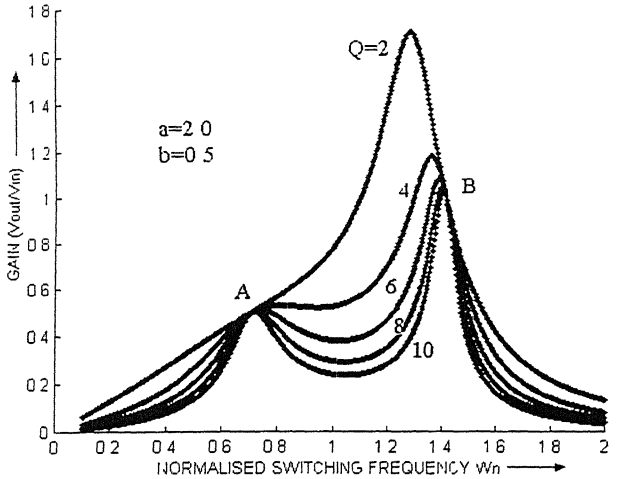

Fig 2.6(a) Voltage gain variation of the the four-element resonant tank.

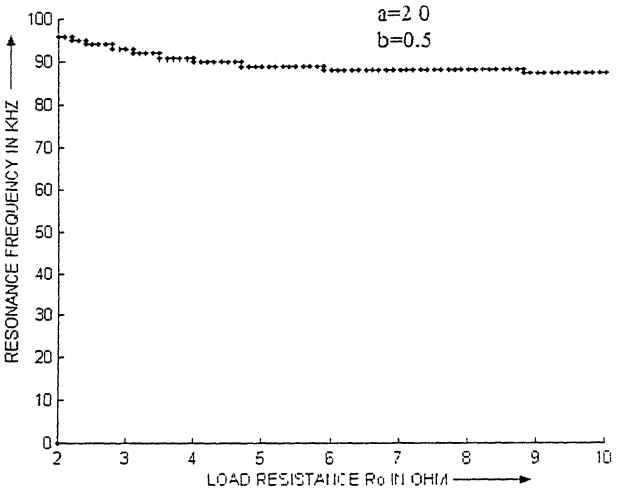

Fig. 2.6(b) Resonance frequency variation of four element resonant tank.

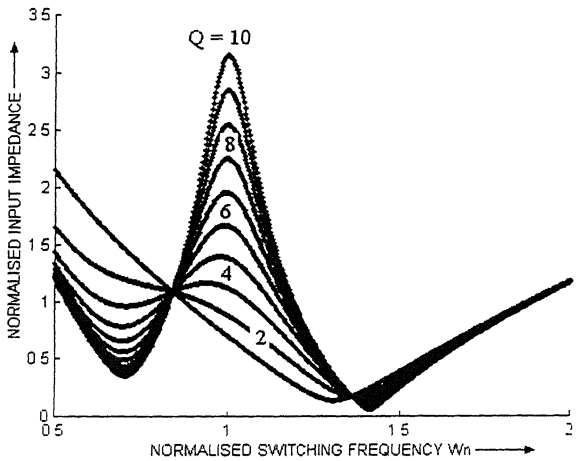

Fig. 2.7 Impedance variation with frequency for different Qs.

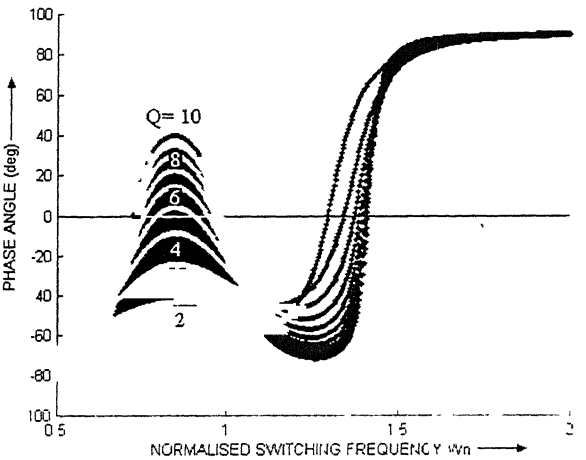

Fig. 2.8 Phase angle variation with frequency for different Qs.

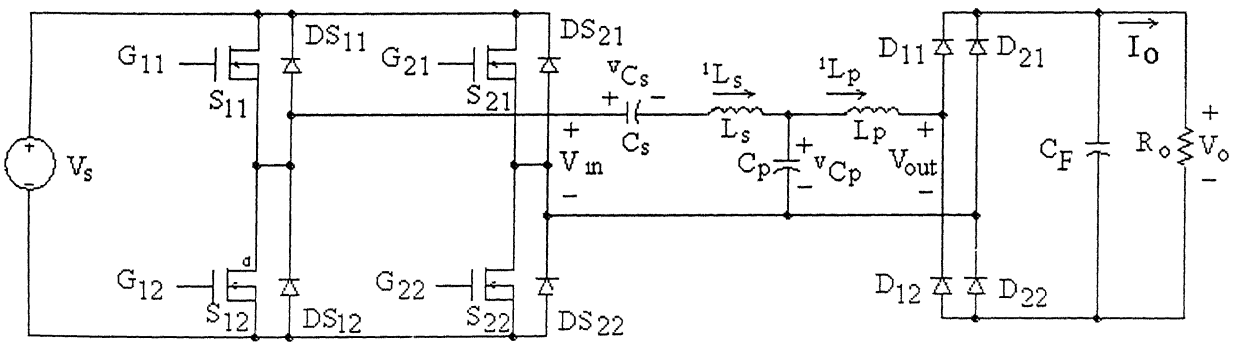

Fig. 2.9 Four-element resonant dc-dc converter.

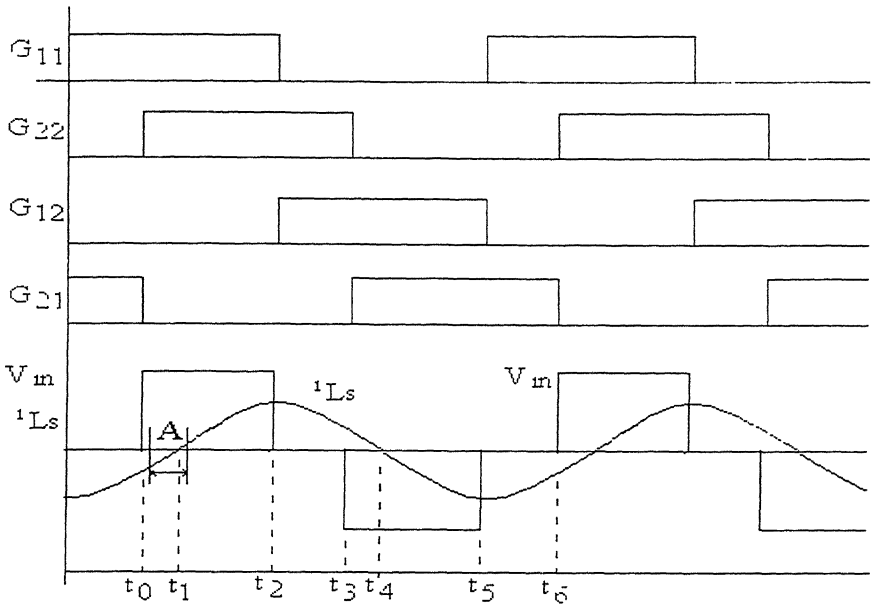

Fig. 2.10 Gating pulses to all MOSFET switches and timing diagram.

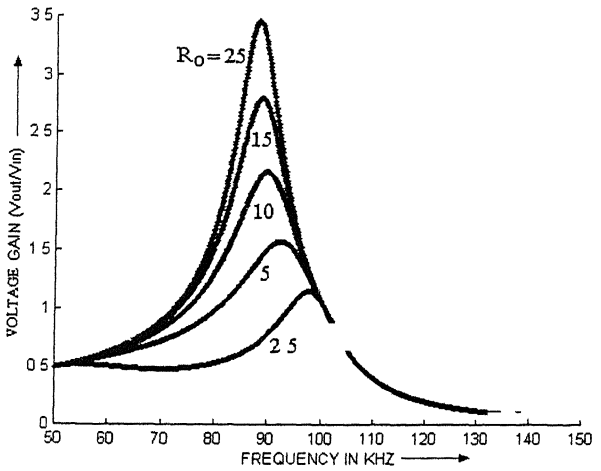

Fig. 2.11(a) Voltage gain variation with switching frequency.

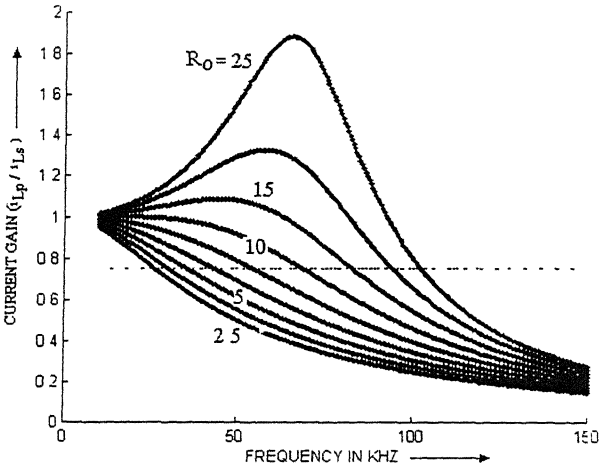

Fig. 2.11(b) Current gain variation with switching frequency.

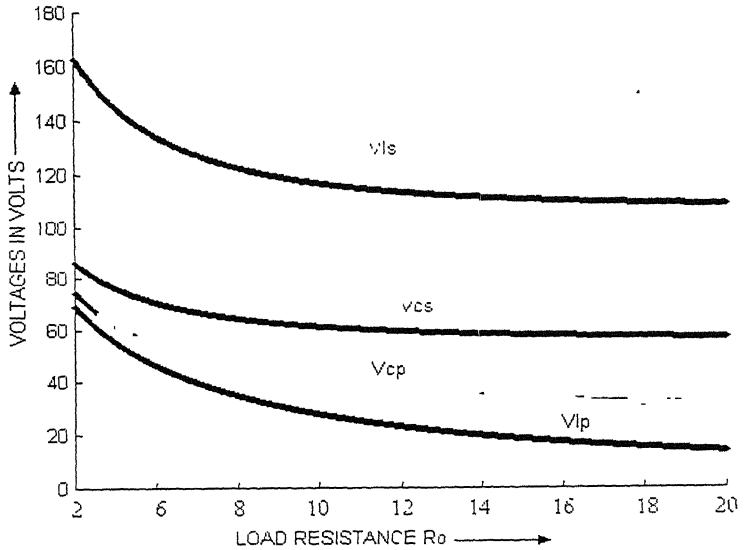

Fig. 2.11(c) Variation of voltage stresses with actual load

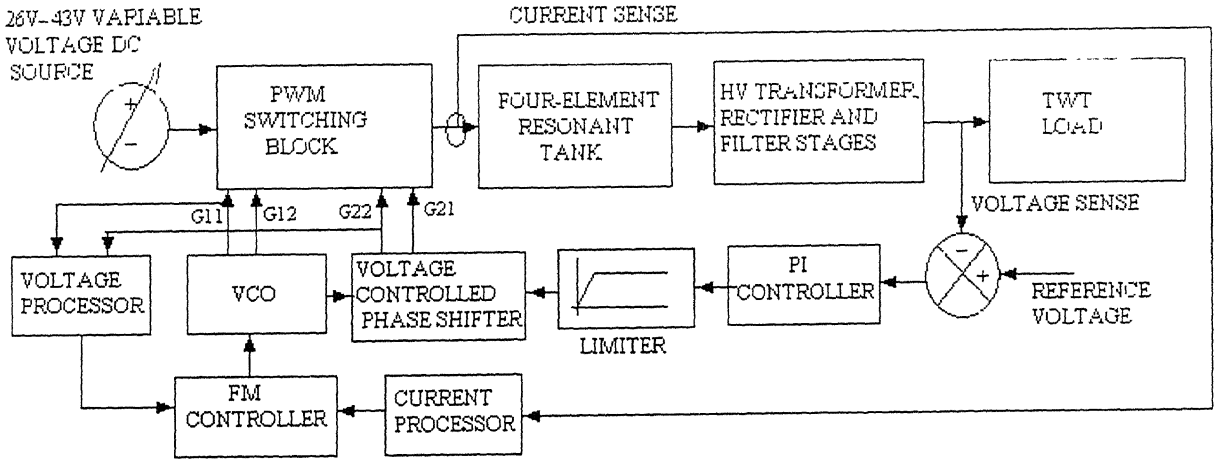

Fig. 2.12 Block diagram of closed loop FM and PWM control.

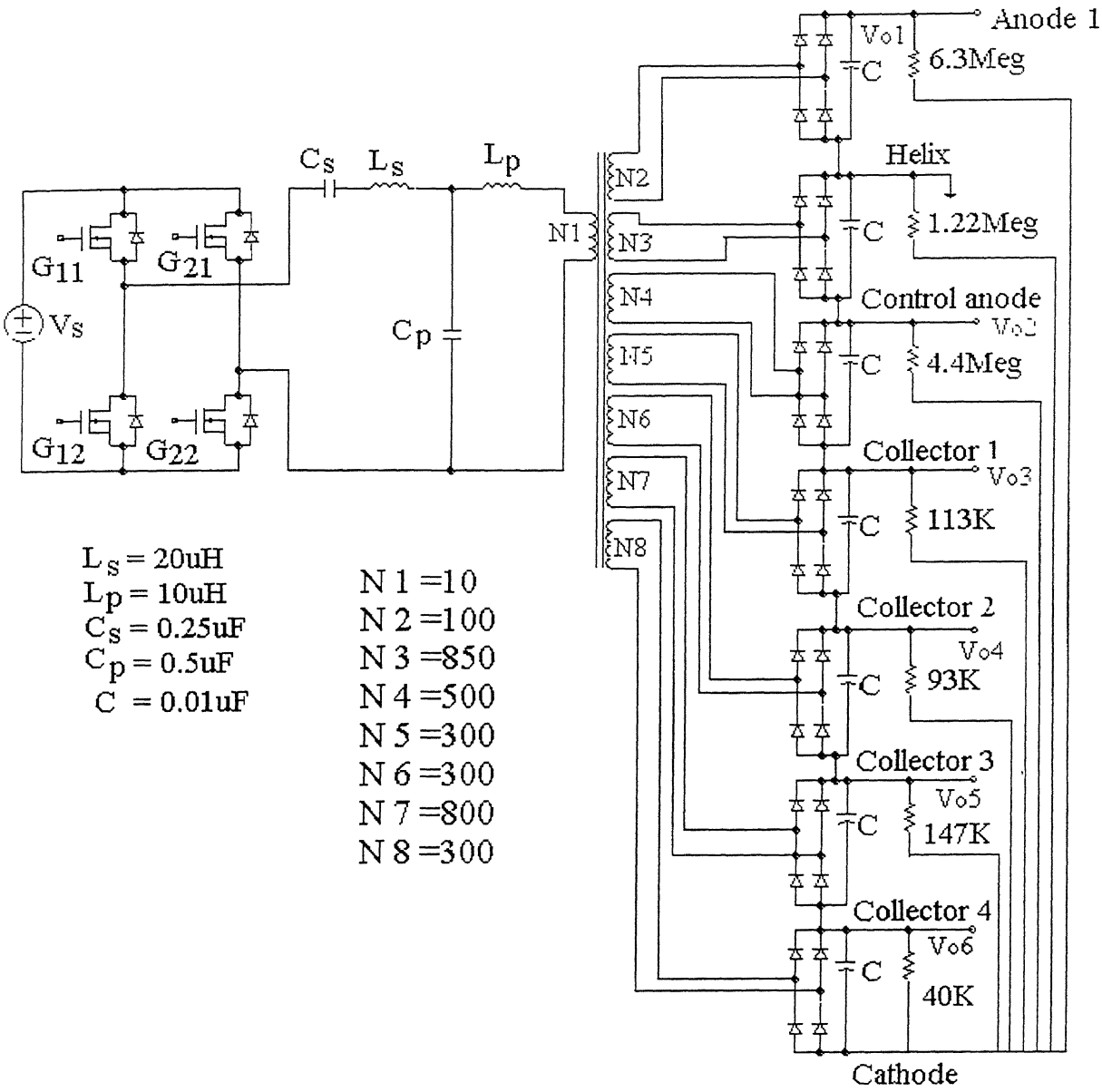

Fig. 2.13 Detailed power circuit of the high voltage converter

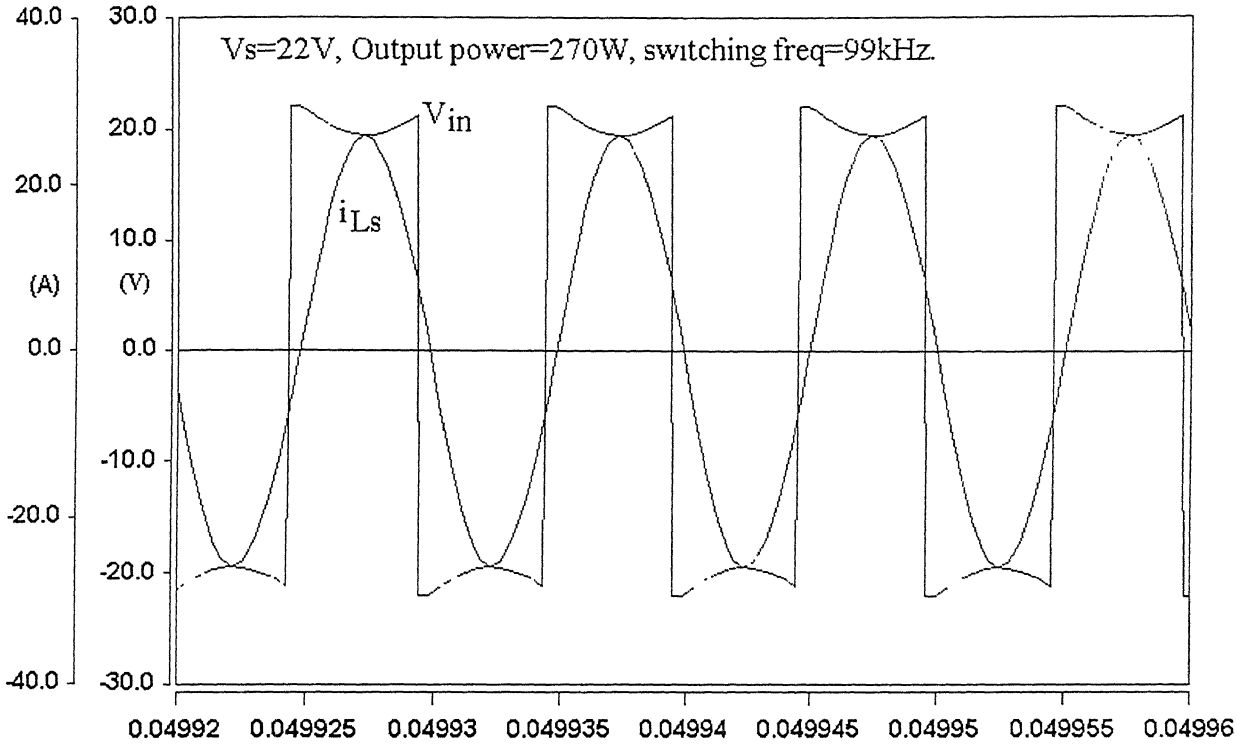

Fig. 2.14(a) Input voltage and current to the resonant tank

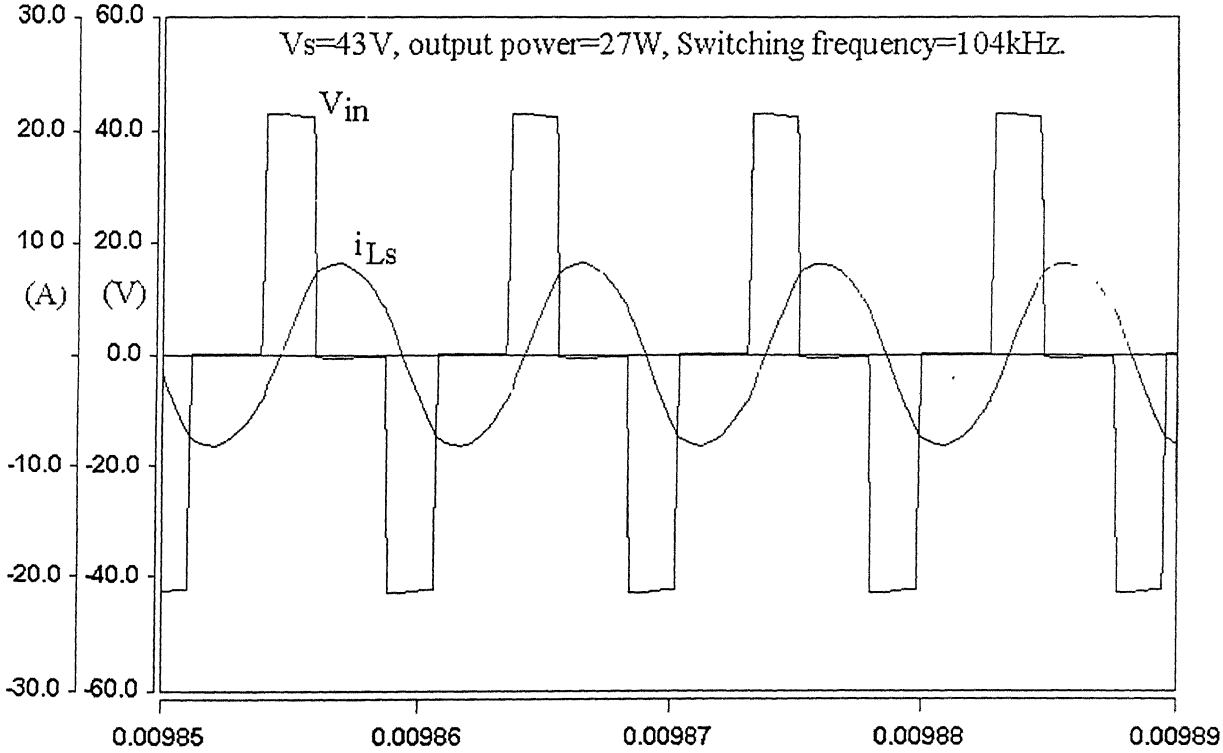

Fig. 2.14(b) Input voltage and current to the resonant tank

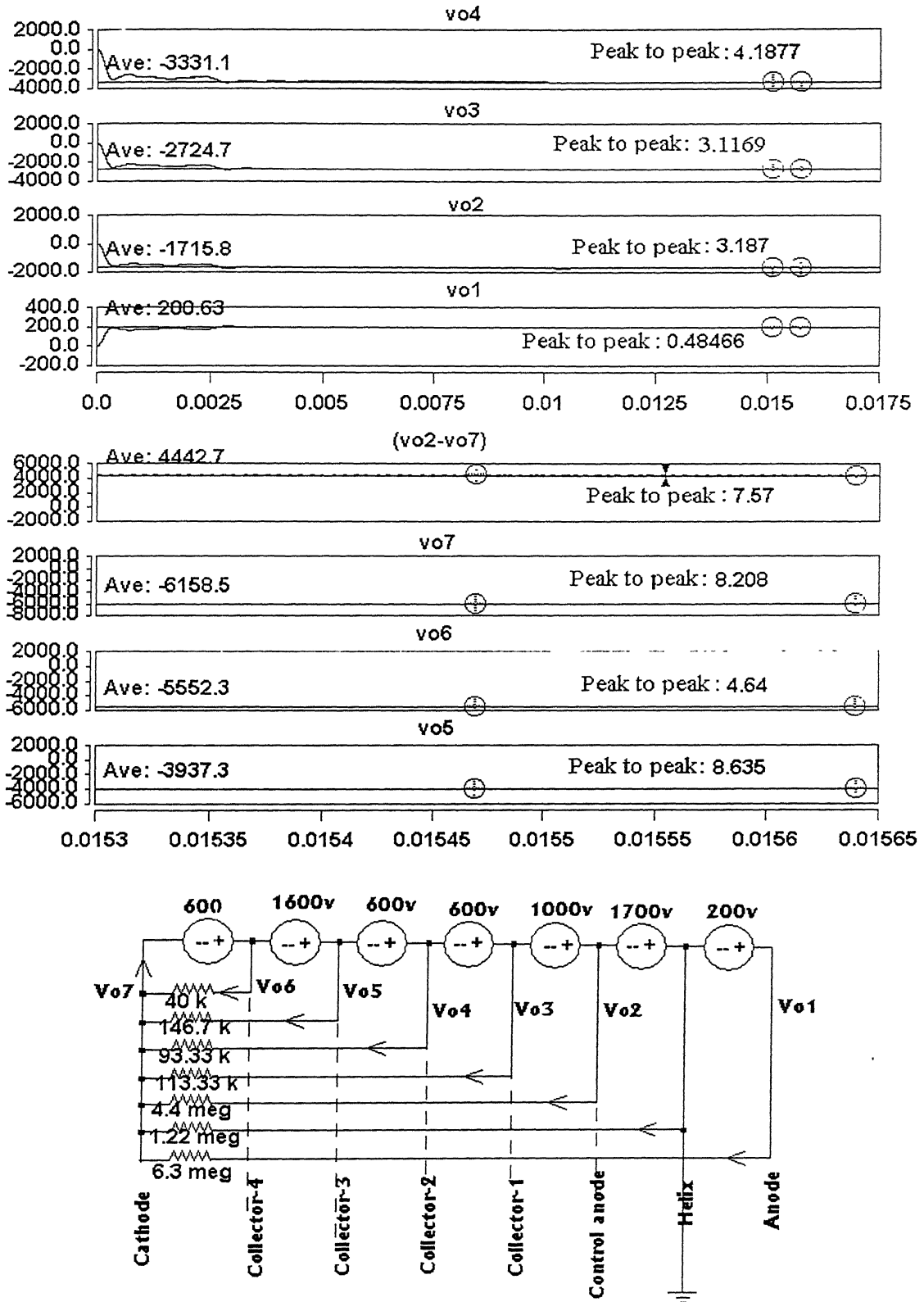

Fig. 2.15(a) The output voltage of the high voltage converter at various electrodes of the TWT.

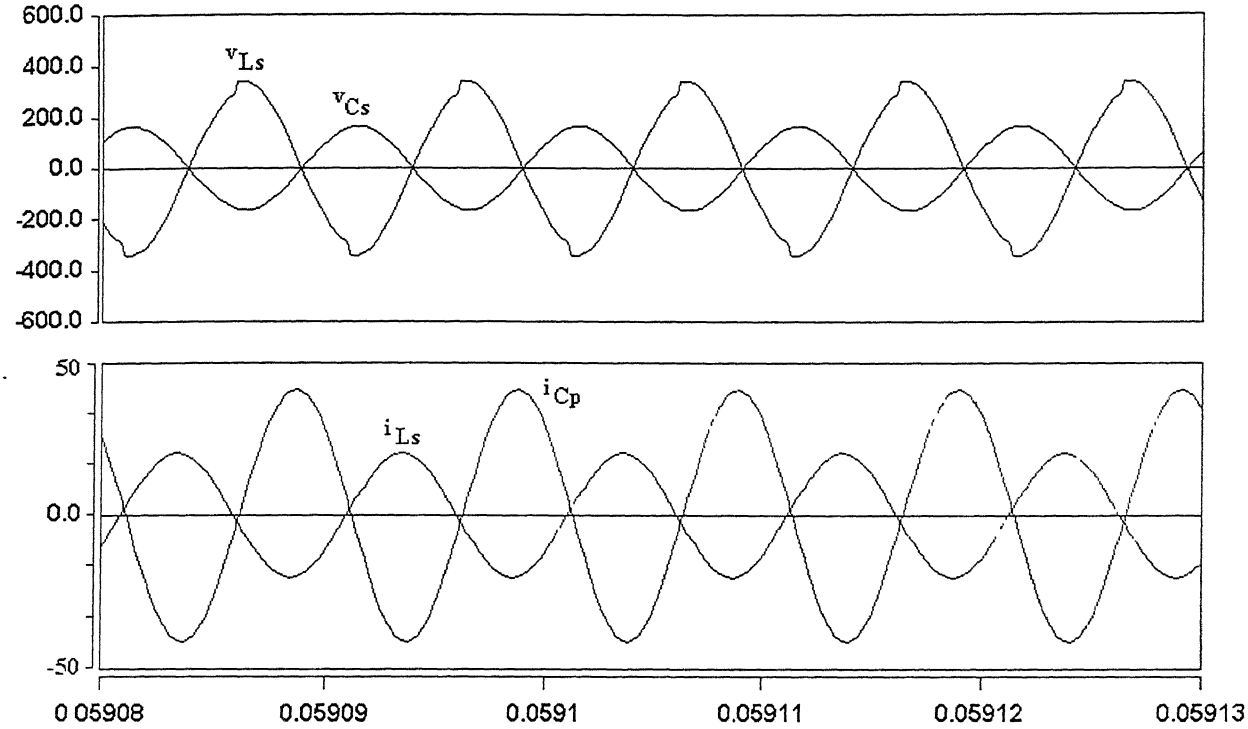

Fig. 2.15(b) Voltage and current stresses in different resonant elements.

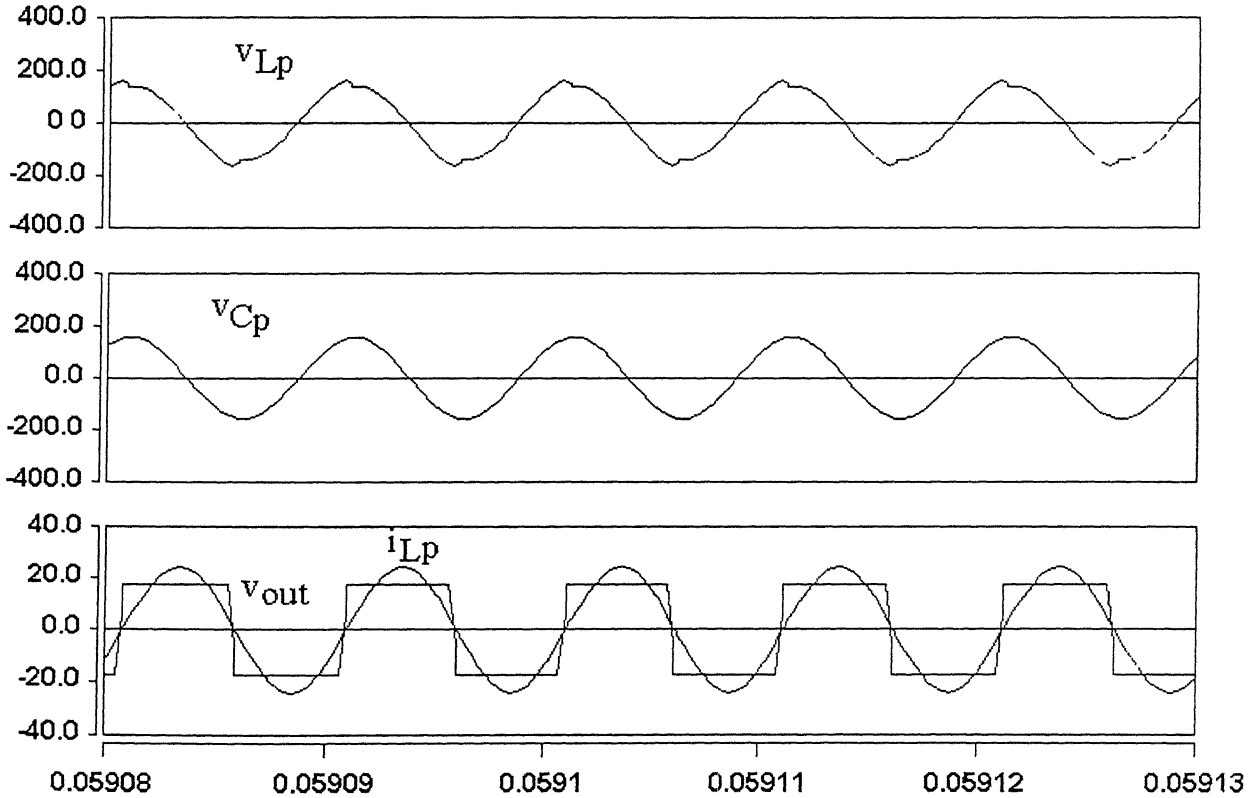

Fig. 2.15(b) (continued) Voltage and current stresses in different resonant elements and the high voltage transformer.

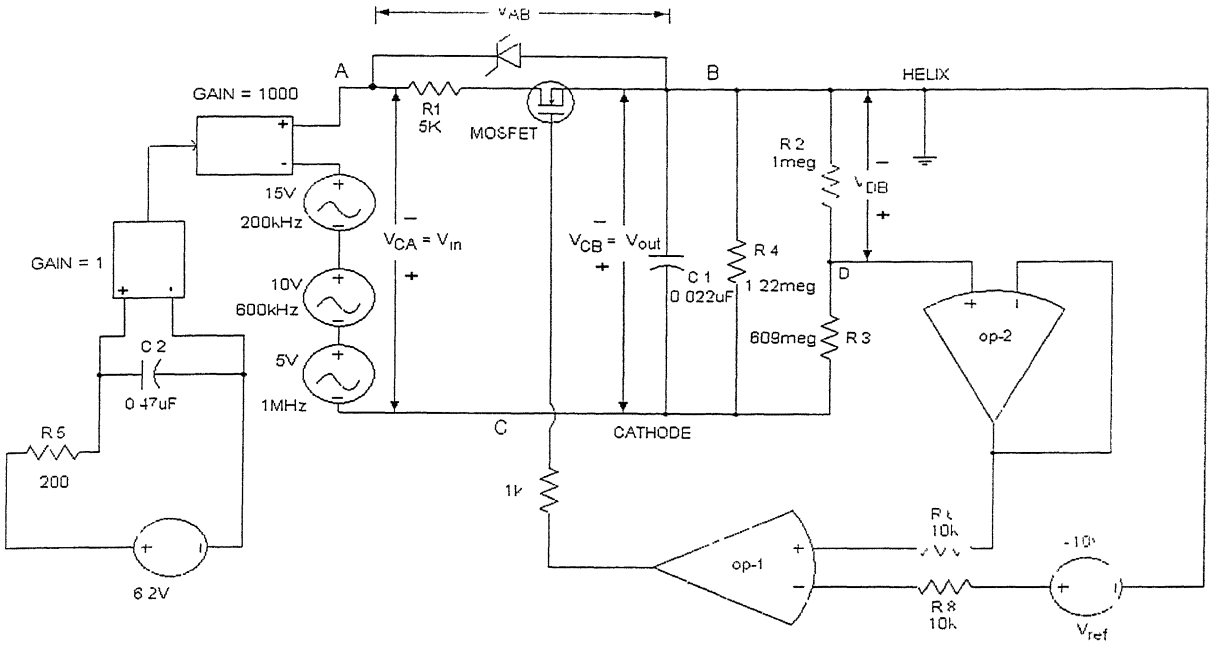

Fig. 2.16 Proposed filter circuit for voltage ripple reduction.

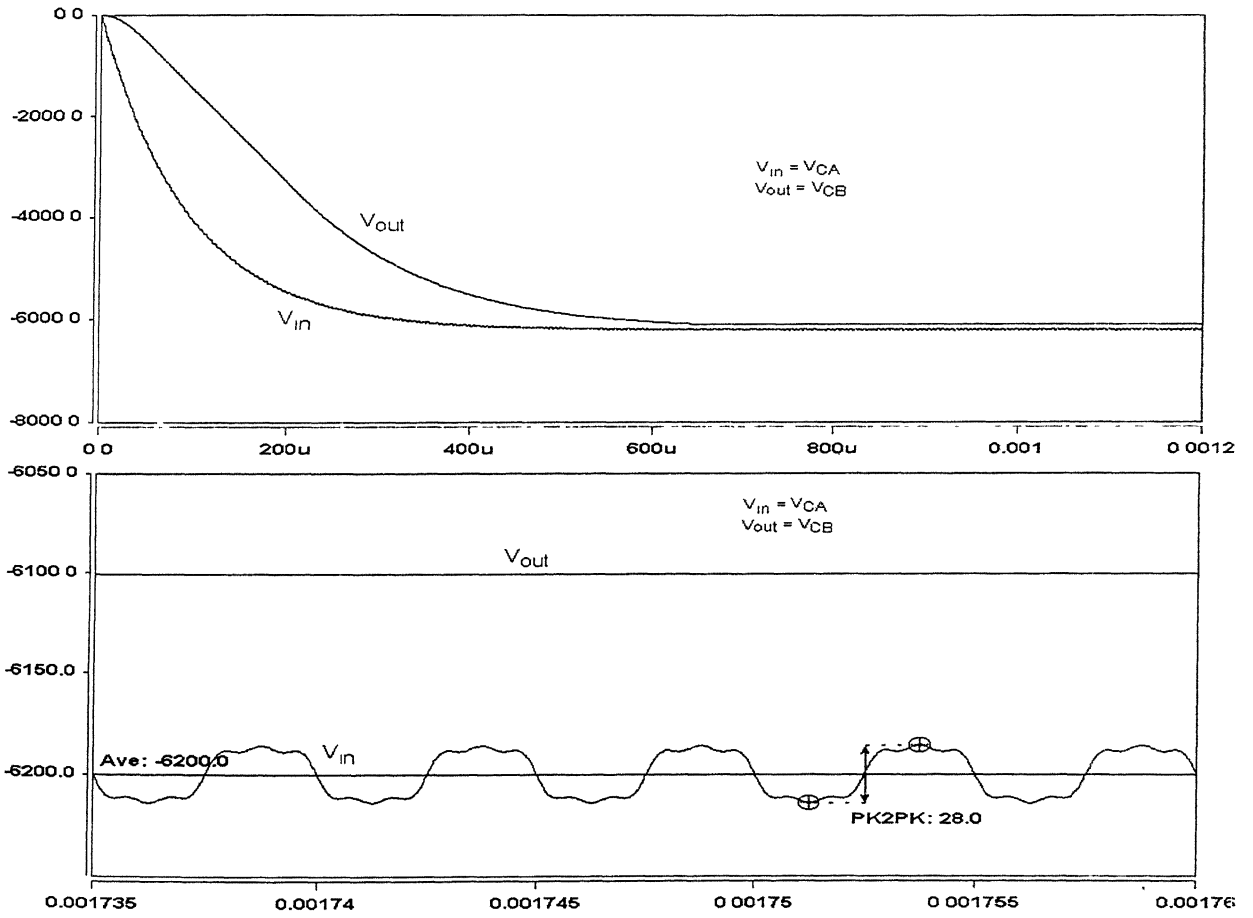

Fig. 2.17 Input and output voltage of the filter.

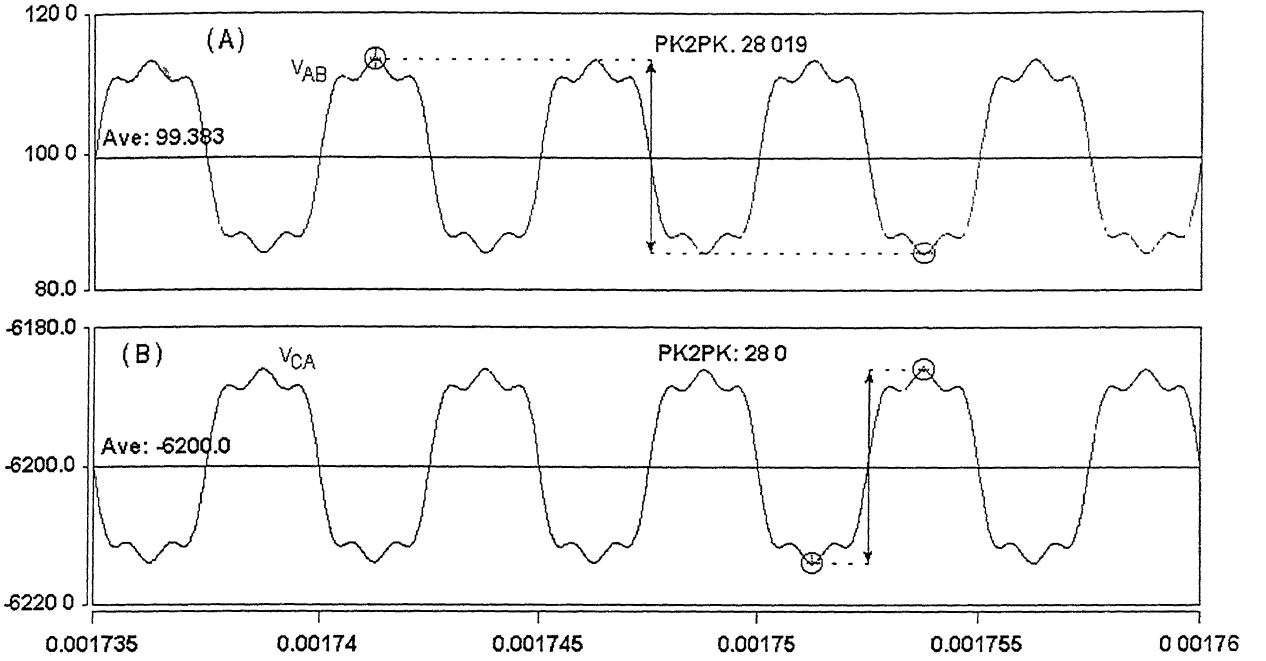

Fig. 2.18 (A) voltage across the MOSFET and resistor R_1
(B) Input voltage to the active filter.

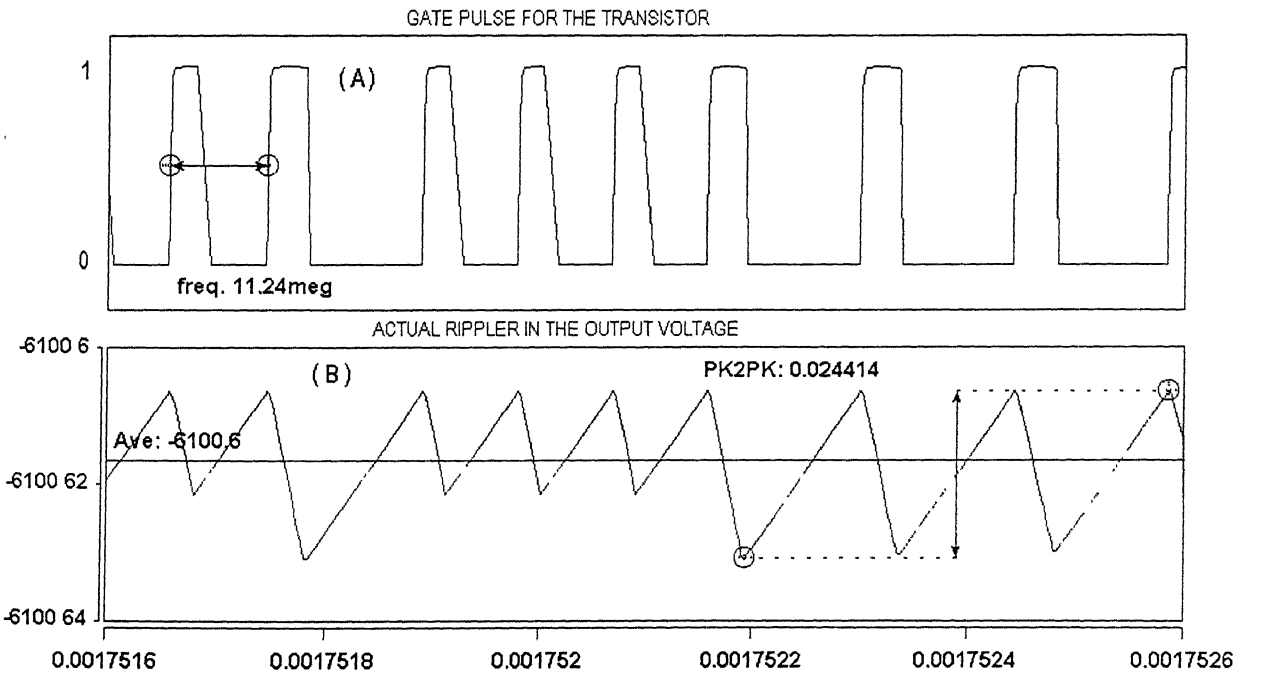

Fig. 2.19 (A) Gate pulse to the MOSFET.
(B) Output voltage of the filter.

CHAPTER 3

ANALYSIS OF TWO STAGE DC-DC POWER CONVERTER

3.1 INTRODUCTION

The substitution of the single stage dc-dc four-element LCLC resonant converter for the high voltage converter of the Electronic Power Conditioner (EPC), as described in the previous chapter, has the problem of high current stress in the resonant elements. The performance of the converter is dependent on the parameters, which vary due to temperature Although the inverter switches turn on at zero current and zero voltage, they turn off at finite current and finite voltage resulting in turn-off losses. The switching losses are directly proportional to the switching frequency. The turn-off losses impose limitation on the maximum switching frequency. In space application where size and weight are of great importance, the converter size should be as compact as possible It should also be highly efficient. EPC has a high voltage multi-output transformer. For a particular power output the size of the transformer varies inversely with the operating frequency. The transformer should be operated at high frequencies and the converter performance should be independent of temperature variation.

A Series Resonant Converter (SRC) provides unity voltage and current gains at resonant frequency independent of load variation and also parameter variation due to temperature. The fundamental component of the voltage and current are always in phase. With full pulse width voltage applied at the input of the resonant tank, the inverter switches turn on and turn off with zero current and finite voltage resulting in minimum switching losses. With resonant converter operating at the resonant frequency, the topology has the disadvantage that the output voltage cannot be controlled. In order to control the output voltage, some other technique is to be

introduced. As pointed out in chapter 2, the second method comprising of a pre-regulator (buck converter) followed by a high frequency series resonant converter (two-stage) is considered for detailed study in this chapter. The dc voltage across the load is controlled using single pulse width modulation (PWM) by controlling the duty ratio of the buck converter. The buck converter is operated at low frequency due to hard-switching. The Series Resonant Converter with multi-output transformer is operated at high frequency. Closed-loop frequency control makes it possible to operate the inverter switches of the SRC at resonant frequency to minimize switching losses.

3.2 ANALYSIS

3 2 1 Two Stage dc-dc Converter Scheme

Fig. 3.1 shows the block diagram of the proposed two-stage dc-dc power converter. The first stage is a conventional buck converter. The output of the buck converter is fed to an uncontrolled high frequency Series Resonant Converter (SRC), operated exactly at the tank resonance frequency. Controlling the duty ratio of the buck converter controls the output dc voltage across the load. The voltage gain and current gain of a SRC operated at resonant frequency is unity. They are independent of the load resistance. Duty ratio control of the buck converter is required to take care of the input voltage variation.

3 2 2 Buck Converter

Fig. 3.2 shows a conventional buck converter. The switching frequency of the buck converter is kept constant. The output voltage of the buck converter is controlled using single PWM by controlling the duty ratio of the switch S_1. When switch S_1 is on, the current through the inductor increases and the source supplies power to the inductor, capacitor and the load. When S_1 is off,

the source is completely disconnected from the converter. The inductor current decreases freewheeling through the diode D_1.

Referring to Fig. 3.3, the switch S_1 is on for a period of T_{ON} and it is off for the rest of the time in a switching cycle of time period T. The average output voltage across the output of the converter is given by

$$V_O = \frac{T_{ON}}{T} = DV_S \qquad (3.1)$$

Where D is the duty ratio.

When S_1 is on,

$$V_L = (V_S - V_O)$$

$$\frac{\Delta i_{on}}{\Delta T} = \frac{\Delta i}{DT} = \frac{V_S - V_O}{L}$$

The rise in the inductor current is

$$\Delta I_{on} = \frac{V_S - V_O}{L} DT \qquad (3.2)$$

When S_1 is off,

$$V_L = - V_O$$

The fall in the inductor current is

$$\Delta I_{off} = \frac{-V_O(1-D)T}{L} \qquad (3.3)$$

$\Delta I_{on} = \Delta I_{off} = \Delta I$, Equating (3.2) and (3.3) we have

$$V_O = \frac{T_{ON}}{T} = DV_S$$

$$I_{max} = \frac{V_O}{R} + \frac{\Delta I}{2} = \frac{V_O}{R} + \frac{V_O(1-D)T}{2L} \qquad (3.4)$$

$$I_{min} = \frac{V_O}{R} - \frac{\Delta I}{2} = \frac{V_O}{R} - \frac{V_O(1-D)T}{2L} \qquad (3.5)$$

For just continuous conduction,

$$I_{min} = 0$$

The minimum value of inductance for just continuous conduction from (3.5) is

$$L_{min} = \frac{(1-D)R}{2f} \qquad (3\ 6)$$

$f = \frac{1}{T}$, switching frequency of the buck converter.

The charge stored in the output capacitor

$$Q = CV_O$$

$$\Delta Q = C\Delta V_O$$

$\Delta Q = \frac{1}{2}\frac{\Delta i_C}{2}\frac{T}{2}$, change in stored charge in one half cycle.

$$\Delta Q = \frac{T\Delta i}{8} \qquad (3.7)$$

Substituting for ΔQ and Δi from above and simplifying we have

$$\frac{\Delta V_O}{V_O} = \frac{(1-D)}{8LCf^2} \qquad (3.8)$$

$$C = \frac{(1-D)}{8Lf^2}\frac{V_O}{\Delta V_O} \qquad (3.9)$$

3.2.3 Series Resonant Converter (SRC)

A conventional series resonant converter (SRC) with a single secondary high voltage transformer is shown in Fig. 3.4. The resonant tank circuit is formed by series combination of an inductor L_S and a capacitor C_S. The leakage inductance of the transformer is included within L_S. The magnetizing inductance of the transformer is neglected because of its high value. The diode junction capacitance and transformer inter-turn capacitance are neglected for analysis because of

their low values. The inverter switches are operated at 50% duty ratio impressing a square wave ac voltage across the resonant tank input. The circuit is operated exactly at the tank resonant frequency. The impedances offered by the tank to other harmonic frequencies are very high. For the purpose of analysis, sinusoidal excitation may be considered.

(a) *Voltage gain*

The voltage gain of the resonant tank is given by

$$M = \frac{V_{out}}{V_{in}}$$

Referring to Fig. 3.4

$V_{in} = V_{out} + I\left(j\omega_S L_S + \frac{1}{j\omega_S C_S}\right)$, ω_S is the angular switching frequency.

$$= V_{out} + \frac{V_{out}}{R}\left(j\omega_S L_S + \frac{1}{j\omega_S C_S}\right),$$

$$= V_{out}\left(1 + j\frac{\left(\omega_S L_S - \frac{1}{\omega_S C_S}\right)}{R}\right) \qquad (3.10)$$

R is the load equivalent ac resistance at the output of the resonant tank

The output is a voltage sink. From equation (2.1)

$R = \frac{8R_o}{\pi^2}$, R_o is the actual dc load resistance.

Quality factor $Q = \frac{\omega_O L_S}{R_O} = \frac{1}{\omega_O C_S R_O}$

$\omega_O = \frac{1}{\sqrt{L_S C_S}}$, the angular resonance frequency of the series resonant tank

$\omega_n = \frac{\omega_s}{\omega_O}$, the normalized frequency

Substituting these in equation (3.10), we have

$$M = \frac{V_{out}}{V_{in}} = \frac{1}{1 + j\frac{\pi^2 Q}{8}\left(\omega_n - \frac{1}{\omega_n}\right)} \qquad (3\ 11)$$

$$|M| = \frac{1}{1 + \left(\frac{\pi^2 Q}{8}\left(\omega_n - \frac{1}{\omega_n}\right)\right)^2} \qquad (3\ 12)$$

The variation of the voltage gain M with normalized switching frequency is shown in Fig. 3.6. As the switching frequency deviates from the resonant frequency, the voltage gain decreases. The gain curves become steeper as Q increases

(b) *Input impedance*

Referring to Fig. 3.5, the input impedance of the resonant tank at fundamental switching frequency is given by

$$Z_I = R + j\omega_S L_S + \frac{1}{j\omega_S C_S}$$

$$= R + j\left(\omega_S L_S - \frac{1}{\omega_S C_S}\right)$$

$$= R\left(1 + j\frac{1}{R}\left(\omega_S L_S - \frac{1}{\omega_S C_S}\right)\right)$$

$$= R\left(1 + j\left(\frac{\pi^2 Q}{8}\left(\omega_n - \frac{1}{\omega_n}\right)\right)\right) \qquad (3.13)$$

Normalized impedance $Z_n = \frac{Z_I}{Z_O}$

$Z_0 = \sqrt{\frac{L_S}{C_S}} = \frac{L_S}{\sqrt{L_S C_S}} = \omega_O L_S$, the characteristics impedance of the series resonant tank

$$Z_n = \frac{R}{\omega_O L_S}\left(1 + J\left(\frac{\pi^2 Q}{8}\left(\omega_n - \frac{1}{\omega_n}\right)\right)\right) \quad = \frac{R}{QR_O}\left(1 + j\left(\frac{\pi^2 Q}{8}\left(\omega_n - \frac{1}{\omega_n}\right)\right)\right)$$

$$= \left(\frac{8}{Q\pi^2} + J\left(\omega_n - \frac{1}{\omega_n}\right)\right)$$

$$|Z_n| = \sqrt{\left(\left(\frac{8}{Q\pi^2}\right)^2 + \left(\omega_n - \frac{1}{\omega_n}\right)^2\right)} \qquad (3.14)$$

$$\angle Z_n = \tan^{-1}\left(\frac{\left(\omega_n - \frac{1}{\omega_n}\right)}{\frac{8}{Q\pi^2}}\right) \quad (\text{rad})$$

$$= \tan^{-1}\left(\left(\frac{\pi^2 Q}{8}\left(\omega_n - \frac{1}{\omega_n}\right)\right)\right) \quad (\text{rad}) \qquad (3.15)$$

Fig. 3.7 shows the variation of normalized impedance with normalized frequency. The variation of phase angle of the input impedance with normalized frequency is shown in Fig. 3.8

(c) Peak v*oltage Stress across* L_s

Assuming the amplitude of the input current to the resonant tankas I_m, the Maximum voltage stress across L_S is

$$V_{LS(max)} = I_m\, \omega_S L_S = I_m\, \omega_n \omega_O L_S = I_m\, \omega_n Q R_O \qquad (3\ 16)$$

The output is a voltage sink load. Substituting the dc load current $I_O = \frac{2Im}{\pi}$ in (3.16), we have

$$V_{LS(max)} = \frac{\pi I_O}{2}\omega_n Q R_O$$

Normalized maximum voltage stress across L_S is

$$\frac{V_{LS(max)}}{V_O} = \frac{\pi}{2}\omega_n Q \qquad (3.17)$$

Where $V_O = I_O R_O$

(d) Peak voltage stress on C_S

Maximum voltage stresses across C_S is

$$V_{CS(max)} = I_m \frac{1}{\omega_S C_S} = I_m \frac{1}{\omega_n \omega_O C_S} = I_m Q \frac{R_O}{\omega_n} = \frac{\pi I_O}{2} Q \frac{R_O}{\omega_n}$$

Normalized maximum voltage stress across C_S is

$$\frac{V_{CS(max)}}{V_O} = \frac{\pi}{2} \frac{Q}{\omega_n} \qquad (3.18)$$

Figs. 3.9 and 3.10 show the variation of maximum voltage stresses across L_S and C_S with normalized frequency. For a particular value of Q, the voltage stress is directly proportional to the switching frequency for the inductor and inversely proportional to the switching frequency for the capacitor. For a given switching frequency, the voltage stress increases with an increase in Q for both inductor and capacitor.

3.3 PRINCIPLE OF OPERATION

3 3 1 Buck Converter

The buck converter can be thought of as a voltage controlled power voltage source. The output voltage is proportional to the control voltage. The control voltage adjusts the duty ratio of the buck converter. The maximum duty ratio is unity. Comparing the control voltage with a fixed frequency triangular wave derives the gate pulse to the switch of the buck converter as shown in Fig. 3.11. In a complete switching cycle, the switch is on for a duration T_{ON} and rest of the time it is off. This strategy produces a chopped voltage waveform V_X as shown in Fig. 3.11. This voltage is passed through an LC filter to reduce the ripple and is applied to the load which is the second stage. When the switch is turned off, the inductor current freewheels through the diode D_1.

3.3.2 *Series Resonant Converter*

Referring to Fig. 3.4, in a complete switching cycle, switches S_{11}, S_{22} and S_{12}, S_{21} conduct during alternate half cycles. The gate pulses to inverter switches are shown in Fig. 3.12. The inverter produces a square wave ac voltage of amplitude equal to the dc voltage at the inverter input. This voltage is applied to the input of a frequency selective resonant tank circuit The square wave inverter is operated exactly at the resonant frequency The impedance offered by the tank to higher order harmonics is very high. Therefore, the current response is close to sinusoidal and is in phase with the input voltage to the resonant tank. All the inverter switches turn on and turn off at zero current and finite voltage. The inherent anti-parallel diode across each inverter switch does not conduct any current. The input dc source current is shown in Fig. 3 12. There is no regenerative or freewheeling interval. Output of the resonant tank is connected to a diode bridge rectifier through a high voltage transformer. The output voltage of the diode bridge rectifier is applied to the load through a capacitive filter. The filter capacitor at the diode bridge rectifier output maintains a constant dc voltage V_O across the load. At the input of the diode bridge rectifier, the output voltage is reflected as a square wave of amplitude V_O. Both sides of the resonant tank, there are square wave voltage excitations. The circuit is tuned exactly at the resonant frequency. Most of the energy from the input source is transferred to the load by fundamental frequency. The resonant tank circuit acts as a short circuit for the fundamental frequency while it offers high impedance to other harmonics.

3.4 CLOSED-LOOP CONTROL

The high voltage two-stage dc-dc converter should be able to keep its dc output voltage constant at the reference value, for all possible load variation and input voltage variation. There are two-control techniques introduced to keep the output voltage constant

(a) Duty ratio control of the low frequency buck converter for input voltage variation,

(b) FM (Frequency Modulation) control of the high frequency inverter to ensure zero current turn-on and turn-off of the inverter switches.

The block diagram of the closed-loop control of the two-stage dc-dc converter is shown in Fig 3.13. The output voltage across the load is sensed and compared with a reference voltage (proportional to the desired dc voltage across the load) in an analog comparator. The comparator output is applied to the PI controller. The output of the PI controller through the limiter is the control voltage of the buck converter, which decides the duty ratio of the switch S_1. The buck converter output voltage is applied to the input of the SRC. If the output dc voltage across the load is less than the reference value, the control voltage (PI controller output) increases, which in turn increases the duty ratio of S_1. The output voltage of the buck converter increases. As a result, the output dc voltage across the load increases. Similarly, it reduces the output voltage when it is greater than the reference voltage.

The resonant frequency of the SRC is uniquely determined by the values of resonant inductor and capacitor. It is independent of the load resistance. In practical SRC the values of the resonant elements are not constant. They vary with temperature, aging etc. The high voltage transformer has magnetizing inductance and inter-turn capacitance; the diode bridge rectifier has some junction capacitance. The actual resonant circuit is indeed a multi-element complex circuit, which makes the resonant frequency slightly dependent on the load resistance. The FM control loop adjusts the switching frequency of the high frequency inverter so as to operate the converter exactly at the resonant frequency of the complex system. This strategy ensures soft-switching under all possible load variation and parameter variation. The FM control is a Phase Locked Loop (PLL) circuit, which locks the output frequency of the VCO to the resonant frequency of the tank circuit. Whenever the input current to the resonant tank tends to lag behind the rising edge of the input voltage to the resonant tank, the input voltage to the VCO decreases and correspondingly the output frequency of the VCO, which is the switching frequency of the SRC,

decreases. The opposite happens whenever the input current has a tendency to lead the input voltage. This may happen during load variation and/or parameter variation The FM controller needs two control signals for its operation. These correspond to the input current and the voltage to the resonant tank. Although the input voltage to the resonant tank can be fabricated from the gating pulses of devices, a current sensor is required for obtaining the input current to the resonant tank.

3 5 CONCLUSION

The detailed analysis of the two-stage dc-dc converter shows that the desirable features of the SRC can be maintained with load variation coupled with output voltage control. The voltage control is made possible by the front-end buck converter and the load independent operation by the SRC. Due to hard-switching, the buck converter is operated at low frequency to reduce the switching loss. Allowing discontinuous conduction in the inductor of the buck converter, the switch can be turned on at zero current and finite voltage, minimizing the turn-on losses. The study of closed-loop block diagram reveals that the FM control always adjusts the switching frequency of the SRC to the resonant frequency of the tank. The inverter switches turn on and turn off at zero current and finite voltage resulting in minimum switching losses. The SRC can thus be operated at very high switching frequency to reduce the size of the high voltage multi-output transformer, output filter capacitor and resonant elements. The converter gain is independent of the parameter variation due to temperature, aging or replacement. No snubber circuit is required for the inverter switches.

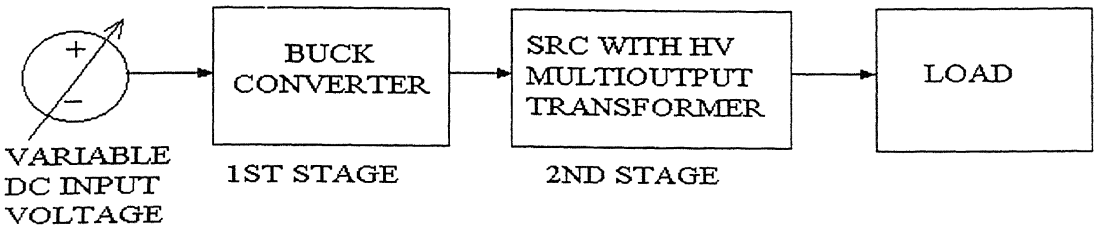

Fig. 3.1 Block diagram of proposed two-stage dc-dc converter

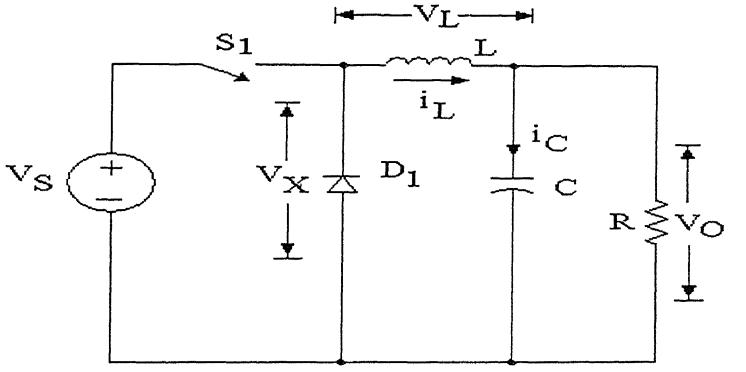

Fig. 3.2 Buck converter

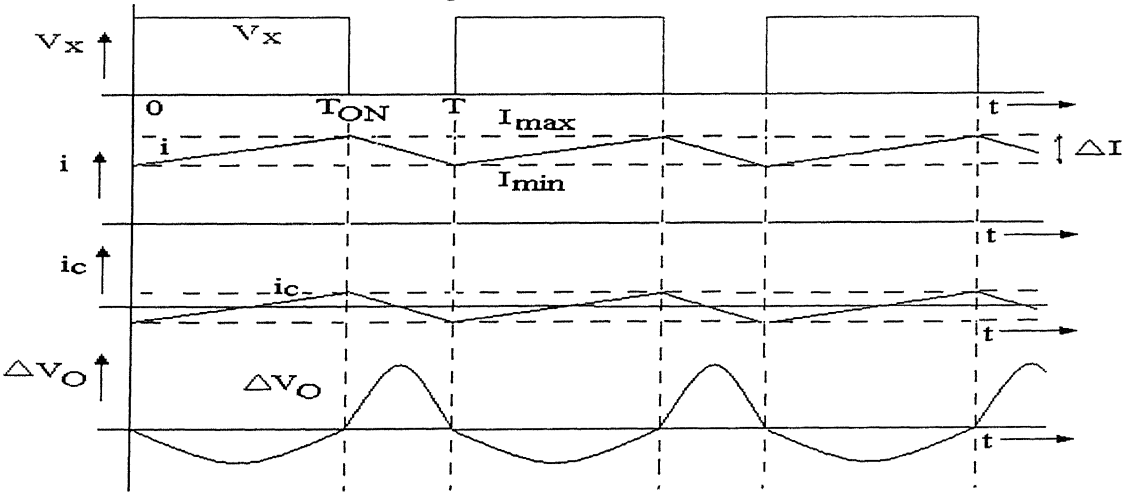

Fig. 3.3 Voltage and current waveforms of the Buck converter.

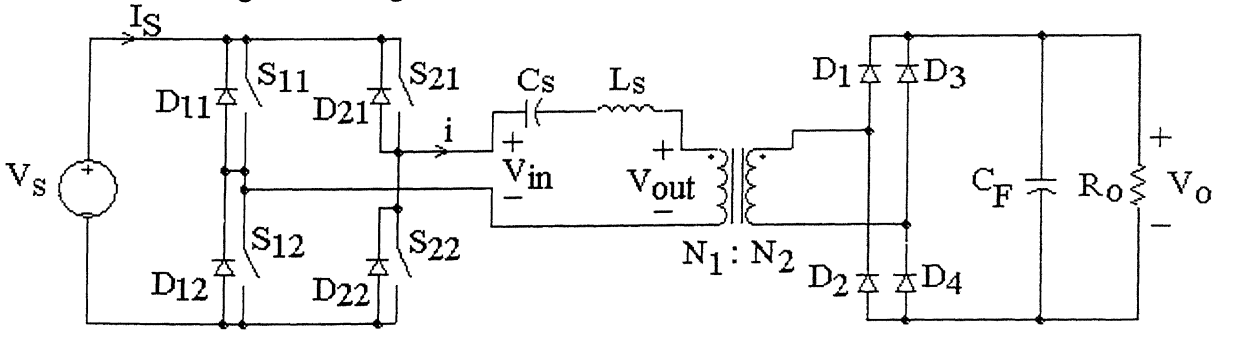

Fig. 3.4 Series Resonant Converter

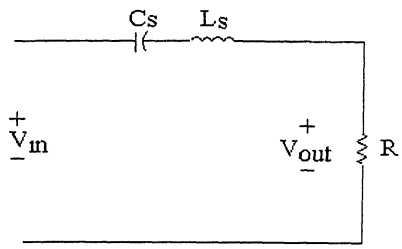

Fig. 3.5 Fundamental equivalent circuit of the resonant tank

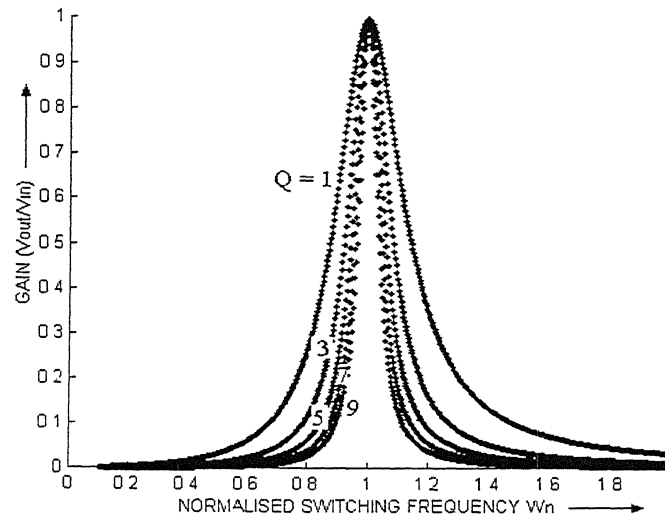

Fig. 3.6 Variation of voltage gain of the series resonant tank with normalized switching frequency

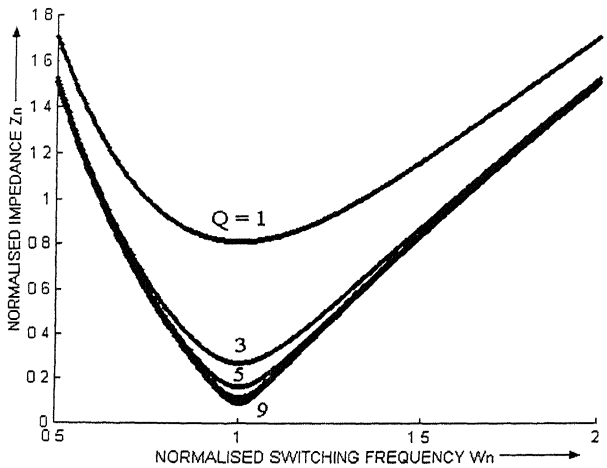

Fig. 3.7 Impedance variation with frequency for different Q

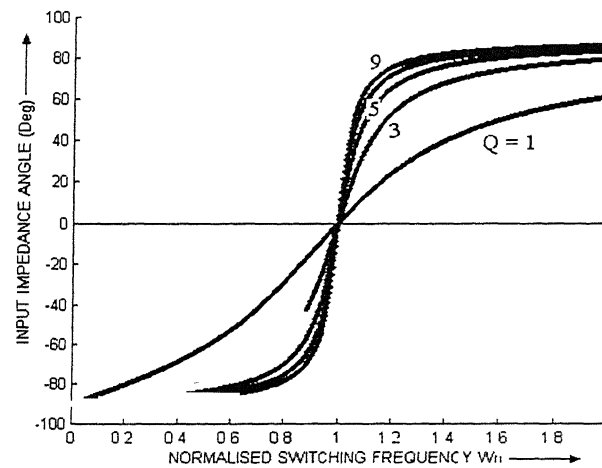

Fig. 3.8 Phase angle variation with frequency for different Q

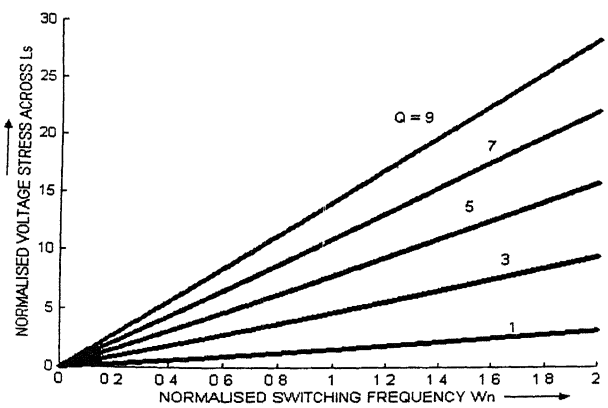

Fig. 3.9 Variation of maximum voltage stress across L_S with normalized frequency

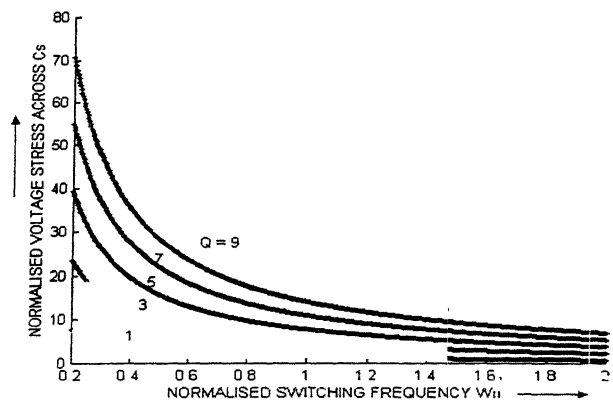

Fig. 3.10 Variation of maximum voltage across C_S with normalized frequency.

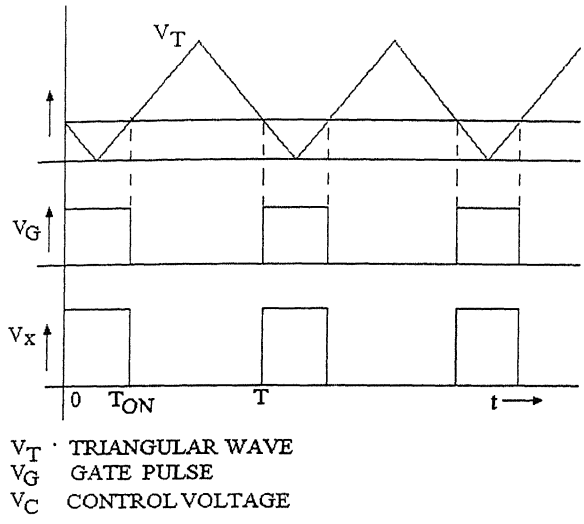

Fig. 3.11 Gate pulse generation of Buck Converter

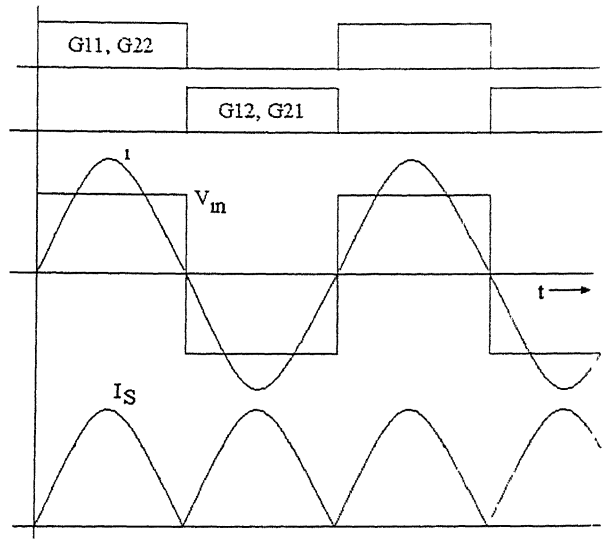

Fig. 3.12 Gate pulses of SRC

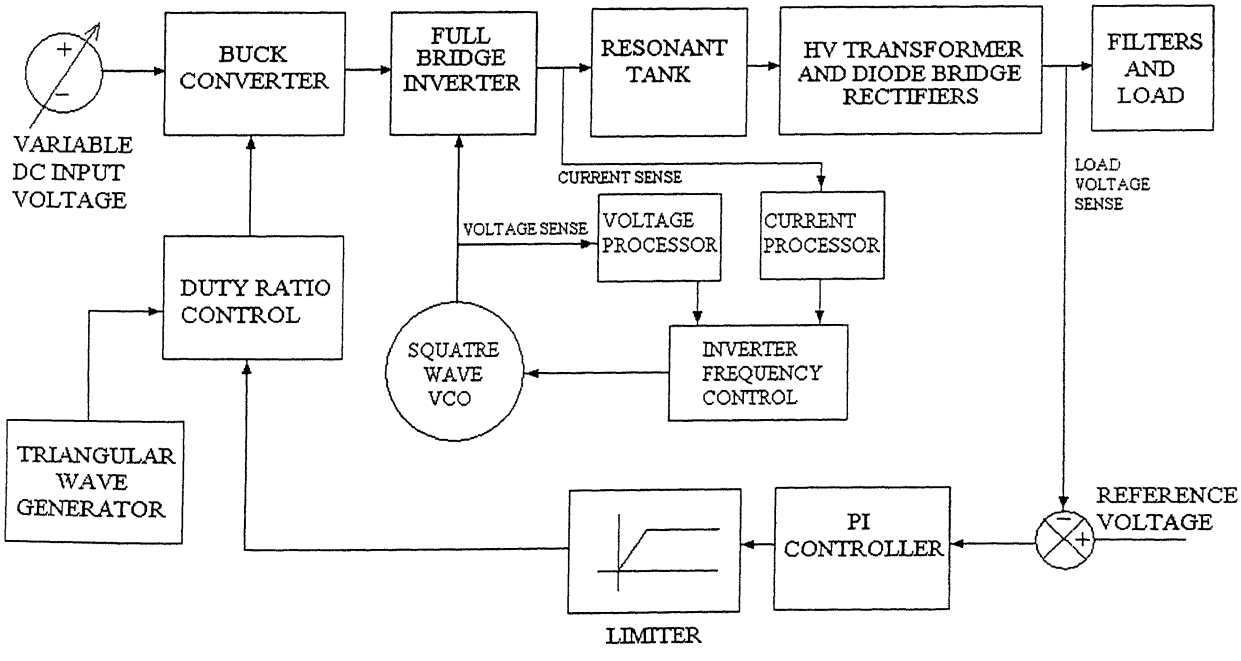

Fig. 3.13 Block diagram of closed loop Duty ratio and FM control

CHAPTER 4.

DESIGN AND SIMULATION OF TWO-STAGE DC-DC POWER CONVERTER

4.1 INTRODUCTION

The high voltage converter of the Electronic Power Conditioner (EPC) for the TWTA can be implemented either by a single stage high frequency dc-dc resonant converter or by a two-stage dc-dc converter. The power circuit of the high voltage converter with multiple secondary transformer is described in Chapter 2. Chapter 3 deals with the detailed analysis of two-stage dc-dc power converter. The first stage is a conventional single pulse width modulated (PWM) buck converter, which is followed by the second stage, a high frequency Series Resonant Converter (SRC). The present chapter considers the two-stage dc-dc converter with a single secondary high voltage transformer for detailed design and simulation. The maximum output power remains same as the actual converter with multiple output stages. The dc output voltage of the converter is taken 6300 V, which is the voltage between Anode-1 and Cathode of the multi-output topology.

4.2 SPECIFICATIONS OF TWO-STAGE POWER CONVERTER

The high voltage two-stage dc-dc converter is designed with following specification.

- Input dc supply: 26 V- 43 V.
- Maximum dc output voltage: 6300 V.
- Maximum output power: 270 W.
- Minimum output power: 27 W (10% full load).

4.3 DESIGN OF THE BUCK CONVERTER

The minimum input voltage to the buck converter is taken as 22 V to take into account the various inherent voltage drops across various parts of the actual two-stage power converter. The design is such that, at minimum input voltage the duty ratio of the buck converter is unity, and the switch S_1 of the converter is on. The output voltage is the same as the input voltage With the change in input voltage from its minimum value, the duty ratio is adjusted in a way to keep the output voltage of the converter to its original minimum value. When the input voltage varies with in the range 22 V - 43 V, the output voltage is held constant at 22 V.

The minimum duty ratio $D_{min} = \frac{22}{43} = 0.512 \approx 0.5$

The converter is designed in such a way that at maximum output power and maximum input voltage the current through the inductor is just continuous.

From (3.6) in chapter 3, the value of the inductor is

$$L = \frac{(1 - D_{min})R_{L(min)}}{2f}$$

$$= \frac{(1-0.5)\times 1.75}{2\times 10\times 10^3} = 43.75\,\mu H \approx 44\,\mu H$$

From the practical considerations, a value of 50 μH is taken.

From (3.9), the value of the capacitor is given

$$C = \frac{(1 - D_{min})}{8Lf^2\ \Delta V_O} V_O$$

f = switching frequency of the buck converter = 10 kHz.

ΔV_O = Permissible voltage ripple at the output voltage of the buck converter = 0.85 V.

$$C = \frac{(1-0.5)\times 22}{8\times 50\times 10^{-6}\times (10\times 10^3)^2\times 0.85} = 322.82\times 10^{-6}\,F \approx 323\mu F\ .$$

From the practical considerations, a value of 330 μF is taken.

4.4 DESIGN OF THE SERIES RESONANT CONVERTER

Whenever the input voltage to the buck converter changes between 22 V – 43 V, it maintains a constant voltage of 22 V at the input of the SRC. The output dc voltage across the load is 6300V. Referring to Fig. 3.6, the voltage gain M of the SRC at load independent point $\omega_n = 1$, is unity.

$M = 1,$

$\omega_n = 1,$

Taking Q =4,

$\omega_o = \frac{1}{\sqrt{L_S C_S}}$ = resonant angular frequency of the tank,

$= 2\pi f_o$ rad/sec

f_O = Resonant frequency = 110 kHz

$$Z_o = \sqrt{\frac{L_S}{C_S}} = QR_O$$

To determine values of L_S and C_S, 1:1 transformer is considered.

Input voltage to the SRC is V_S = 22 V.

Amplitude of the fundamental component of input voltage to the resonant tank input

$$V_{in(max)} = \frac{4V_s}{\pi} = 28\ V$$

Amplitude of the fundamental component of input voltage to the diode bridge rectifier with 1:1 transformer

$V_{out(max)}$ = 28 V (as M = 1)

There is voltage sink load at the output. The expression for the peak voltage at the input of the diode bridge is

$$\frac{4V_O}{\pi} = V_{out(max)}$$

$$V_O = 22 \text{ V}.$$

Load resistance corresponding to 270 W at 22 V is

$$R_O = 1.79\ \Omega.$$

$$Z_O = \sqrt{\frac{L_S}{C_S}} = QR_O \text{ characteristics impedance of the resonant tank}$$

$$= 1.79Q$$

$$L_S = \frac{Z_O}{\omega_O} = \frac{4 \times 1.79}{2 \times \pi \times 110 \times 10^3} = 10.36\ \mu\text{H} \approx 10\ \mu\text{H}.$$

$$C_S = \frac{L_S}{Z_O^{\ 2}} = 0.195\ \mu\text{F} \approx 0.2\ \mu\text{F}$$

With the values chosen, the resonant frequency is,

$$f_o = \frac{1}{2\pi\sqrt{L_S C_S}} = 112.54\ \text{kHz}.$$

In the simulation study an ideal transformer is considered. The amplitude of the fundamental component of the voltage appeared across the primary of the 1:1 transformer is 28 V (calculated above).

The desired output dc voltage is 6300 V.

The amplitude of the fundamental component of the voltage across the input of the diode bridge

$$\text{rectifier} = \frac{4 \times 6300}{\pi} = 8021.4 \text{ V}$$

$$\text{The required turns ratio} = \frac{8021.4}{28} = 286.48$$

In the simulation, we have taken a turns ratio of 300, as the actual voltage available across the primary of the transformer is less than 28V due to turn-on and turn-off delay, conduction drop etc.

4.5 SABER SIMULATION

Fig. 4.1 shows the complete power circuit topology of the two-stage dc-dc power converter for simulation study in SABER simulator. As shown in Fig. 3.13, the simulation is carried out with closed-loop voltage control (duty ratio control) and frequency control.

The converter is simulated with the following data, which are fed to the SABER simulator.

4 5 1 Buck Converter (first stage)

Switching frequency: 10 kHz

Inductor: L = 50 μH

Initial current = 1 A.

Capacitor: C = 330 μF

Initial voltage = 20 V

Switch S_1: $V_{DS(max)}$ = 100 V

$I_{DS(cont)}$ = 33 A.

Turn-on time = 130 ns

Turn-off time = 150 ns

$R_{ds(on)}$ = 0.050 Ω

Diode D_B: $I_{forward}$ = 33 A

Conduction drop V_{on} = 1 V

Drain to source breakdown voltage =100 V.

4 5 2 Series resonant converter (second stage)

Switching frequency: 112.5 kHz

Inverter switches : $V_{DS(max)}$ = 100 V

S_{11}, S_{12}, S_{21}, S_{22} $I_{DS(cont)}$ = 33 A.

Turn on time = 130 ns

Turn off time = 150 ns

$R_{ds(on)}$ = 0.050 Ω

Resonant inductor : L_S = 10 μH

Initial current = 0 A

Resonant capacitor: C_S = 0.2 μF

Initial voltage = -150 V

High voltage transformer : N_1 = 10, N_2 = 3000

Diodes D_1,D_2,D_3,D_4: $I_{forward}$ = 33 A.

V_{on} = 1 V.

Breakdown voltage = 100 V.

Output filter Capacitor: C_F = 0.022 μF

Initial voltage = 6000 V

The simulation is carried out for the following boundary cases.

Reference output voltage 6300 V

(1) Input dc voltage 22 V

output Load (a)100 % full load

(b) 10 % full load.

(2) Input dc voltage 43 V

output Load (a)100 % full load

(b) 10 % full load.

4 5 3 Initial conditions

The simulation of the complete converter can be started with or without initial conditions of current for inductors and initial conditions of voltage for capacitors. However, with zero initial

conditions the start-up transients are very much severe and the circuit will take long time to settle down to the steady state Further at a switching frequency of 112.5 kHz, the memory requirement in carrying out the simulation would be very high. Hence, the simulation is carried out with certain initial conditions. Those are given above along with the parameter values of inductors and capacitors.

4 5.4 Simulation run time

The simulation study is carried out for a long period of 70 ms and the waveforms are taken after the steady state is reached.

4 5 5 Simulation Results

CASE (1)

The input voltage is 22 V (minimum)

Output power = 270 W.

Output dc voltage across load = 6300 V.

The duty ratio of the buck converter is D = 1.

The switch S_1 is shorted.

The various waveforms are shown in Figs. 4.2 to 4.6

CASE (2)

The input voltage is 22 V (minimum)

Output power = 27 W.

Output dc voltage across load = 6300 V.

The duty ratio of the buck converter is D = 1.

The switch S_1 is shorted

The various waveforms are shown in Figs. 4.7 to 4.11

CASE (3)

The input voltage is 43 V (maximum.)

Output power = 270 W.

Output dc voltage across load = 6300 V.

The duty ratio of the buck converter is less than unity.

The various waveforms of the SRC are same as case (1)

The various waveforms of buck converter are shown in Fig. 4 12.

CASE (4)

The input voltage is 43V(maximum)

Output power = 27W.

Output dc voltage across load = 6300V.

The duty ratio of the buck converter is less than unity.

The various waveforms of the SRC are same as case (2)

The various waveforms of buck converter are shown in Fig. 4.13.

4.6 CONCLUSION

The SABER simulation results of the proposed two-stage dc-dc converter show that the duty ratio variation of the buck converter is required only to take input voltage variation into account. The operation of the SRC at the resonant frequency ensures zero current turn-on and turn-off of the inverter switches, minimizing the switching losses. The input current to the SRC is always positive. This results in minimum reactive power requirement of the SRC. As the buck converter is operated at low frequency, the switching loss in S_1 is reduced Further, the discontinuous conduction in the inductor current of the buck converter provides zero current turn-on for S_1. The turn-on switching loss in S_1 is considerably reduced. The current and voltage stresses in different components are less than for the single-stage dc-dc resonant converter discussed in chapter 2. This reduces the conduction losses in the switches, resonant elements and various parts of the power circuit.

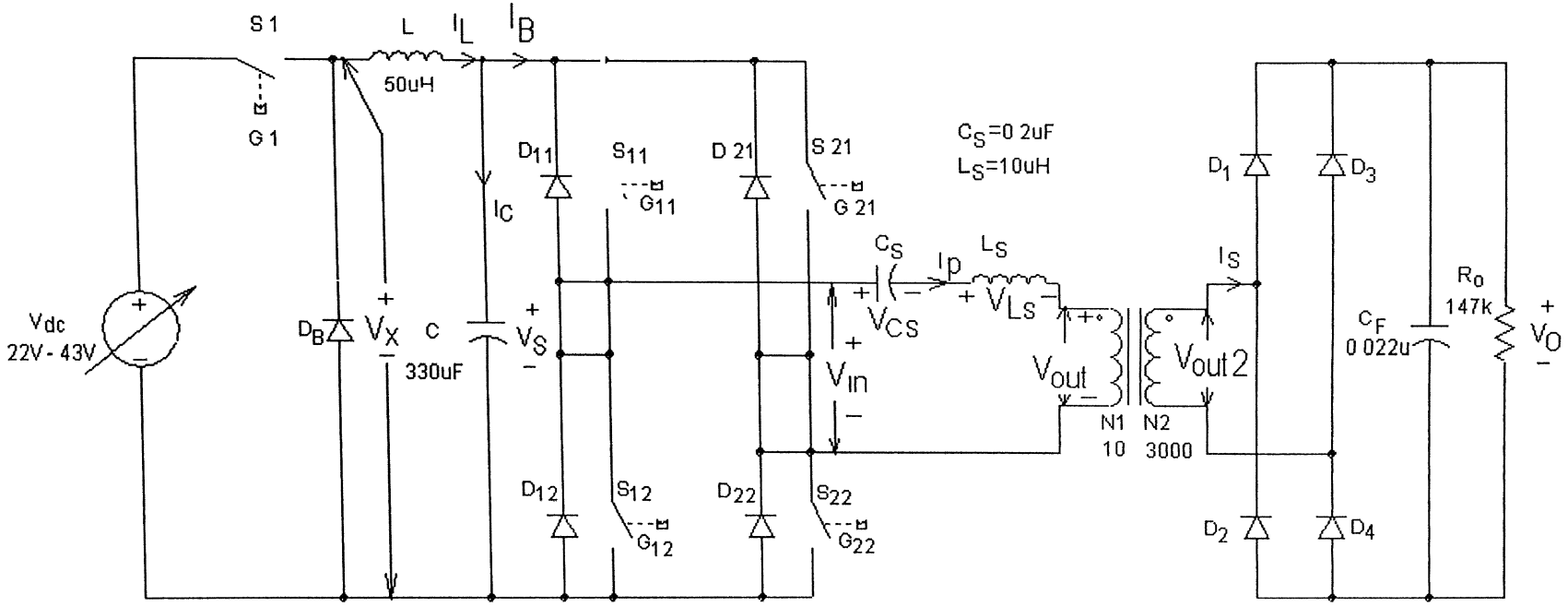

Fig 4 1 Complete power circuit topology of the proposed two stage dc-dc power converter.

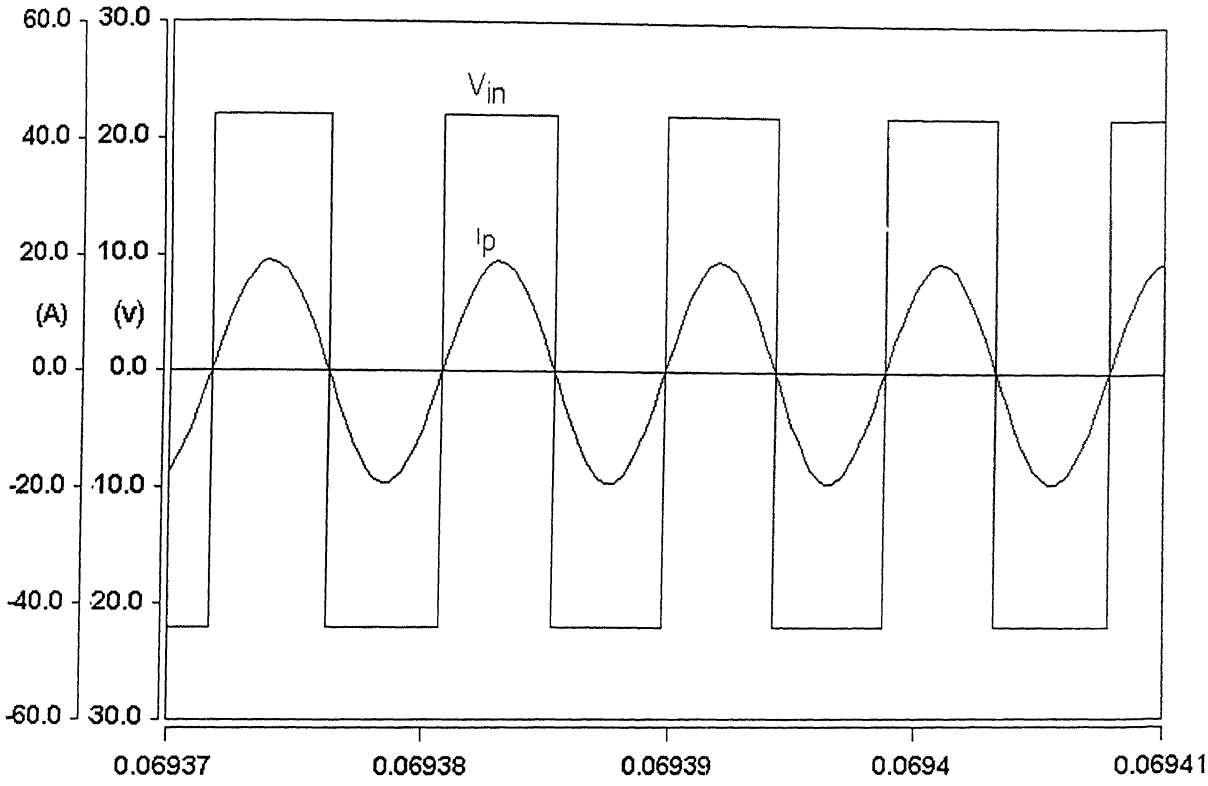

Fig. 4.2 Resonant tank input voltage and current

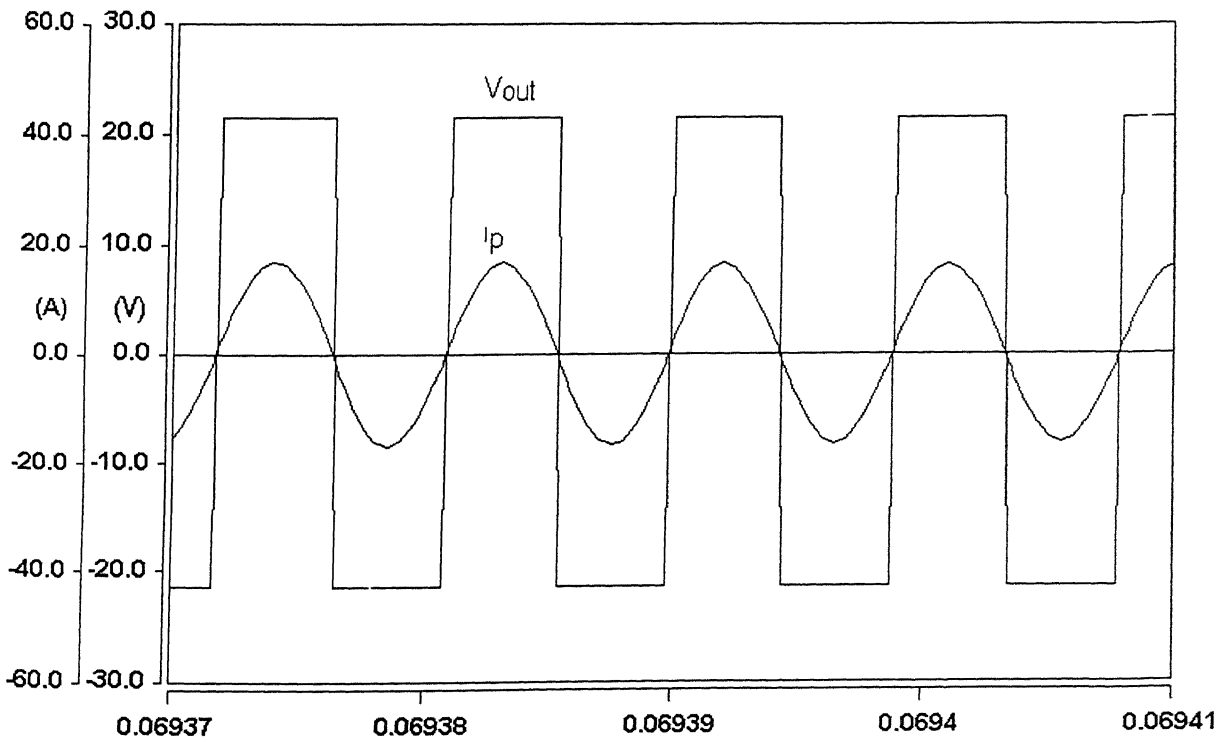

Fig. 4.3 High voltage transformer primary input voltage and current

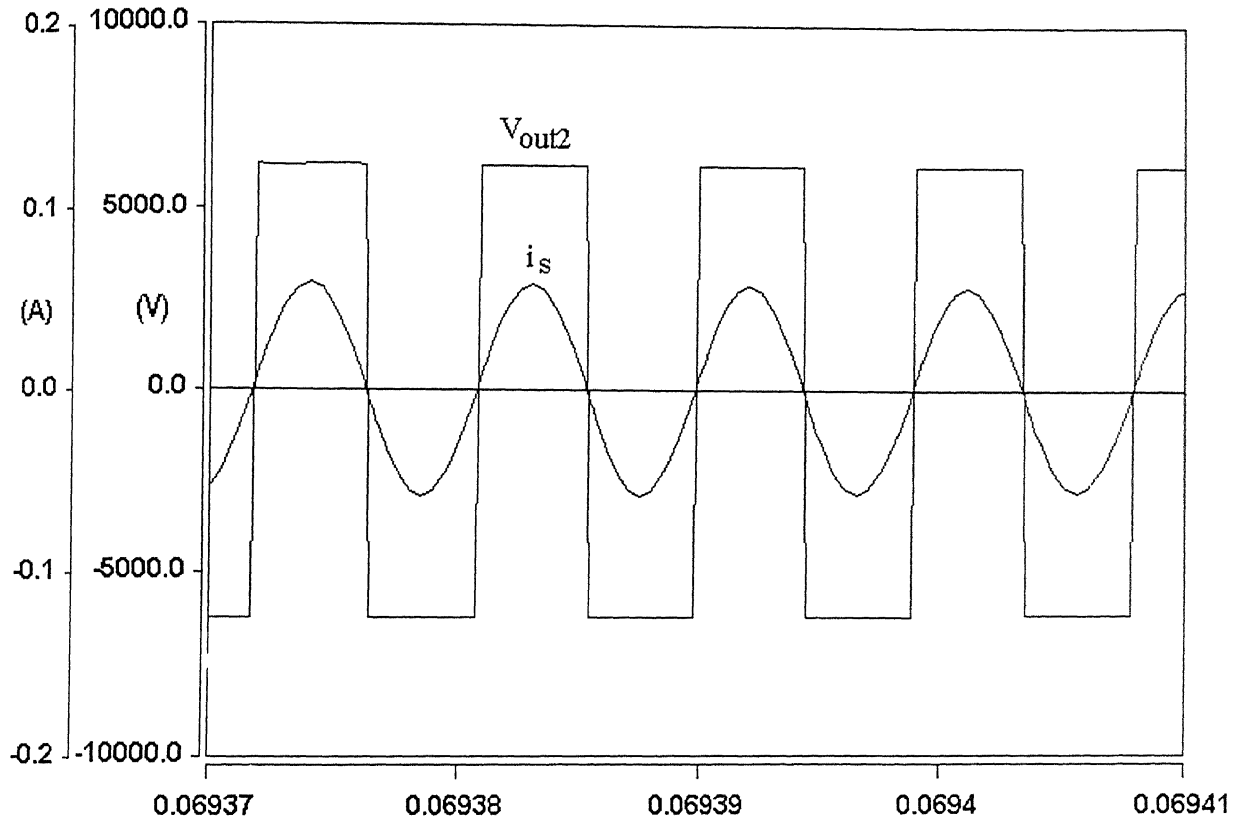

Fig. 4.4 High voltage transformer secondary output voltage and current

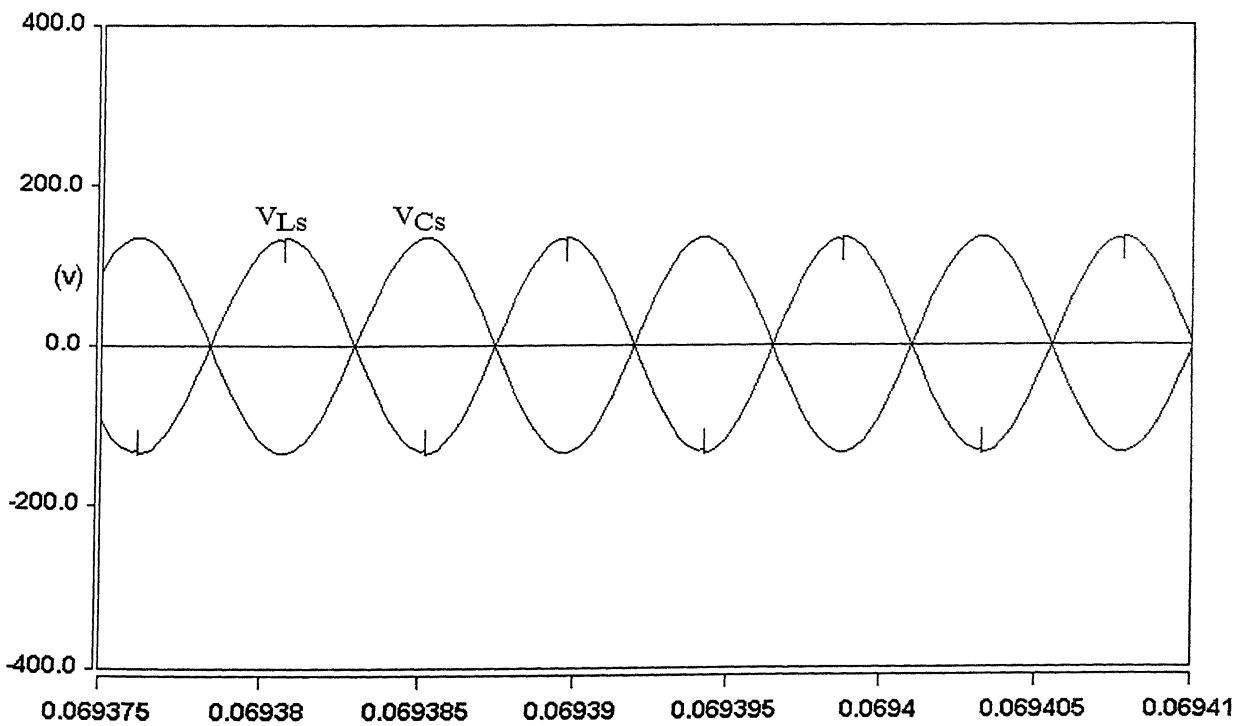

Fig. 4.5 voltage stresses on resonant elements

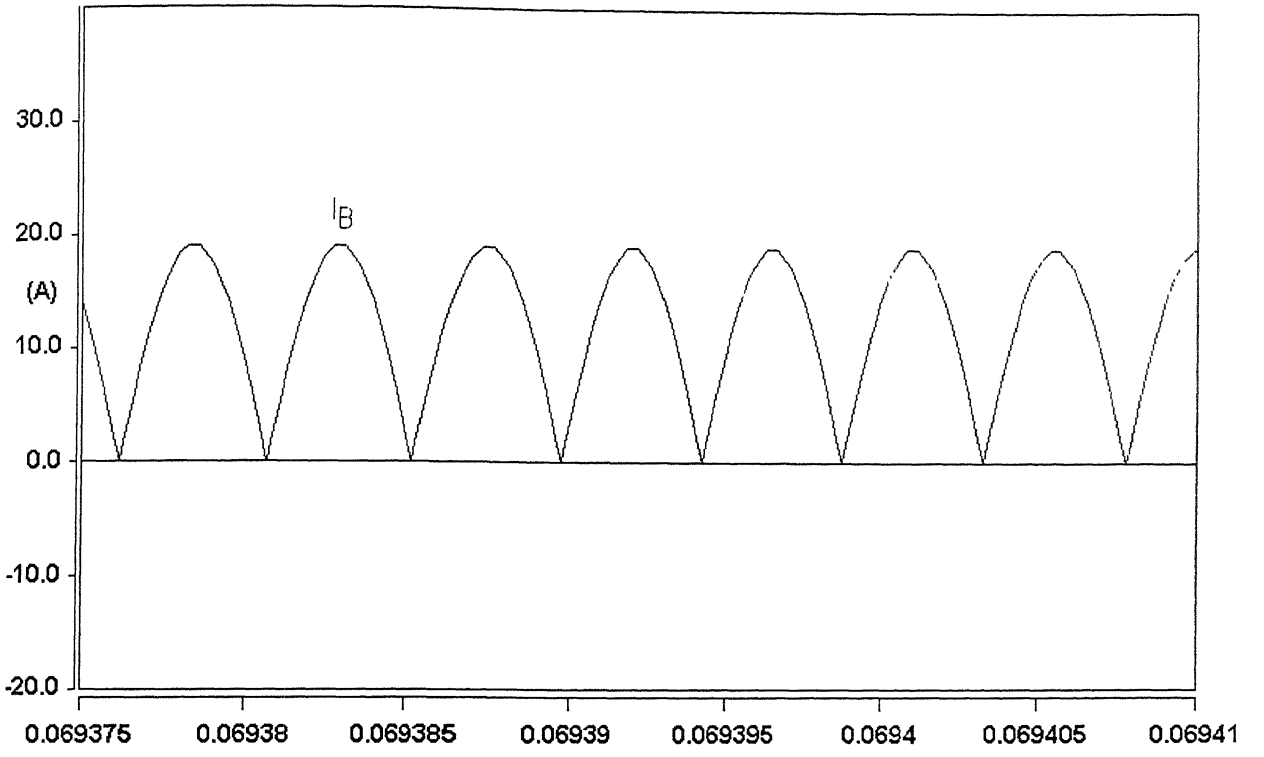

Fig. 4.6 Input current to the SRC

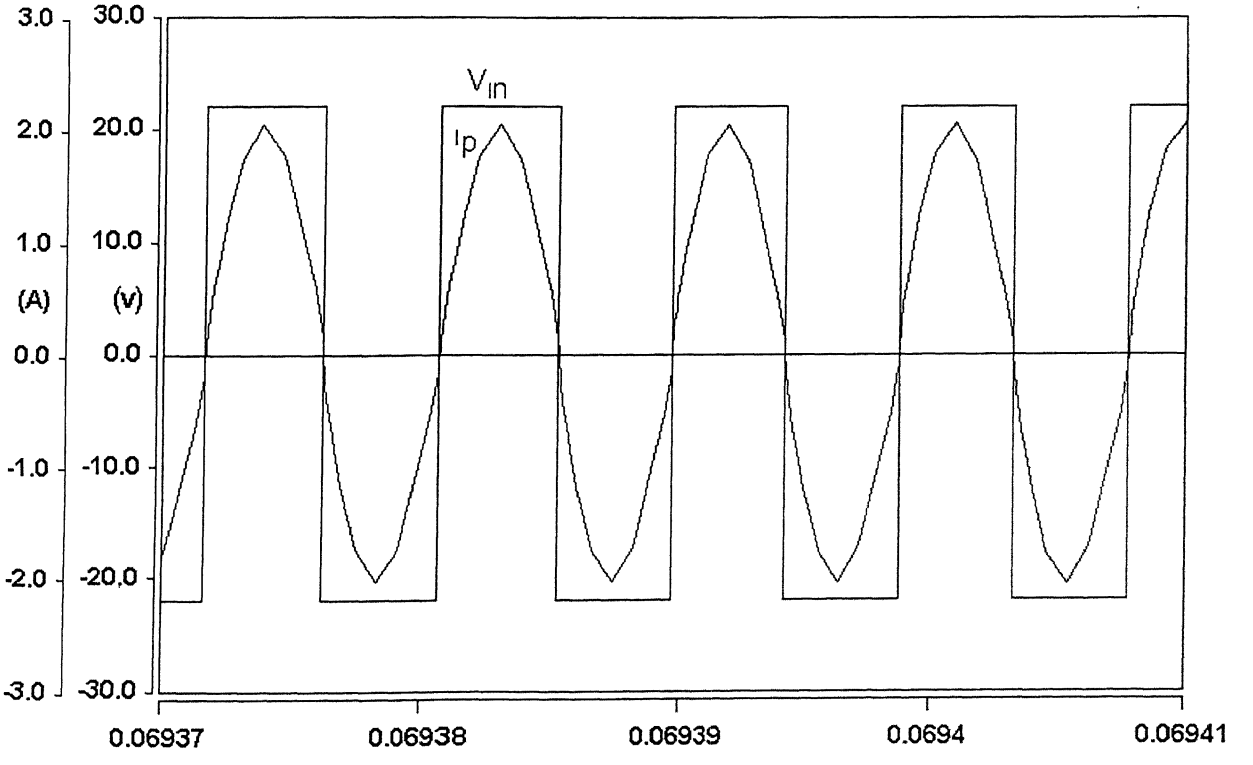

Fig. 4.7 Resonant tank input voltage and current

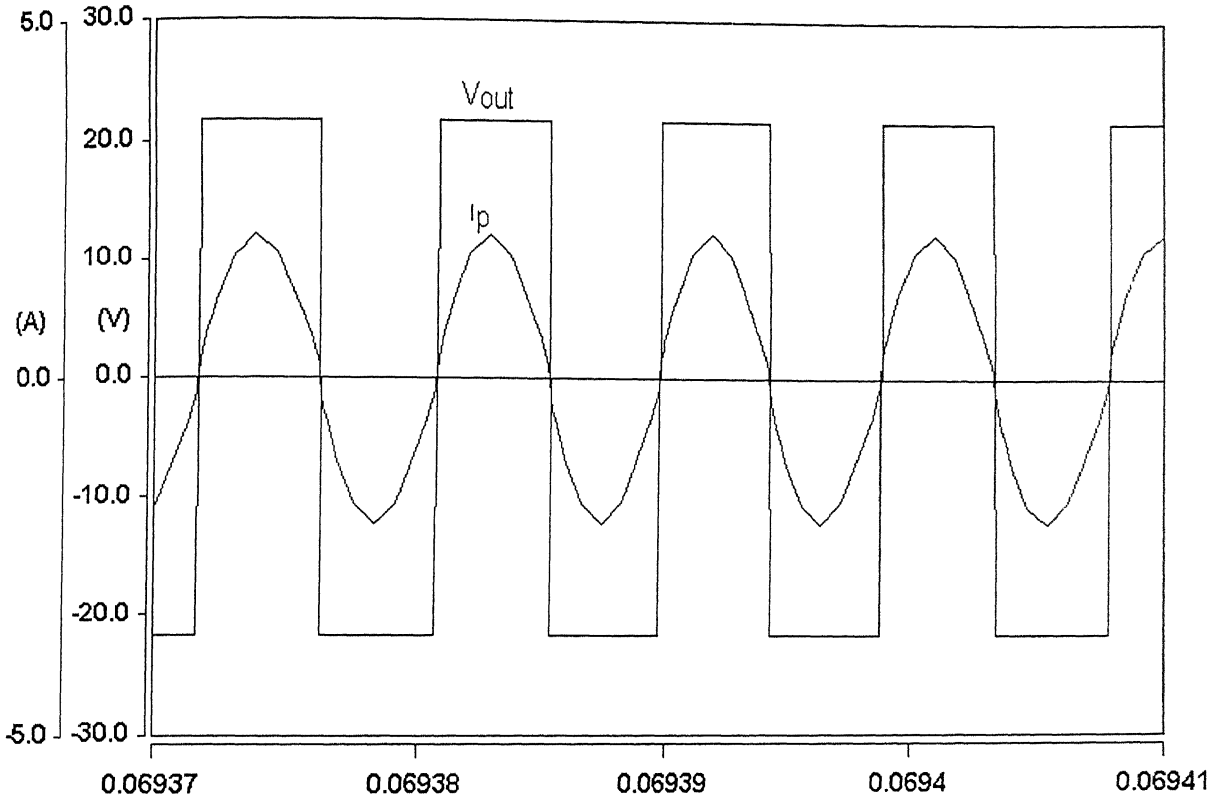

Fig. 4.8 High voltage transformer primary input voltage and current

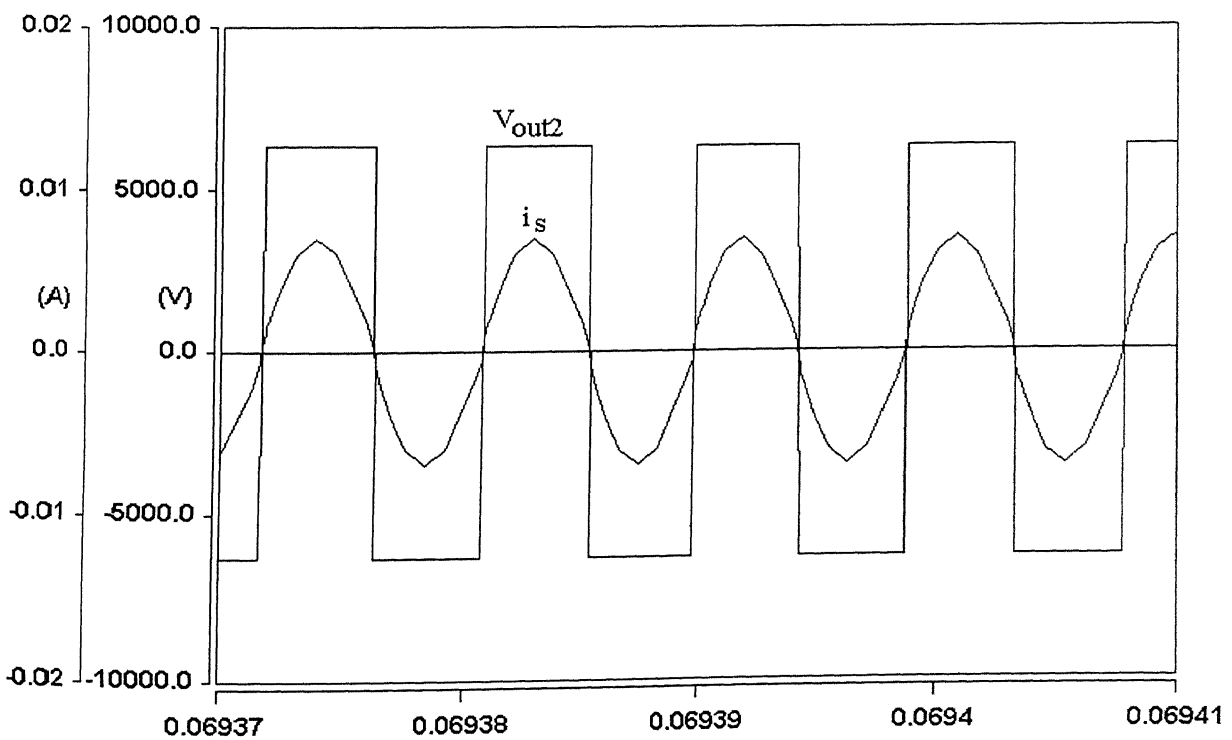

Fig. 4.9 High voltage transformer secondary output voltage and current

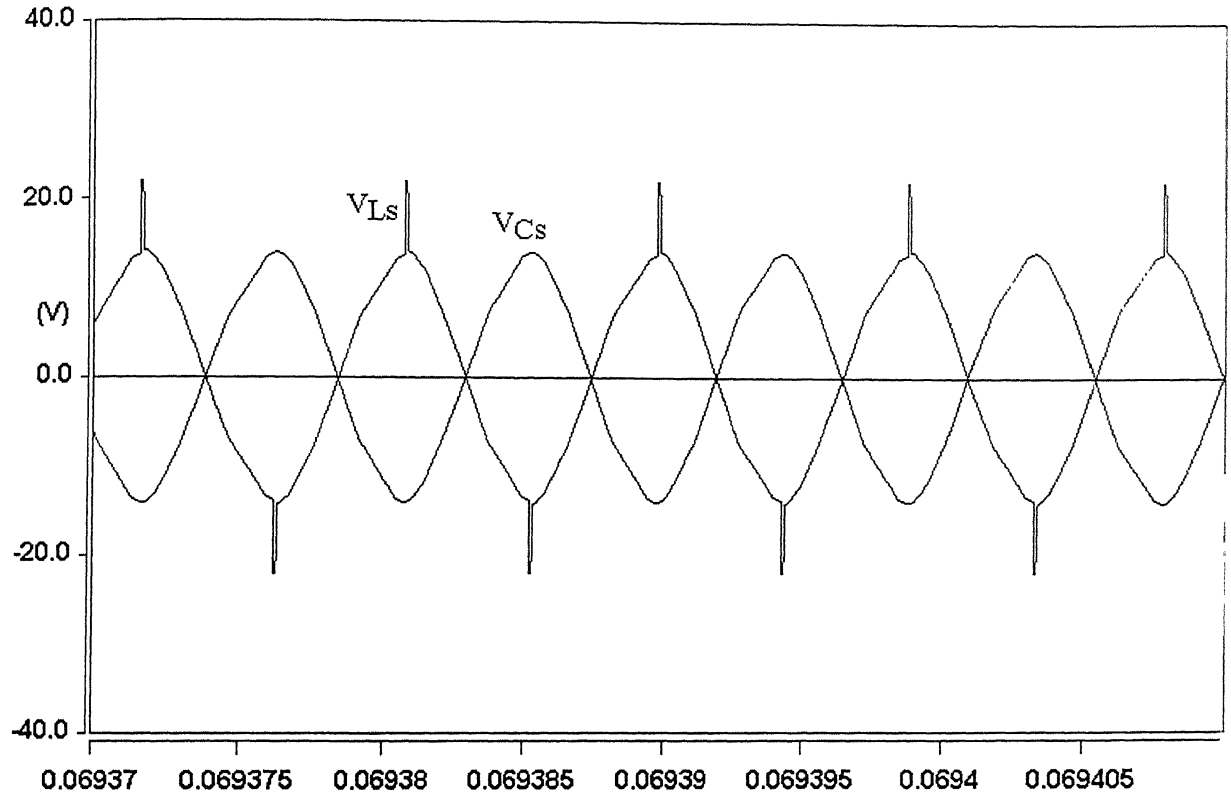

Fig. 4.10 voltage stresses on resonant elements

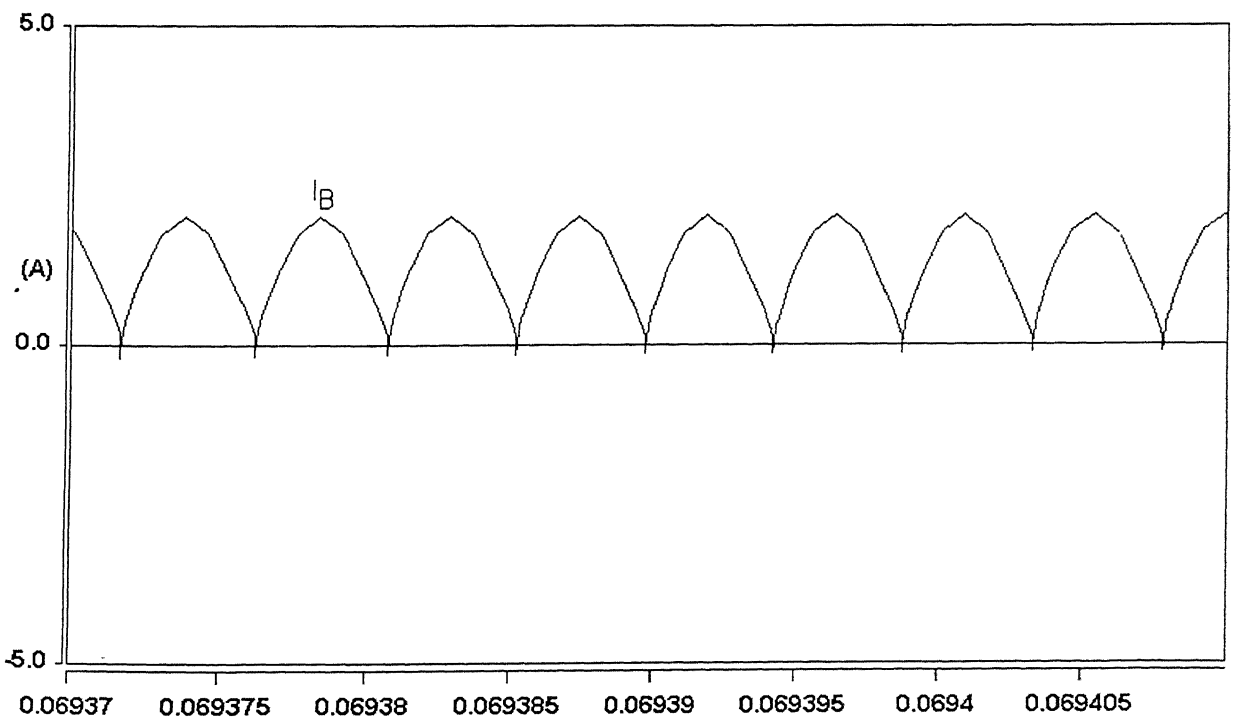

Fig. 4.11 Input current to the SRC

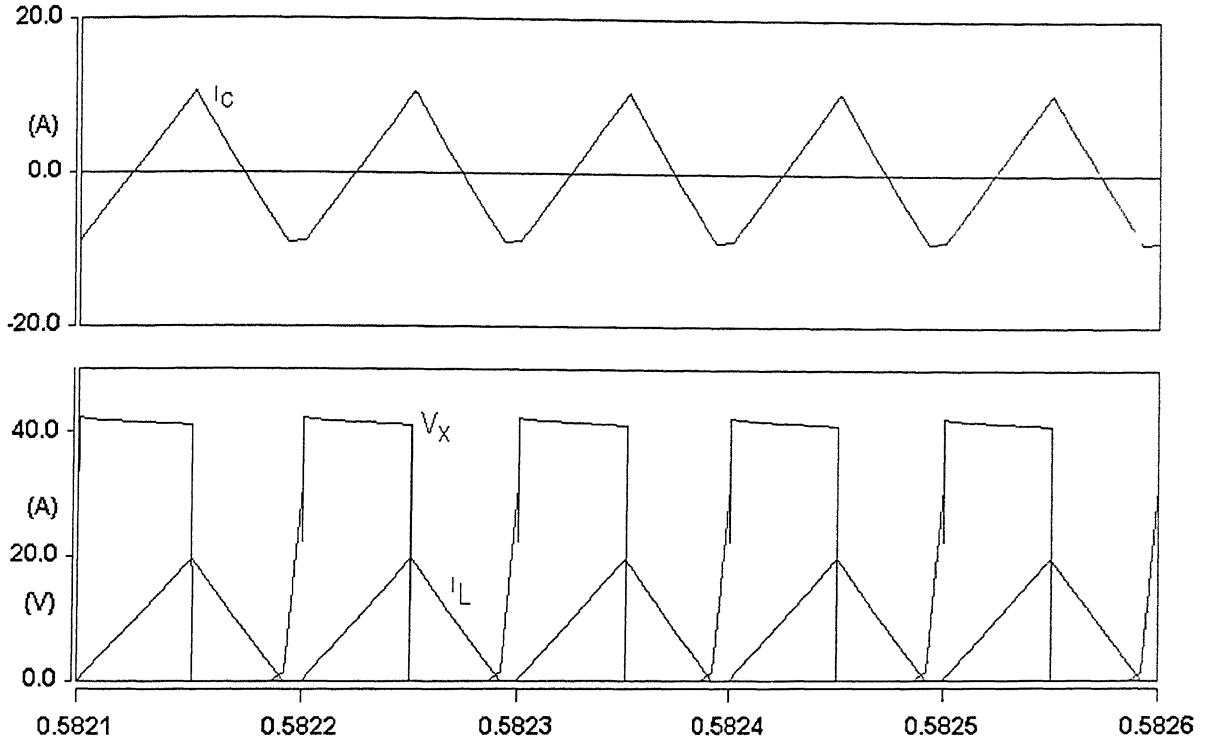

Fig. 4.12 Voltage and current through different elements of the buck converter

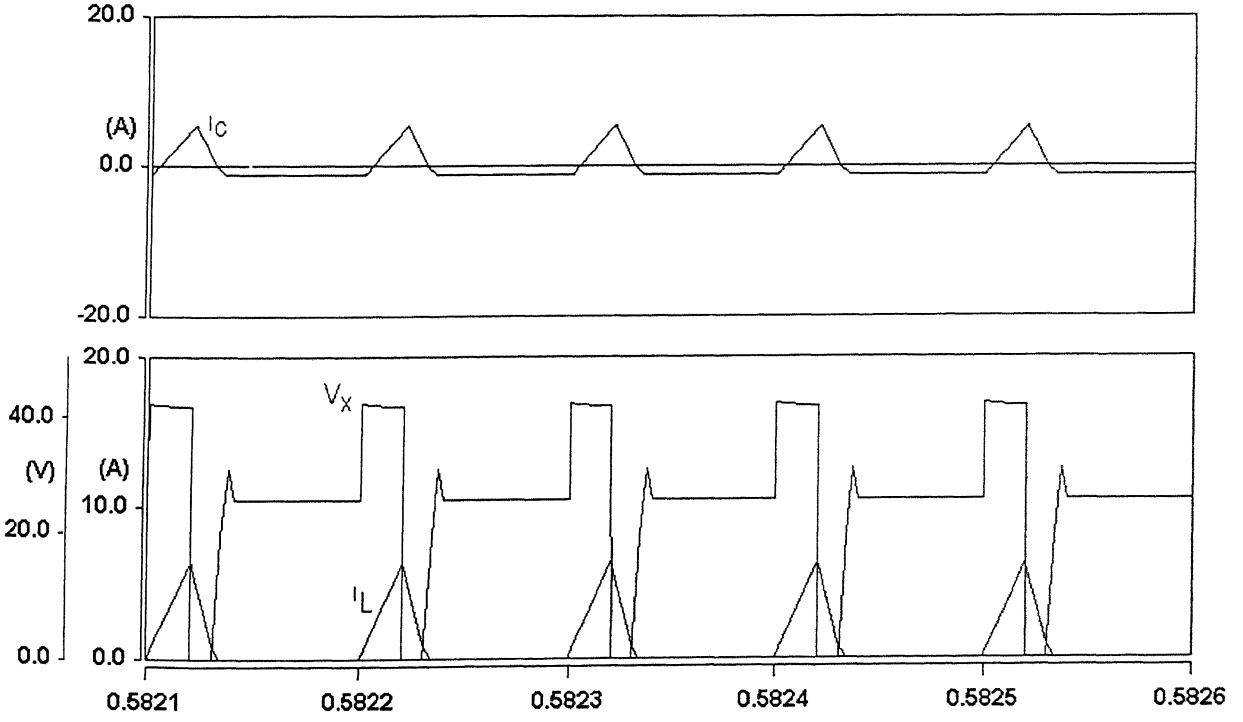

Fig. 4.13 Voltage and current through different elements of the buck converter

CHAPTER 5

IMPLEMENTATION OF TWO-STAGE DC-DC CONVERTER

5.1 INTRODUCTION

A detailed analysis, design and simulation of two-stage dc-dc converter with a single-secondary high voltage transformer according to the need of the Traveling Wave Tube Amplifier (TWTA) are presented in Chapters 3 and 4. A practical two-stage dc-dc converter topology, based on the scheme discussed in Chapter 4, is designed and implemented in this chapter. The output power of the converter is 270 W, which is the same as demanded by the TWTA. The transformer is designed and wound for a dc output voltage of 100V. With ideal transformer and ideal diode bridge rectifier, the resonant frequency of the series resonant tank circuit is independent of load variation. The practical transformer, however, has magnetizing inductance, leakage inductance, and inter-turn capacitance. The output diode bridge rectifier has junction capacitance. These are the parasitic components. The simple two-element series resonant topology is indeed a multi-element complex topology. The resonant frequency of the complex system is slightly dependent on the load resistance. These parasitics are measured with a high precision digital LCR meter The proposed converter is simulated, considering these paracitics and compared with the experimental results. The experimental results agree well with the simulated results.

5.2 SPECIFICATIONS

The converter is designed with the following specifications for practical realization.

- Input dc supply: 35 V-50 V.
- Desired dc output voltage: 100 V.

- Maximum output power: 270 W.
- Minimum output power: 27 W (10 % full load)

5.3 DESIGN MODIFICATIONS OF BUCK CONVERTER

Design of the buck converter is the same as described in Section 4.3. In both simulation and implementation, the following parameter values of different elements are considered.

$L = 50\ \mu H$

$C = 330\ \mu F$

Switching frequency = 10 kHz

5.4 DESIGN MODIFICATIONS OF SERIES RESONANT CONVERTER

The leakage inductance of the transformer is a part of the resonant inductor. Before deciding the value of the external resonant inductor of the SRC, the transformer is designed and wound. The transformer is designed with the following specification,

$$\text{Voltage ratio} = \frac{V_{pri}}{V_{sec}} = \frac{100}{30} = 3.33,$$

Where V_{pri} and V_{sec} are the primary and secondary rms voltages.

Referring to *Appendix-C*,

The number of turns of the primary, N1 = 10.

The number of turns of the secondary, N2 = 34.

The transformer leakage inductance (measured in a high precision digital LCR meter) referred to the primary side is 15.5 μH. This is more than the design requirement, as calculated in section 4.4. Thus, no external resonant inductor is required. Depending upon the availability of the high frequency polypropylene capacitor, the following modifications are made in the SRC.

The resonant elements are put in the secondary side of the high voltage transformer due to the following reasons,

- The current stresses of the resonant elements are reduced due to reduced current handled by the high voltage secondary winding.
- Magnetizing inductance of the transformer comes before the series resonant tank circuit and across the source. It has negligible effect on the voltage gain of the converter
- The use of a high-valued resonant capacitor in the low voltage side of the transformer may be avoided by an equivalent low-valued capacitor in the high voltage side.

Resonant capacitor connected in the secondary side $C_S = 0.01\ \mu F$

Leakage inductance of the transformer referred to the secondary $= 3.33^2 \times 15.5 \approx 172\ \mu H$.

Equivalent resonant inductor in the secondary side $L_S = 172\ \mu H$.

Resonant capacitor referred to primary, $C'_S = 3.33^2 \times 0.01 = 0.11\ \mu F$

Resonant inductor referred to primary, $L'_S = \frac{172}{3.33^2} = 15.5\ \mu H$.

$f_o = \frac{1}{2\pi\sqrt{L_S C_S}}$ = resonant frequency of the resonant tank,

$= 121.35$ kHz

$Z_o = \sqrt{\frac{L'_S}{C'_S}} = QR_O = 11.87$, characteristics impedance referred to primary.

The minimum input voltage to the SRC is taken as 30 V to take various inherent voltage drops within the converter into account. As discussed in section 4.4, the output dc voltage across the load of a SRC (with 1:1 transformer) is the same as the input dc voltage, if it is operated at the resonant frequency. The dc input voltage to the SRC is 30 V. Thus, the dc output voltage is 30 V. Corresponding to a power output of 270 W at 30 V, the load resistance with 1: 1 transformer is $R_O = 3.33\ \Omega$ and the quality factor is $Q = 3.56$.

5.5 SIMULATION AND EXPERIMENTAL RESULTS

The complete two-stage dc-dc converter is fabricated according to the modified design as is shown in Fig. 5.1. The effect of parasitics of the transformer and diode bridge rectifier makes the simple two element resonant tank of a practical SRC into a multi-element complex circuit. In order to verify the experimental results with simulation results, the following additional parameters are measured with a high precision digital LCR meter.

Transformer magnetizing inductance = 140 μH .

Diode bridge junction capacitance = 3 nF.

In order to take copper loss and core loss of the transformer into account, some resistance is inserted in the simulation circuit. The complete power circuit under simulation study is shown in Fig. 5.2. The proposed converter is simulated and tested with closed-loop control for the following cases.

Case 1.

Output power =100 W

Reference output voltage = 100 V

(a) Input voltage = 35 V

(b) Input voltage = 50 V

The corresponding simulation and experimental results are shown in Figs. 5.3 to 5 12.

Case 2.

Output power =75 W

Reference output voltage = 100 V

(a) Input voltage = 35 V

(b) Input voltage = 50 V

The corresponding simulation and experimental results are shown in Figs. 5.13 to 5.22

Case 3.

Output power =50 W

Reference output voltage = 100 V

(a) Input voltage = 35 V

(b) Input voltage = 50 V

The corresponding simulation and experimental results are shown in Figs. 5.23 to 5.32

Case 4.

Output power =25 W

Reference output voltage = 100 V

(a) Input voltage = 35 V

(c) Input voltage = 50 V

The corresponding simulation and experimental results are shown in Figs. 5.33 to 5.42

The range of frequency variation needed to keep the output voltage constant at 100 V is 112 kHz – 115 kHz The frequency is minimum at the maximum load and vice versa.

Current Scale

There are three Hall effect current sensors, used in the power circuit, which gives the current in terms of voltage waveform as shown in the experimental plots. In order to get the actual current, some multiplying factor is necessary. Those are given below,

Multiplying factor for i_L is 0.2

Multiplying factor for i_P is 0.13

Multiplying factor for i_S is 0.1

5 6 CONCLUSION

A practical two-stage dc-dc power converter with a single secondary transformer is designed and implemented. The resonant frequency changes over a small range with load variation. The inverter switches turn on and turn off both at zero current and finite voltage. This feature reduces the switching losses considerably and allow the inverter switches to operate at very high switching frequency. The performance of the proposed two-stage dc-dc converter is not affected by parameter variation due to temperature, aging, etc. The buck converter is operated in the discontinuous current conduction mode for higher input voltage, which ensures zero current turn on of the switch S_1. There is, however, turn-on loss for lower input voltages over a small range. The switch is turned off at finite current and voltage. The switching loss is almost constant in both continuous and discontinuous conduction modes. Since the switching frequency is only about 10 kHz, the switch S_1 is not subjected to appreciable switching loss.

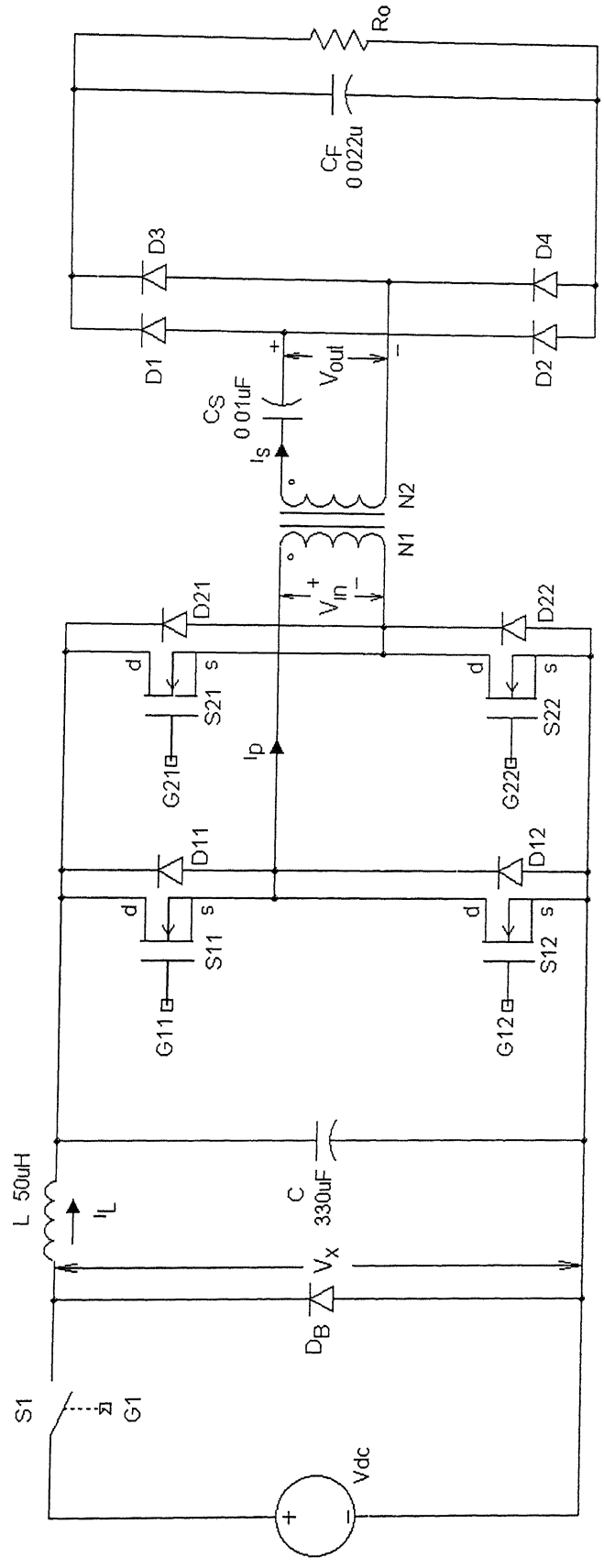

Fig.5.1 The complete power circuit of two-stage dc-dc converter for hardware implimentation.

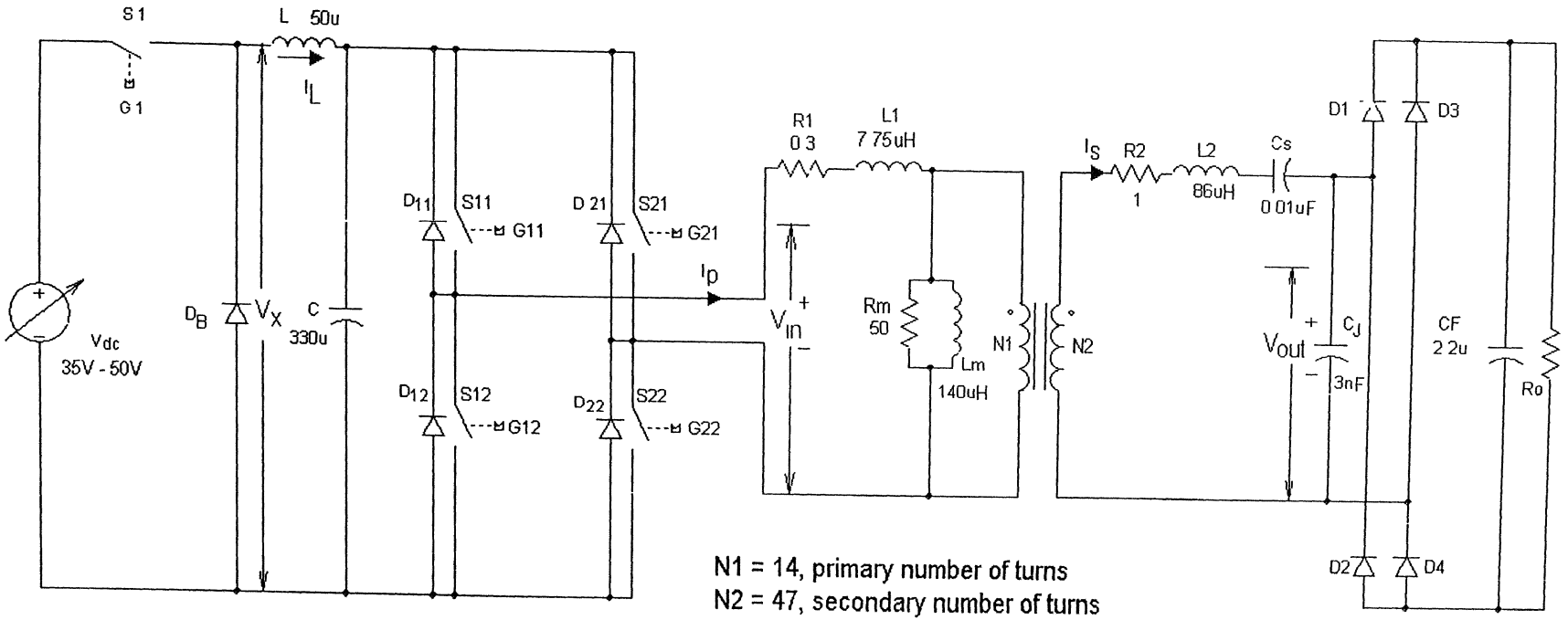

N1 = 14, primary number of turns
N2 = 47, secondary number of turns
Lm = magnetising inductance
R1 = primary winding resistance
R2 = secondary winding resistance
L1 = primary winding leakage inductance
L2 = secondary winding leakage inductance
Rm = resistance representing core loss
CJ = diode bridge junction capacitance

Fig.5.2 The complete power circuit under simulation study.

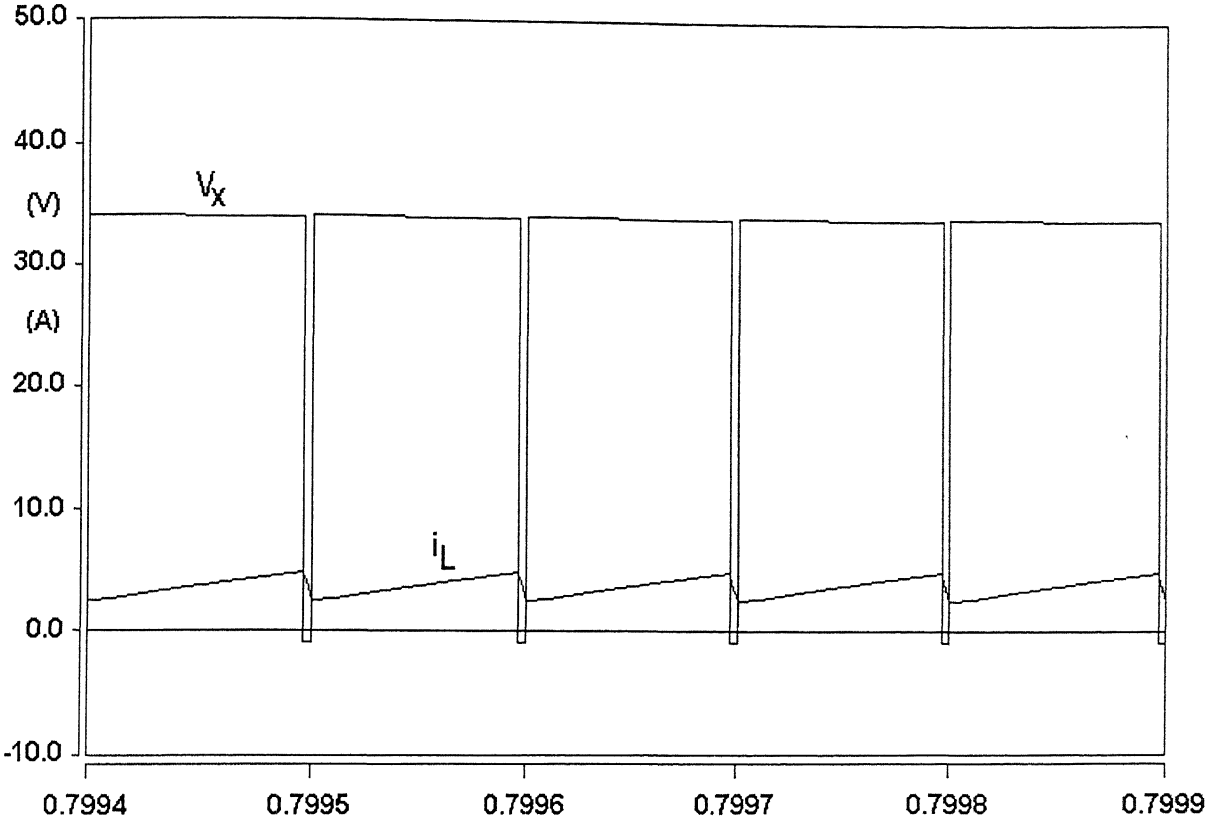

Fig. 5.3 Simulated voltage and current waveforms of the buck converter in Case1 (a).

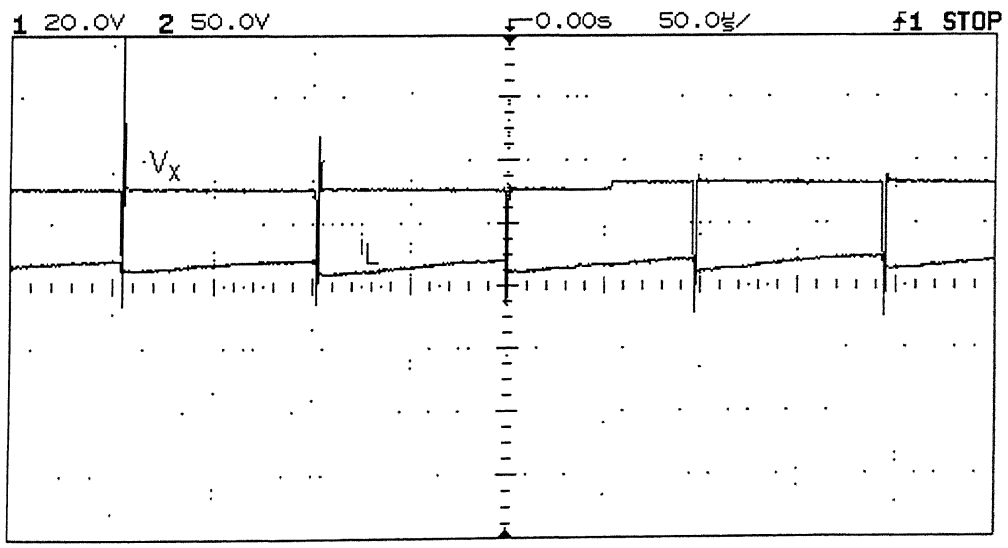

Fig. 5.4 Experimental voltage and current waveforms of the buck converter in Case1 (a).

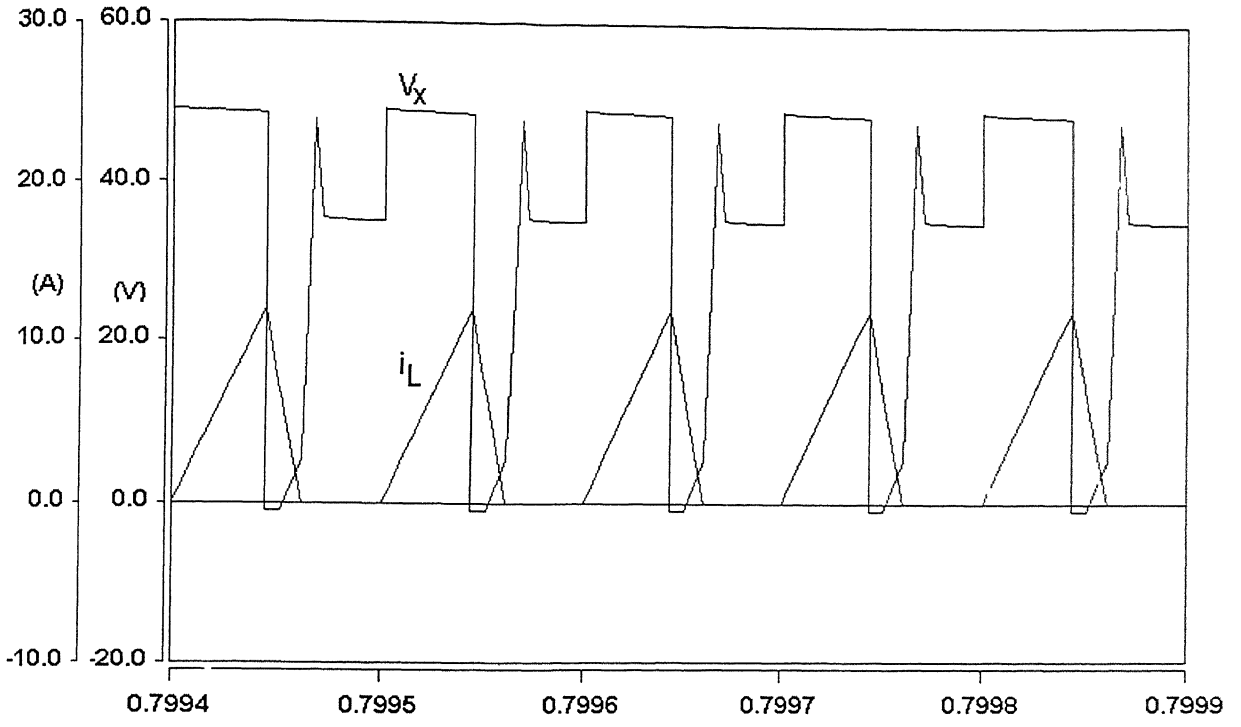

Fig. 5.5 Simulated voltage and current waveforms of the buck converter in Case1 (b).

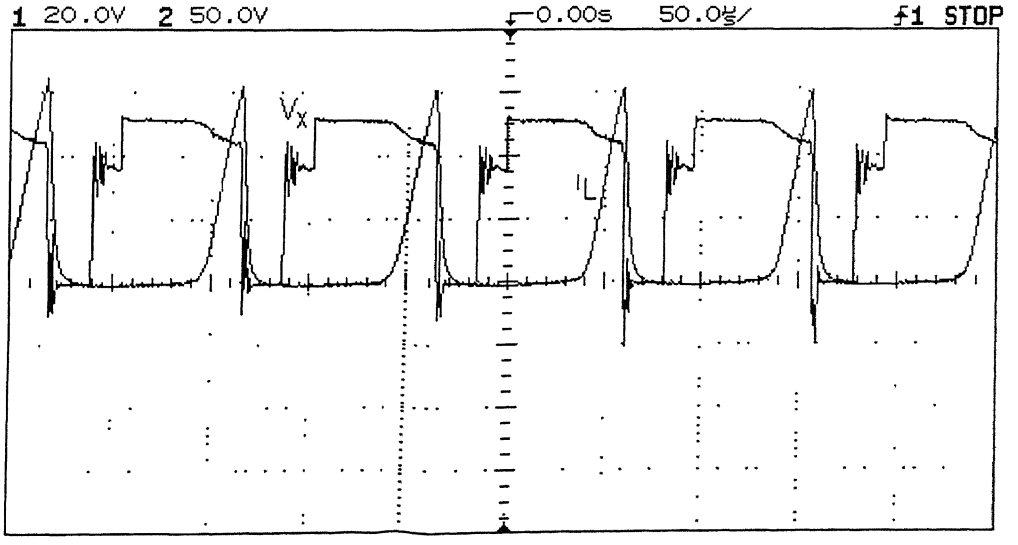

Fig. 5.6 Experimental voltage and current waveforms of the buck converter in Case1 (b).

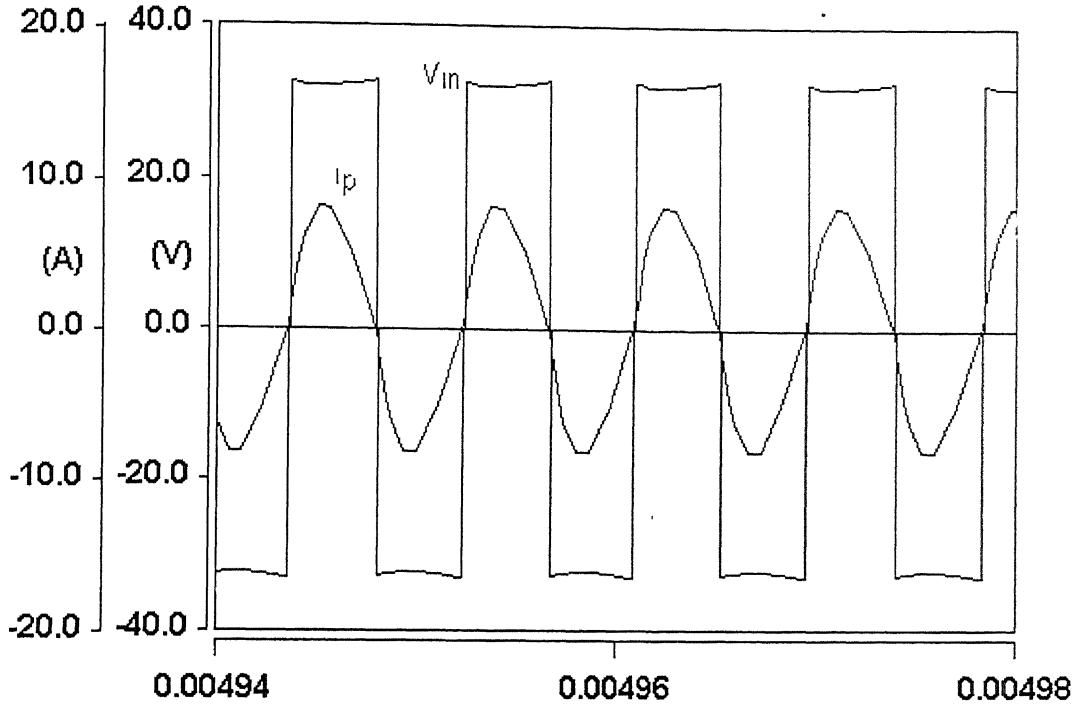

Fig. 5.7 Simulated input voltage and current waveforms to the transformer primary in case1.

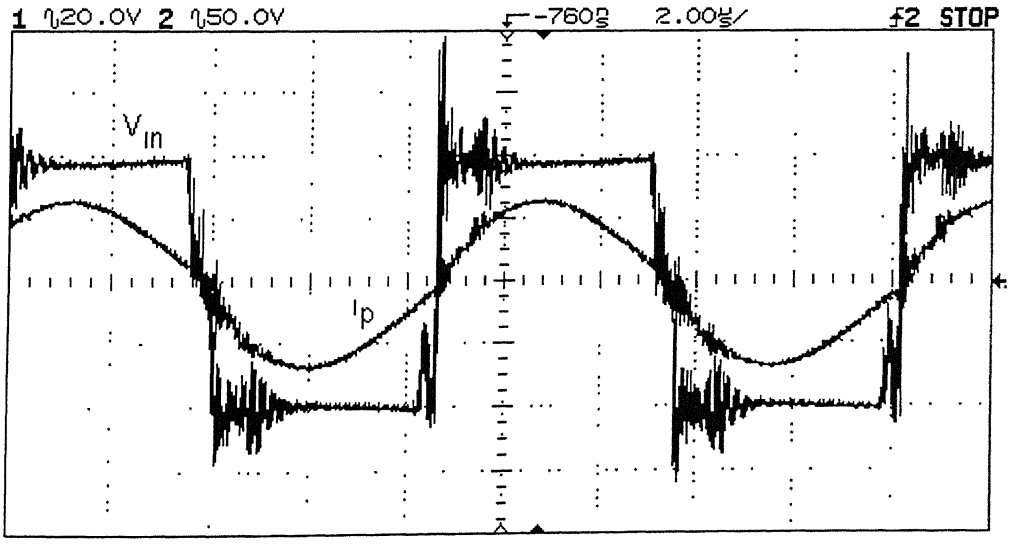

Fig. 5.8 Experimental input voltage and current waveforms to the transformer primary in case1

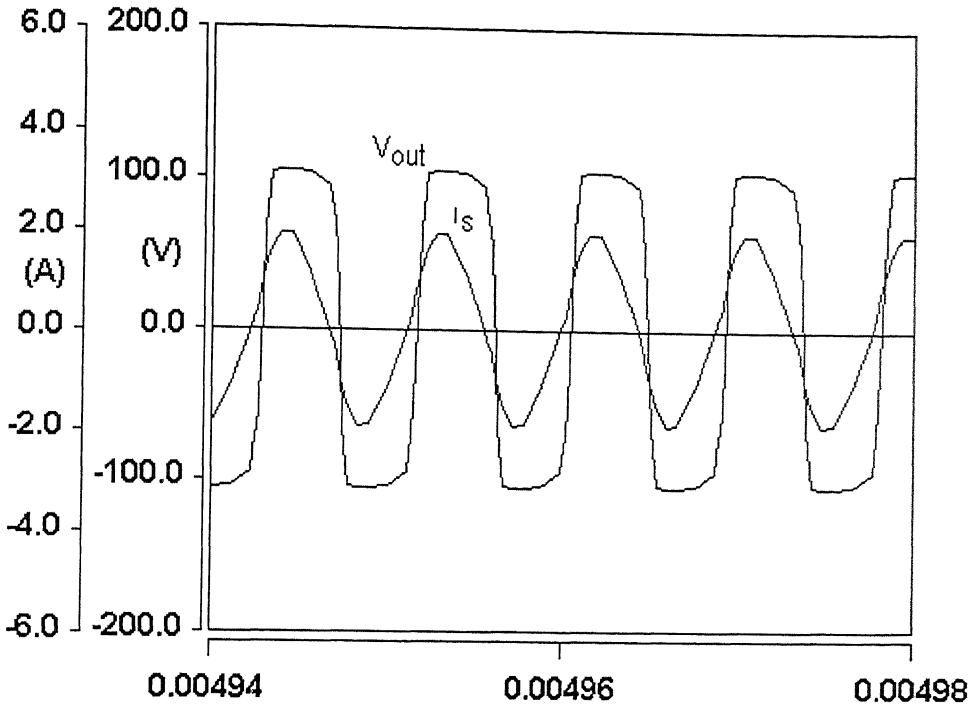

Fig. 5.9 Simulated input voltage and current waveforms to the diode bridge in case1.

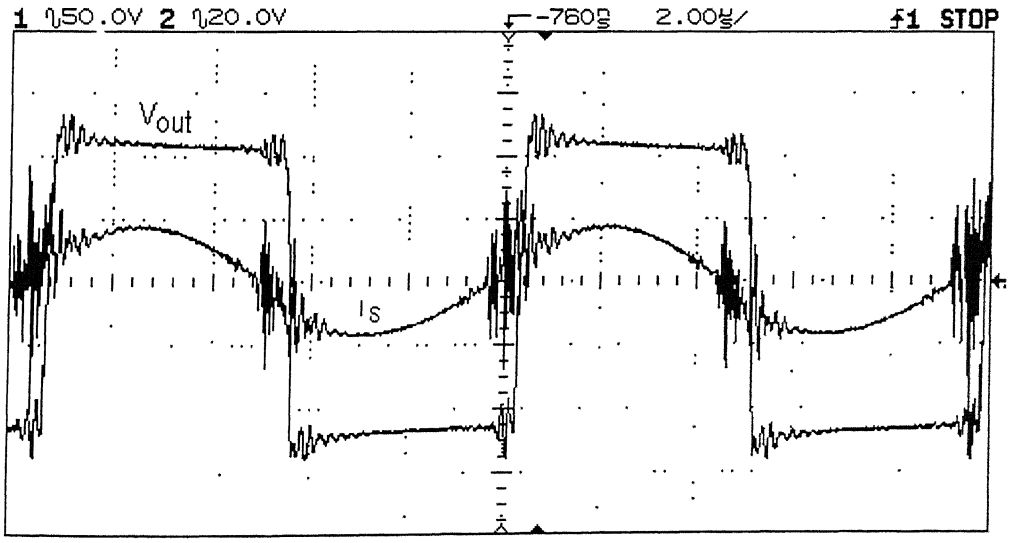

Fig. 5.10 Experimental input voltage and current waveforms to the diode bridge in case1.

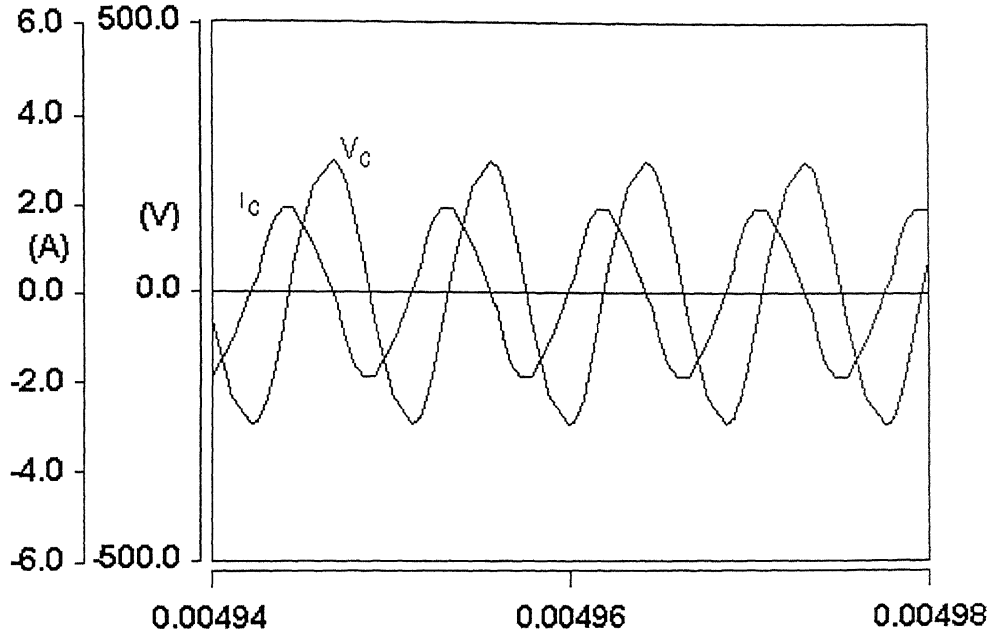

Fig. 5 11 simulated voltage and current waveforms through resonant capacitor, in case1.

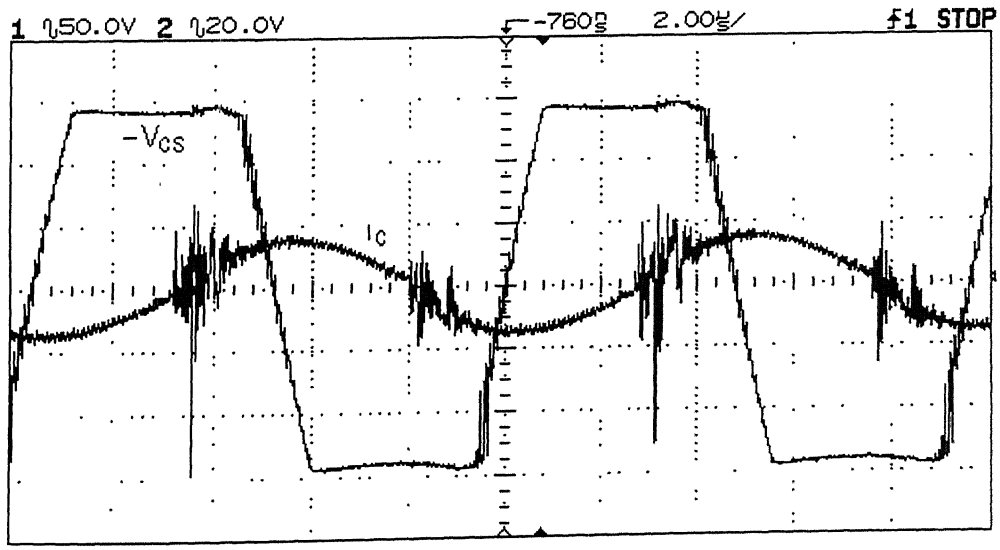

Fig. 5.12 Experimental voltage and current waveforms through resonant capacitor in case1.

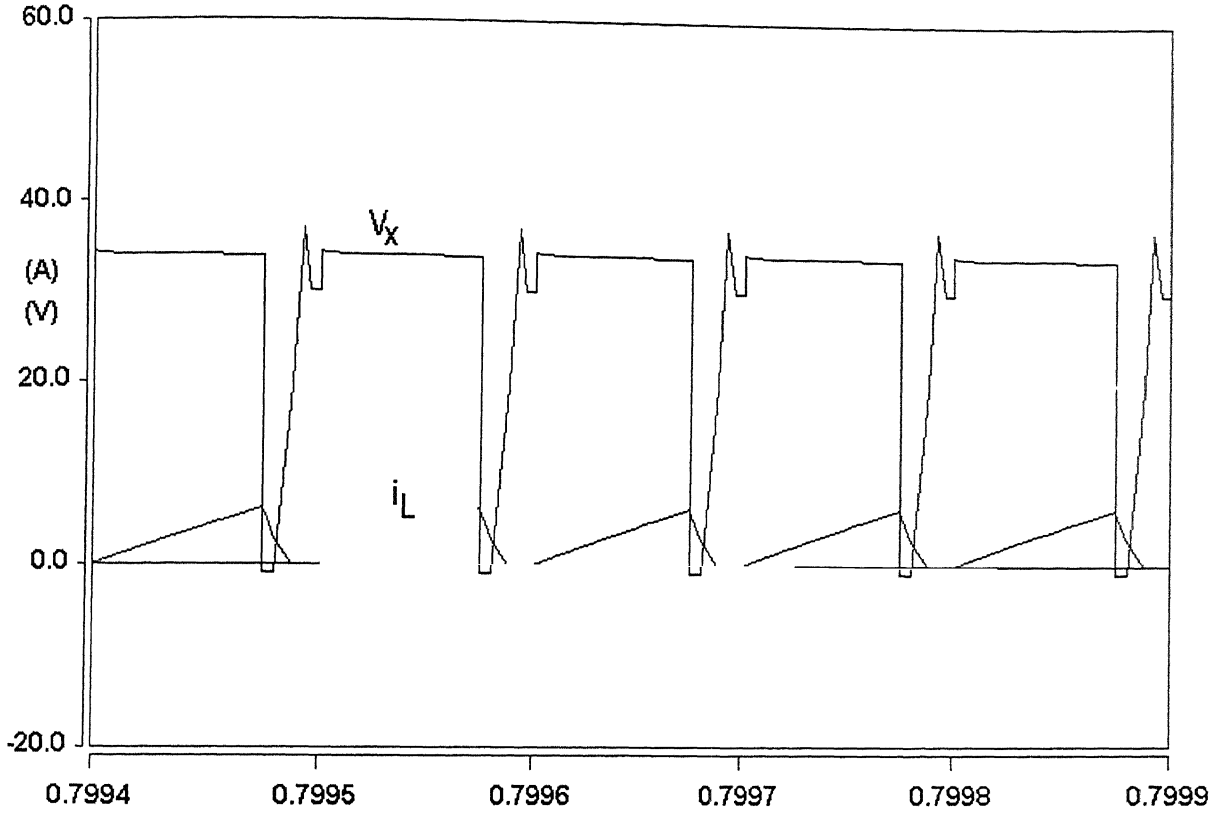

Fig. 5.13 Simulated voltage and current waveforms of the buck converter in Case2 (a).

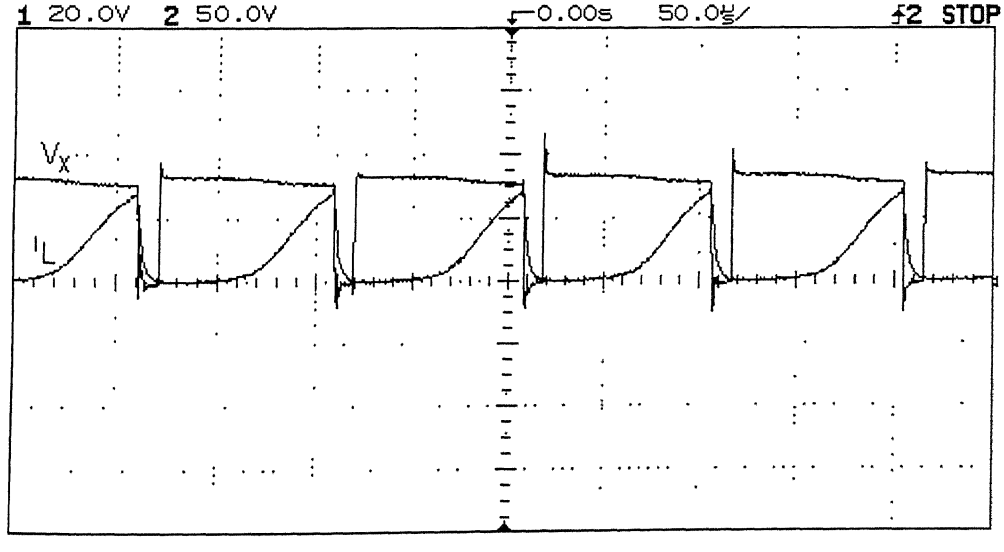

Fig. 5.14 Experimental voltage and current waveforms of the buck converter in Case2 (a).

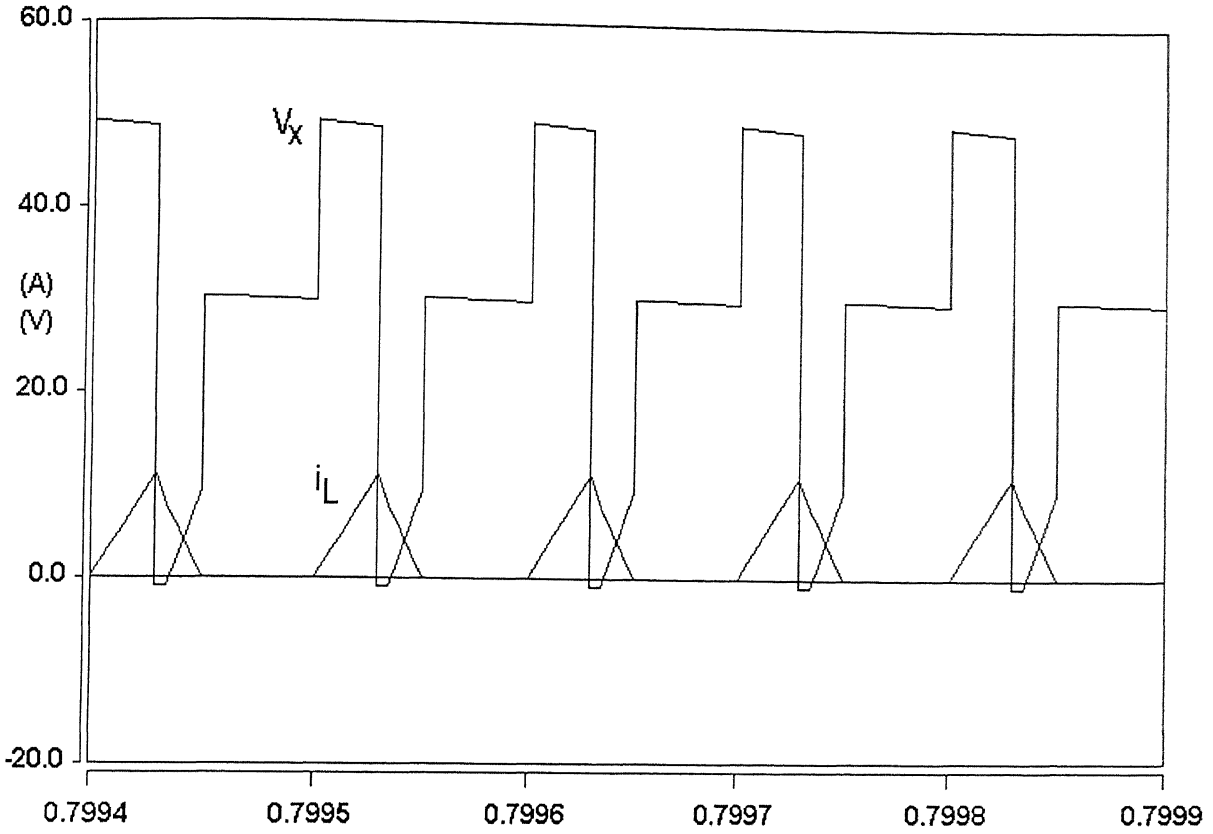

Fig. 5.15 Simulated voltage and current waveforms of the buck converter in Case 2 (b).

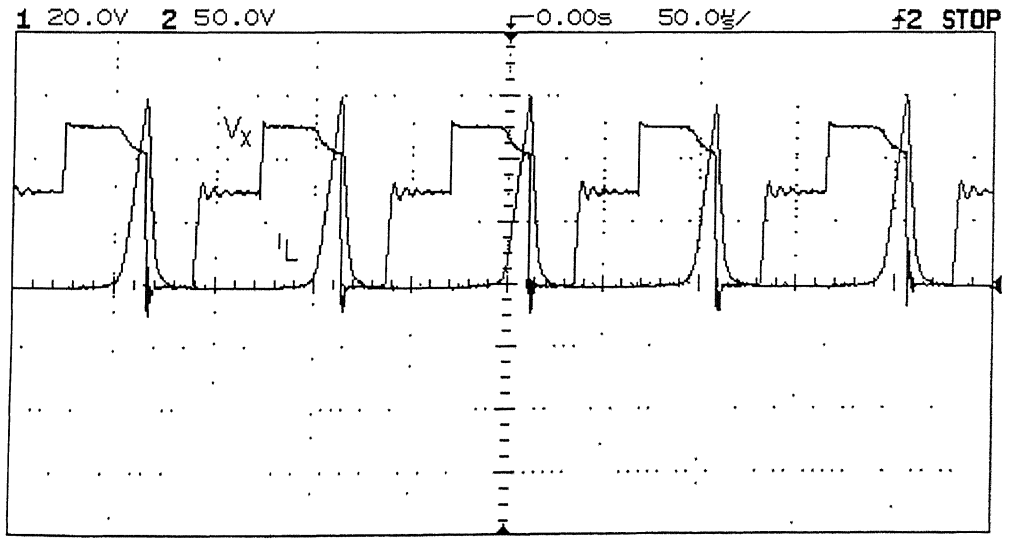

Fig. 5.16 Experimental voltage and current waveforms of the buck converter in Case 2(b).

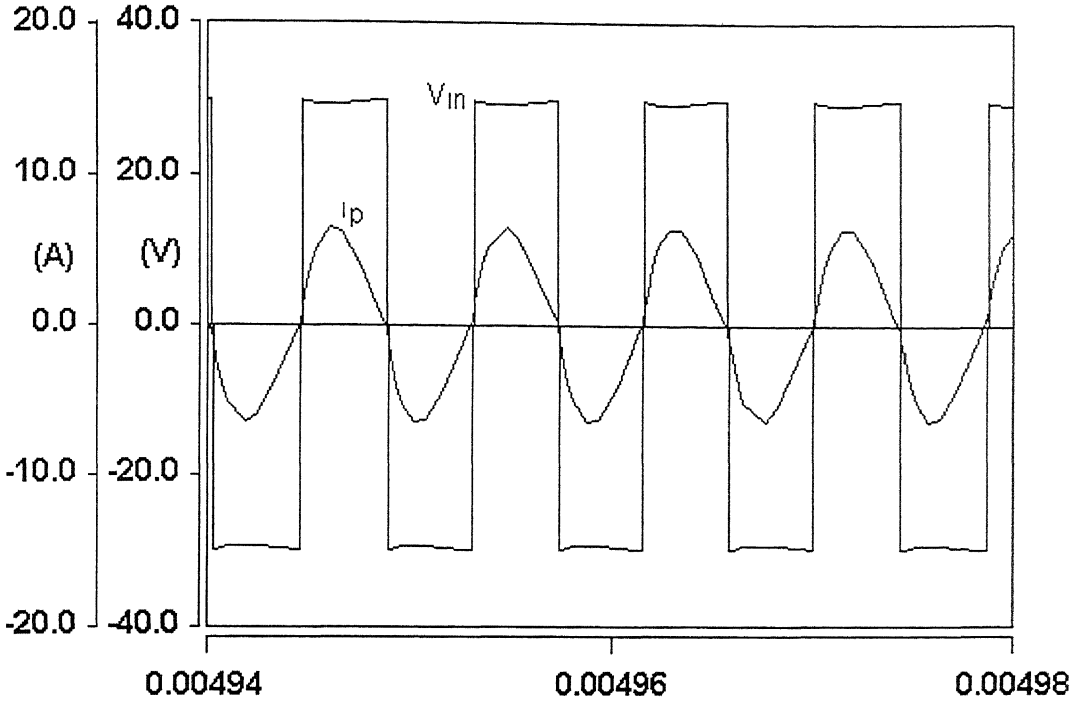

Fig. 5.17 Simulated input voltage and current waveforms to the transformer primary in case2

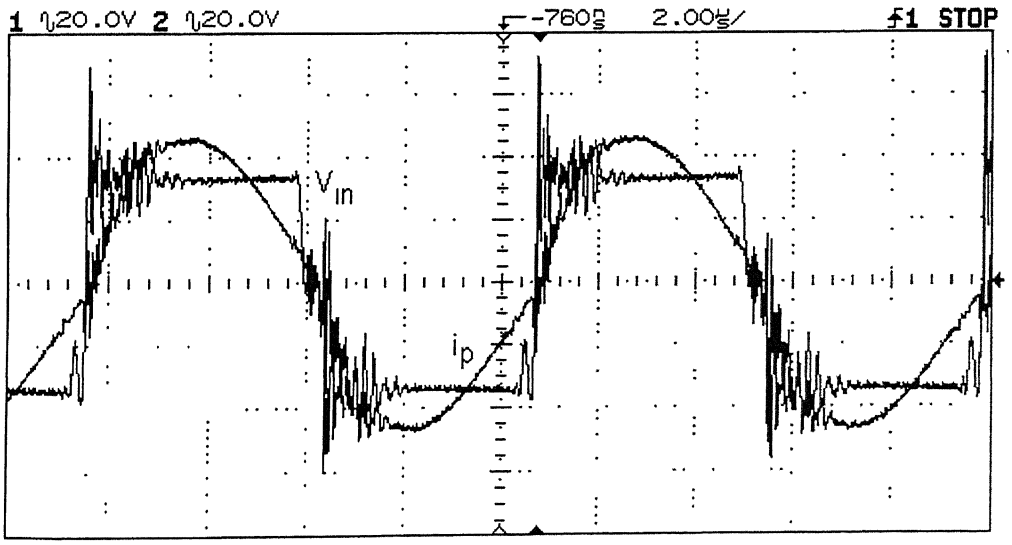

Fig. 5 18 Experimental input voltage and current waveforms to the transformer primary in case2

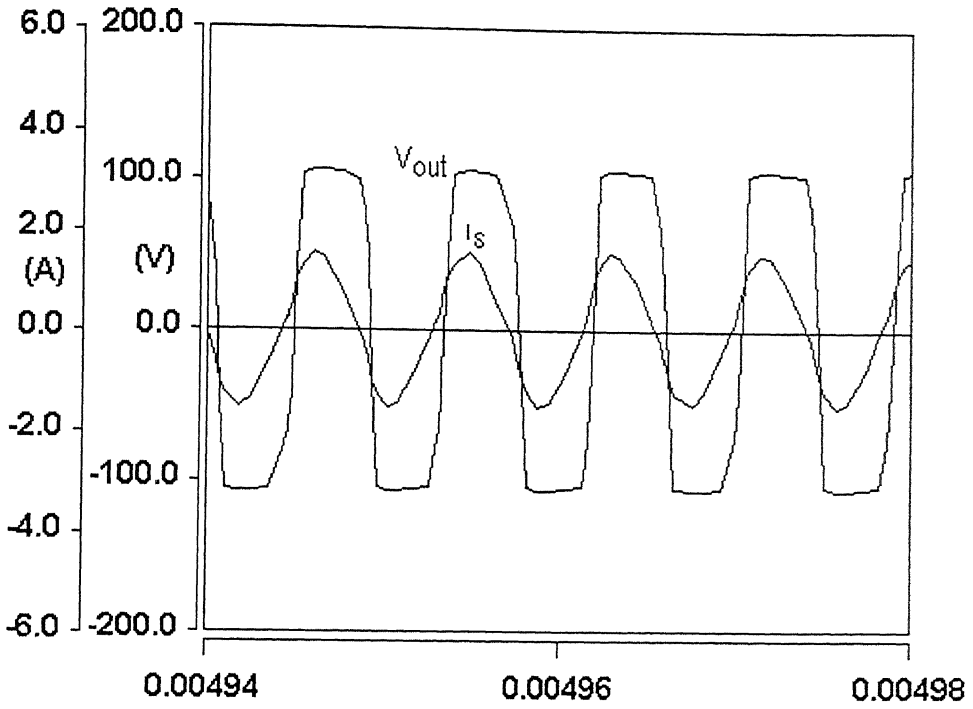

Fig. 5.19 Simulated input voltage and current waveforms to the diode bridge in case2

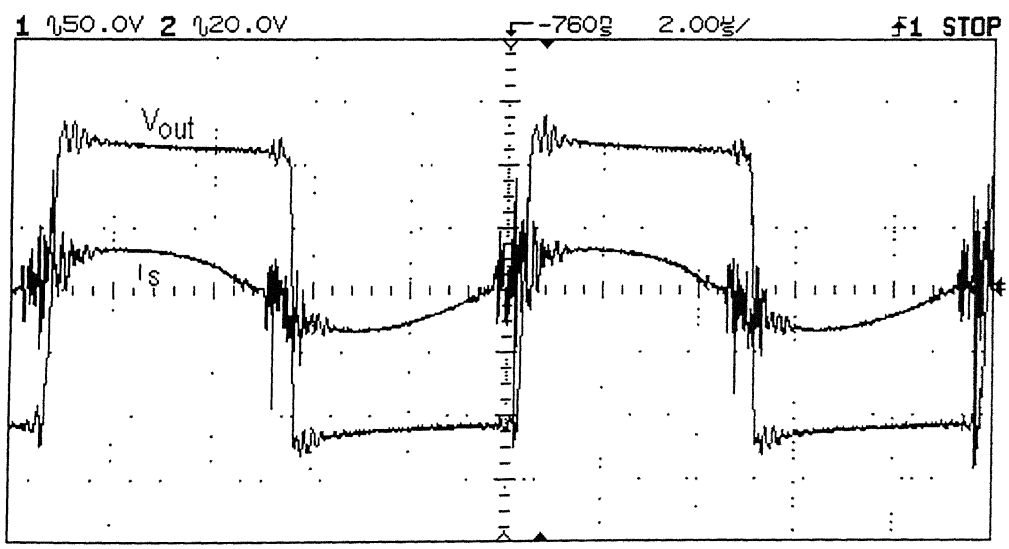

Fig. 5. 20 Experimental input voltage and current waveforms to the diode bridge in case2

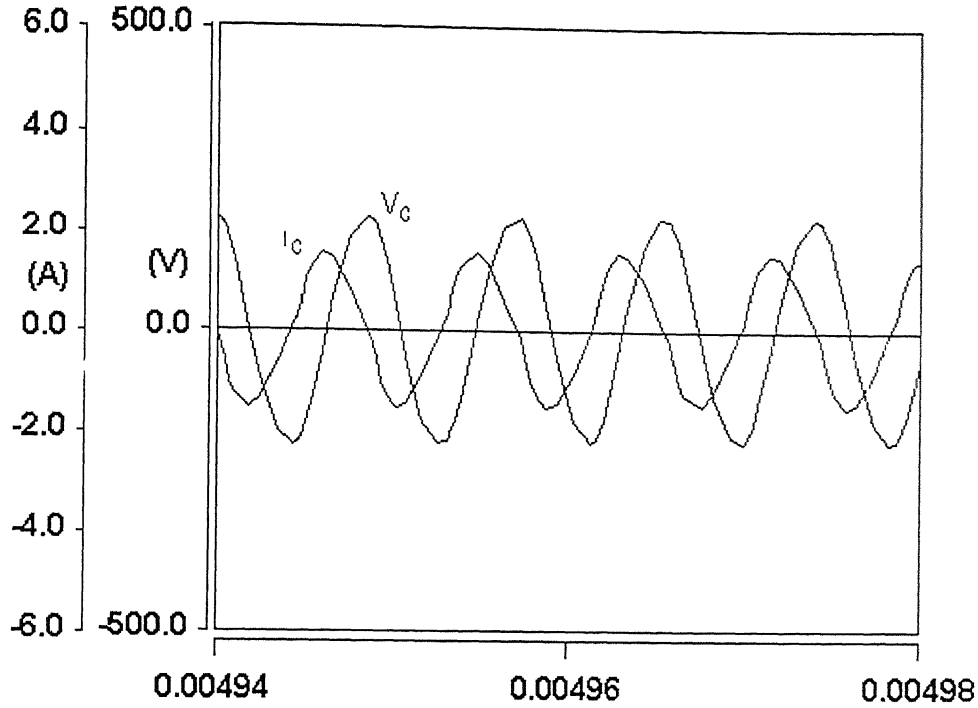

Fig. 5 21 simulated voltage and current waveforms through resonant capacitor, in case2.

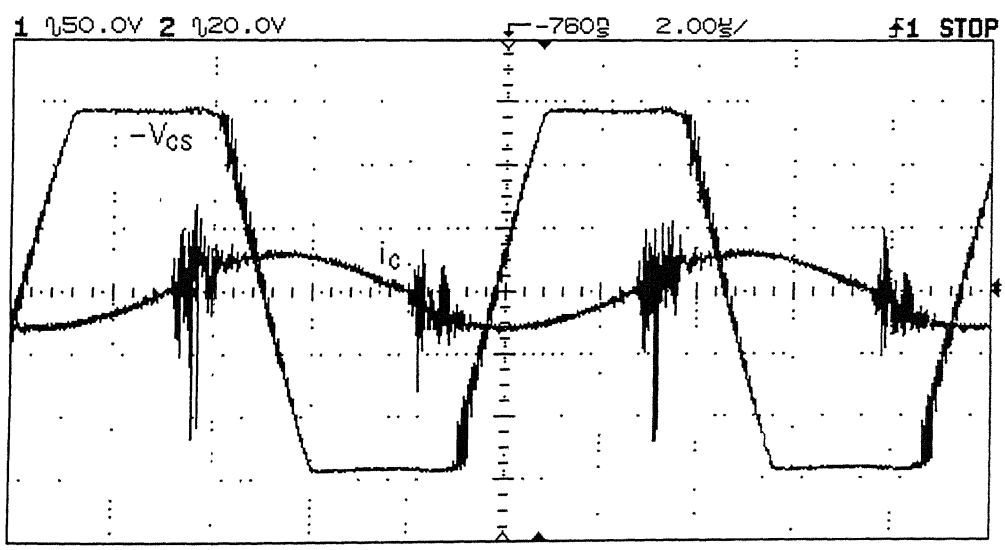

Fig. 5.22 Experimental voltage and current waveforms through resonant capacitor in case2.

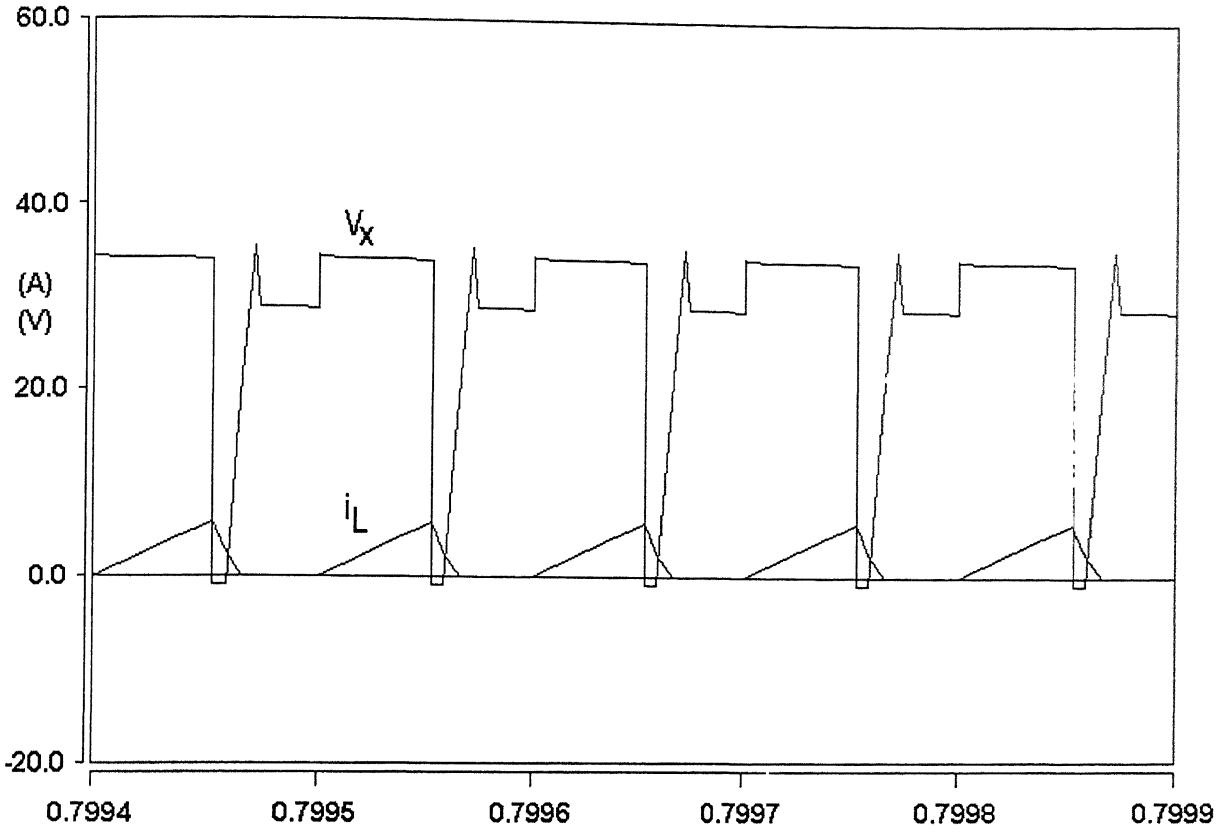

Fig 5.23 Simulated voltage and current waveforms of the buck converter in Case3 (a).

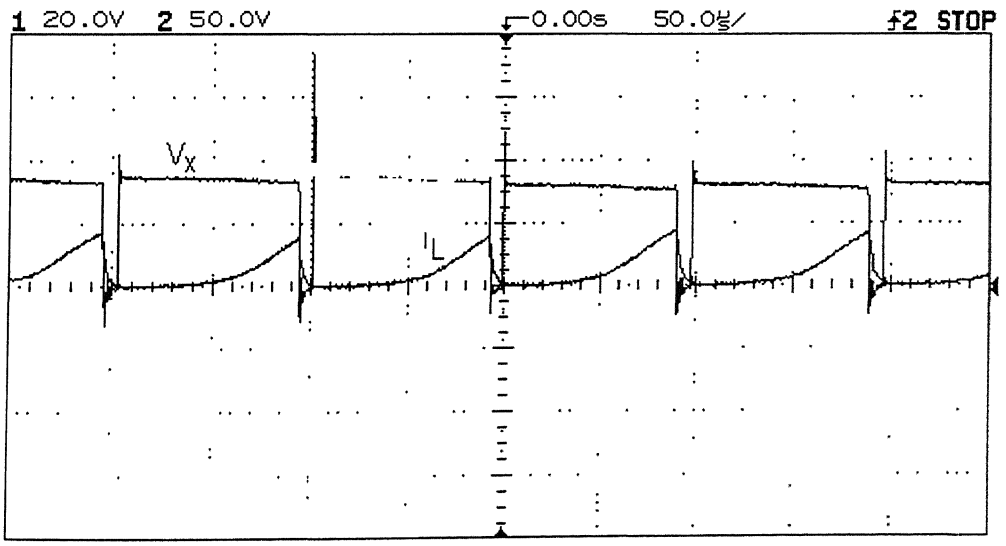

Fig. 5.24 Experimental voltage and current waveforms of the buck converter in Case3 (a).

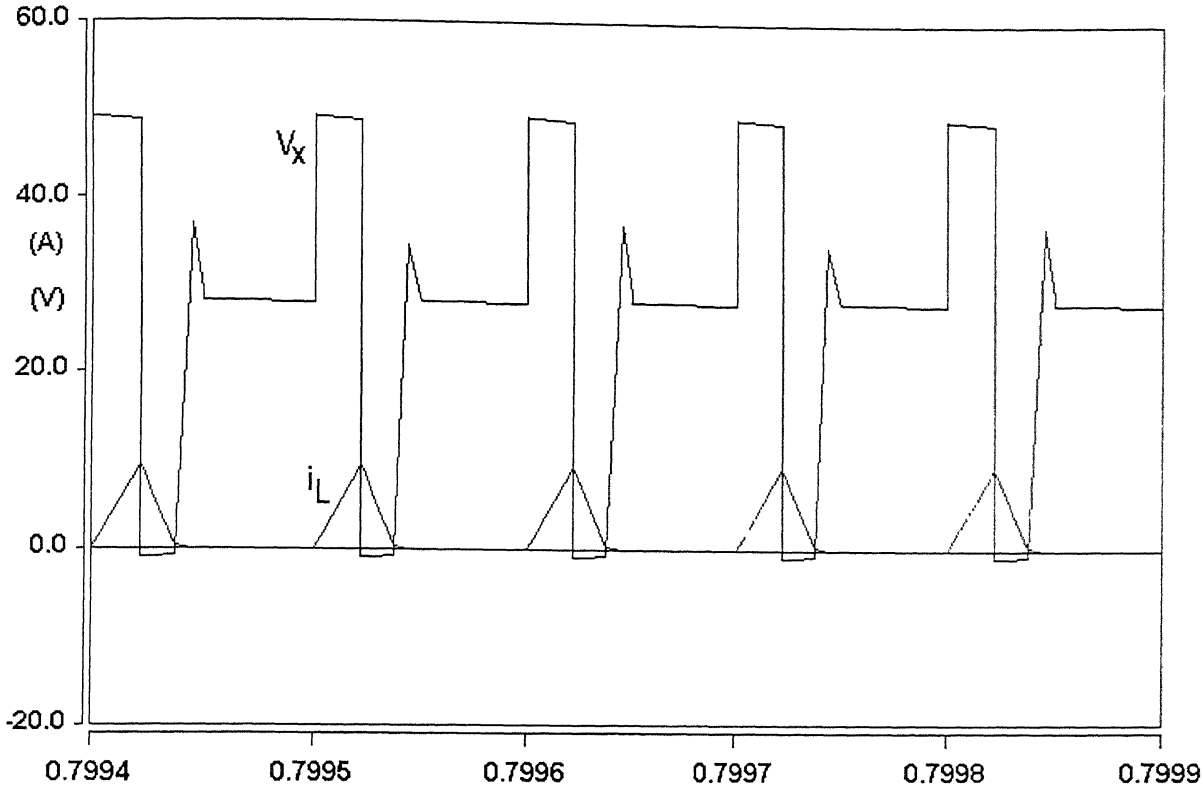

Fig. 5.25 Simulated voltage and current waveforms of the buck converter in Case3 (b).

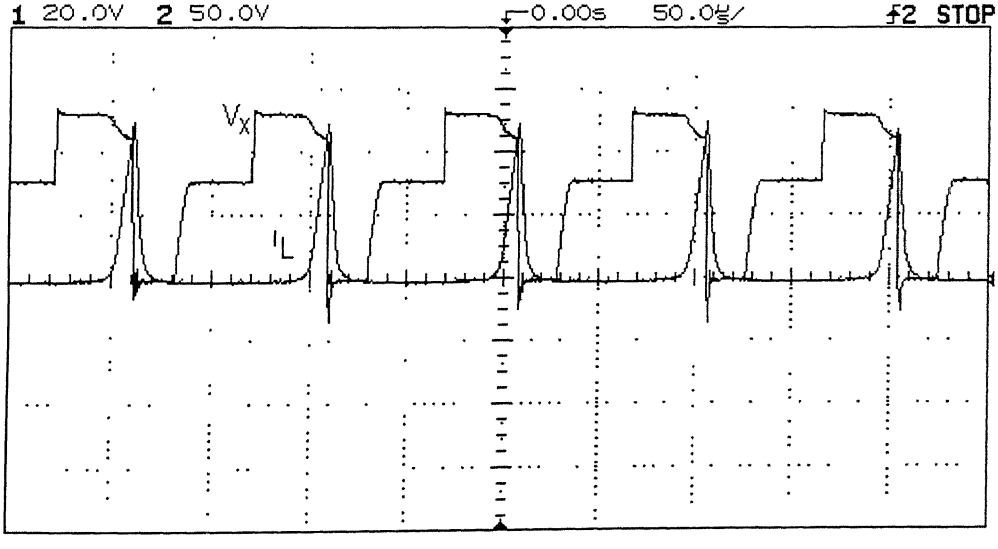

Fig. 5.26 Experimental voltage and current waveforms of the buck converter in Case3 (b).

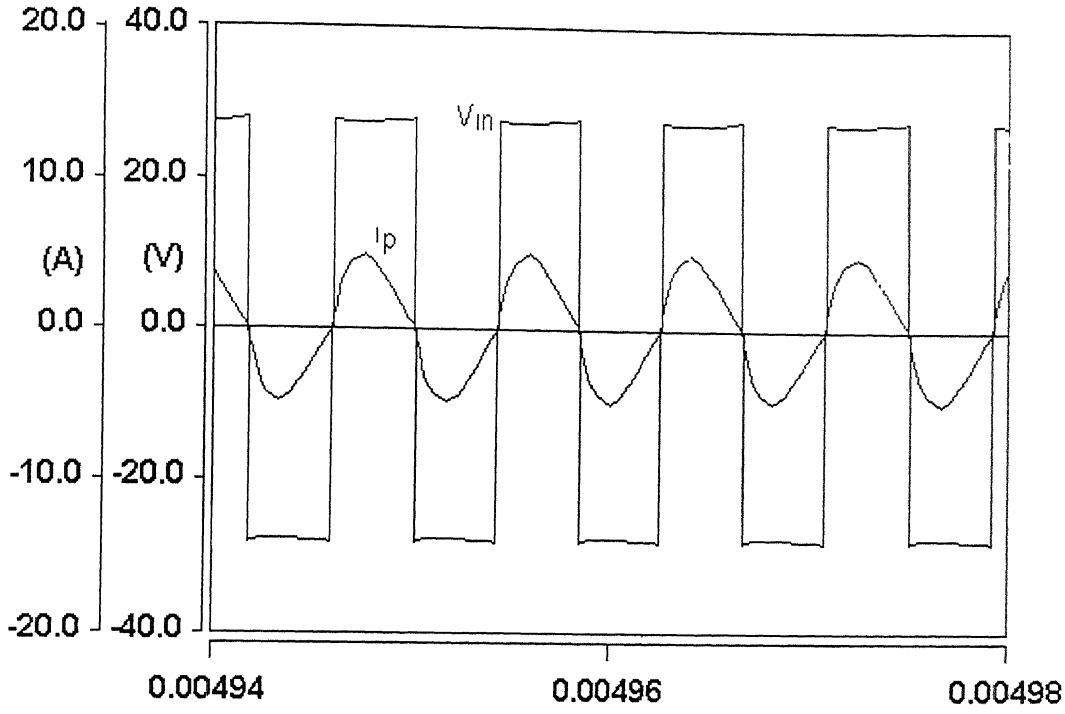

Fig. 5.27 Simulated input voltage and current waveforms to the transformer primary in case3

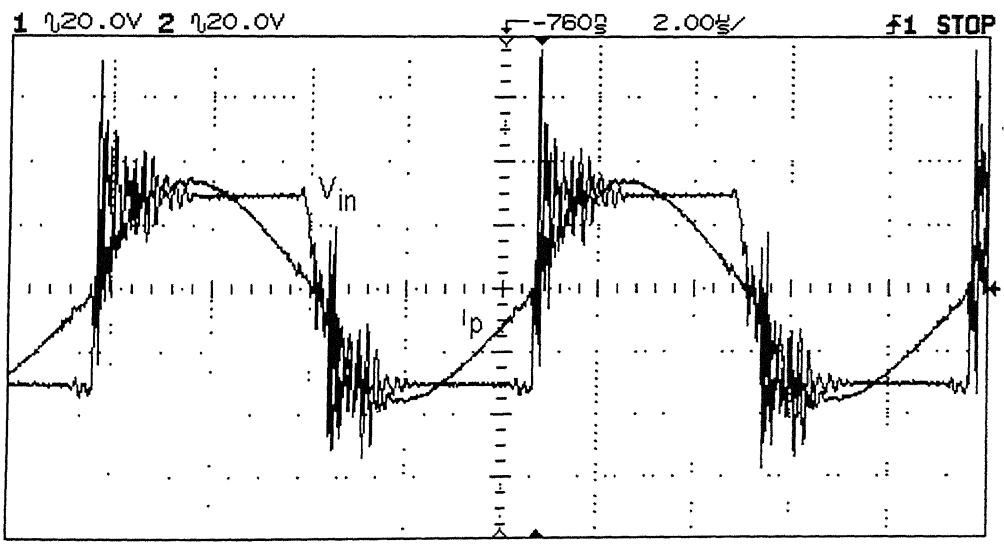

Fig. 5.28 Experimental input voltage and current waveforms to the transformer primary in case3.

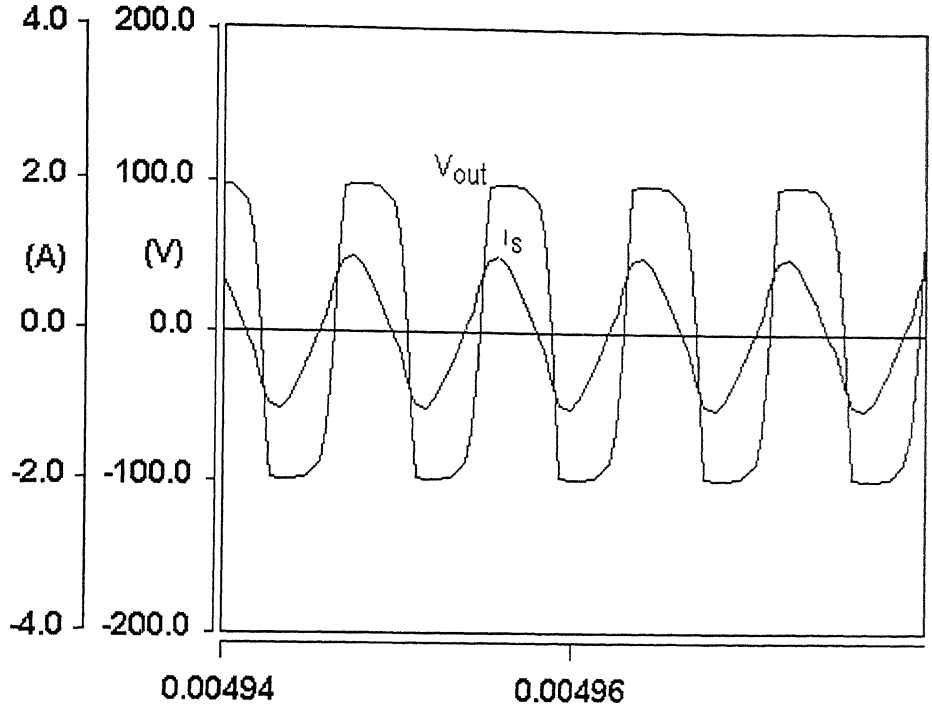

Fig. 5 29 Simulated input voltage and current waveforms to the diode bridge in case3

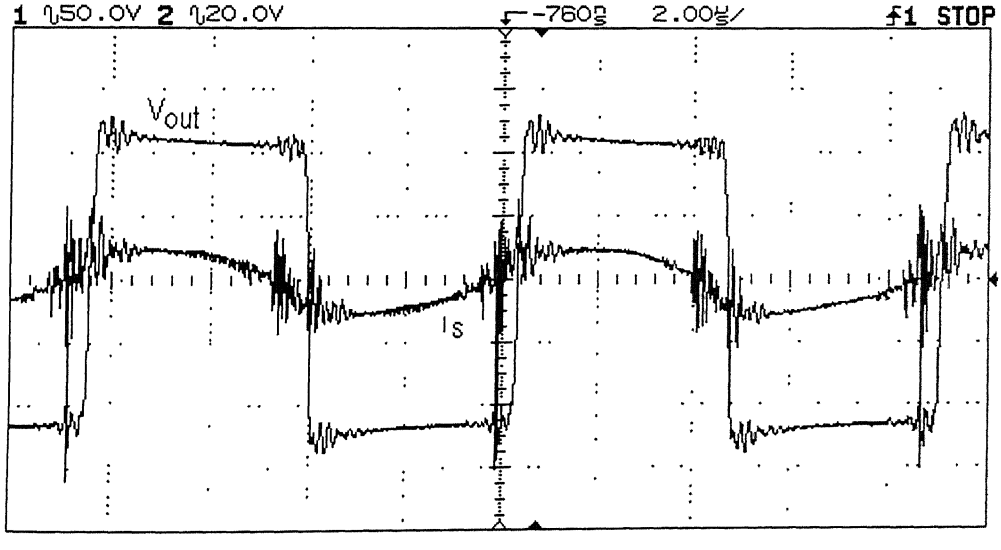

Fig. 5.30 Experimental input voltage and current waveforms to the diode bridge in case3

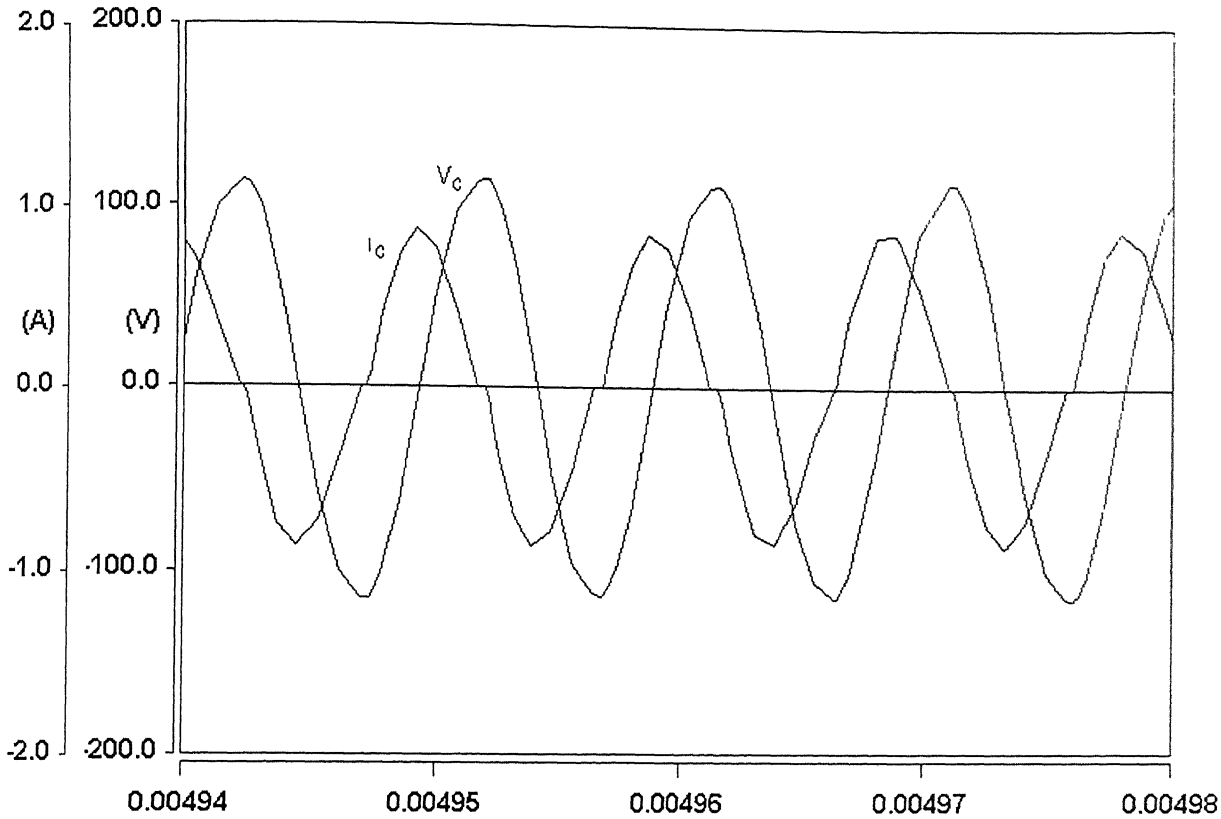

Fig. 5.31 simulated voltage and current waveforms through resonant capacitor, in case3.

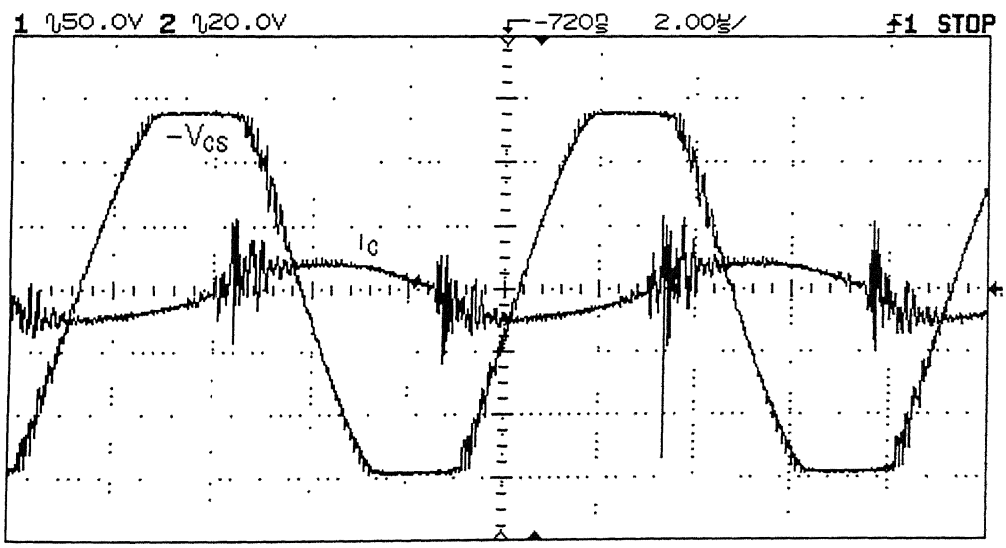

Fig. 5.32 Experimental voltage and current waveforms through resonant capacitor in case3.

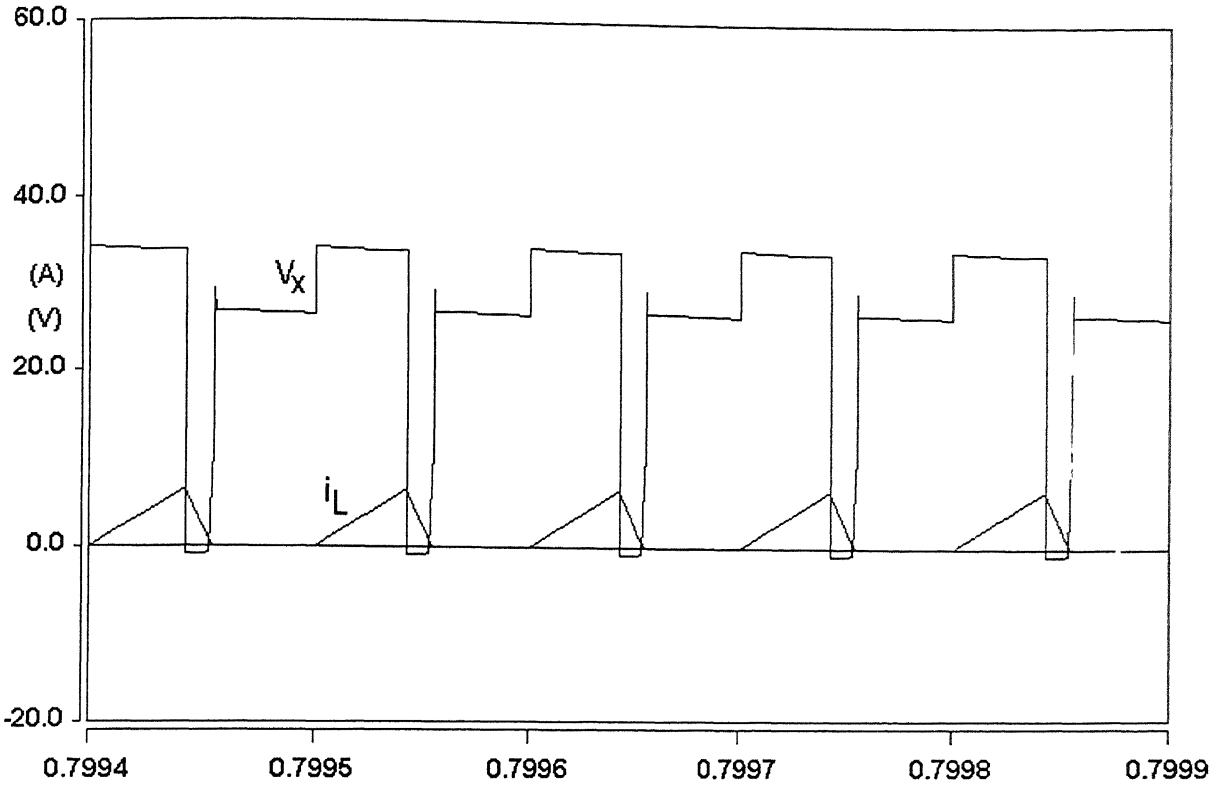

Fig. 5.33 Simulated voltage and current waveforms of the buck converter in Case (4.a).

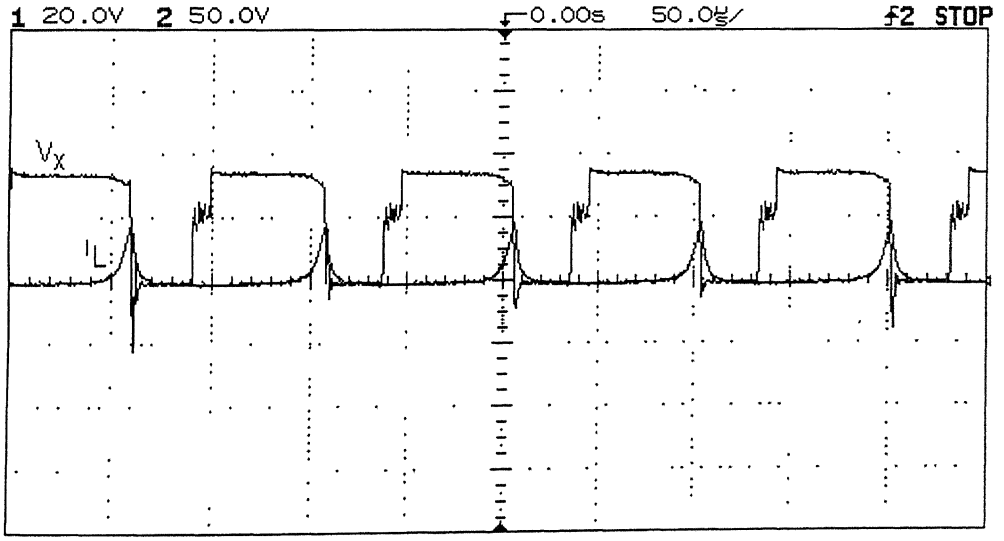

Fig. 5.34 Experimental voltage and current waveforms of the buck converter in Case (4.a).

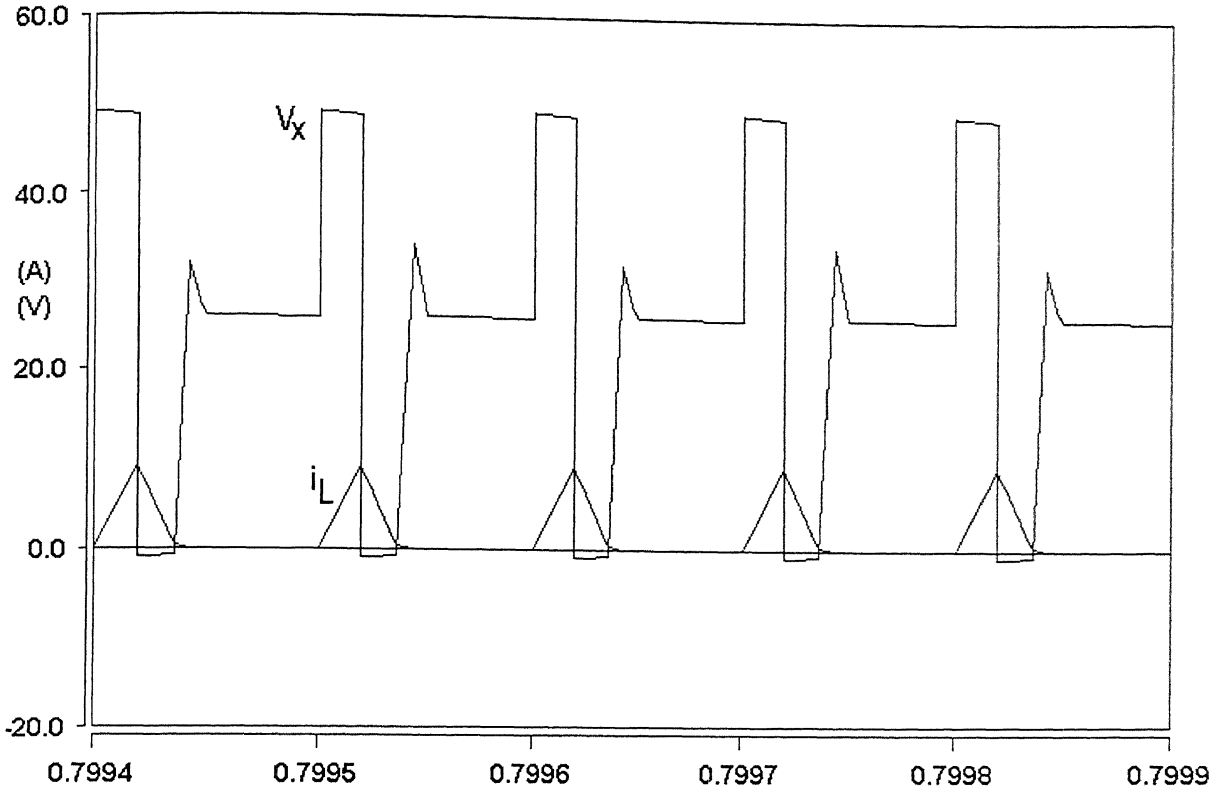

Fig. 5.35 Simulated voltage and current waveforms of the buck converter in Case (4.b).

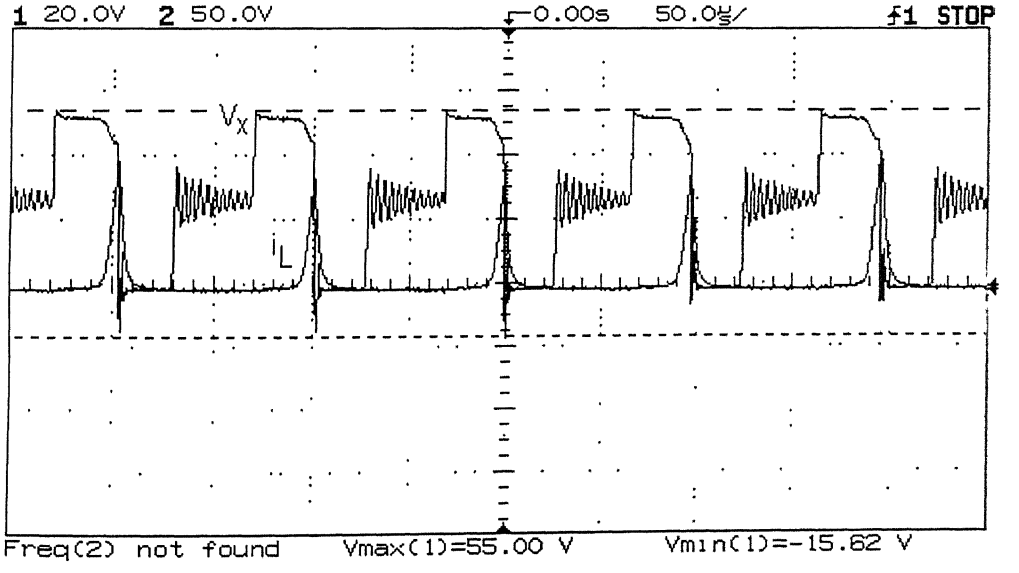

Fig. 5.36 Experimental voltage and current waveforms of the buck converter in Case (4.b).

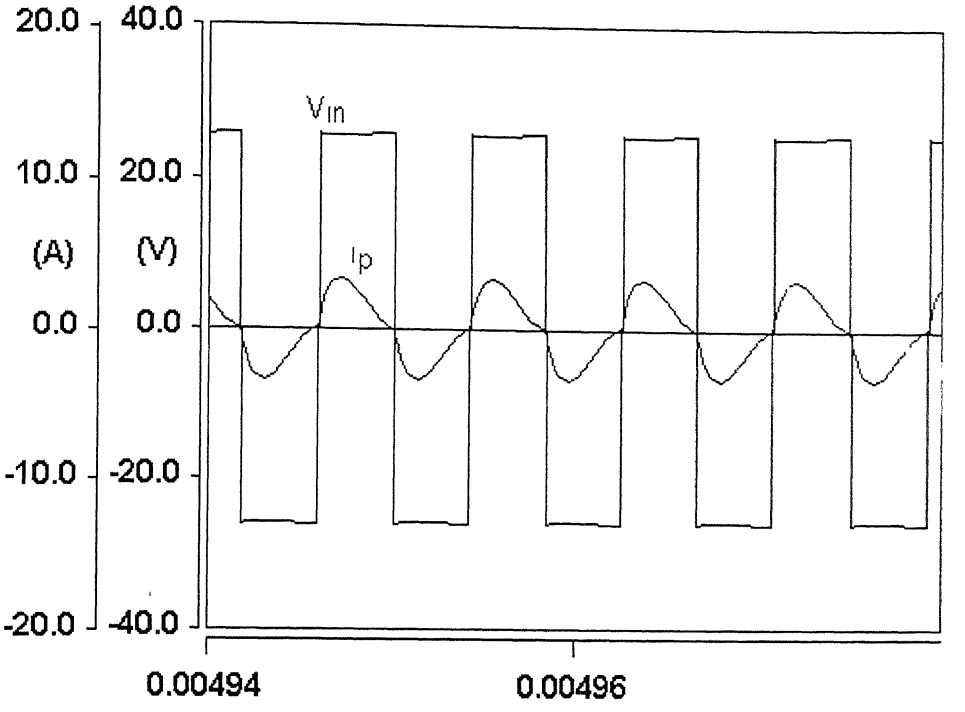

Fig. 5.37 Simulated input voltage and current waveforms to the transformer primary in case4.

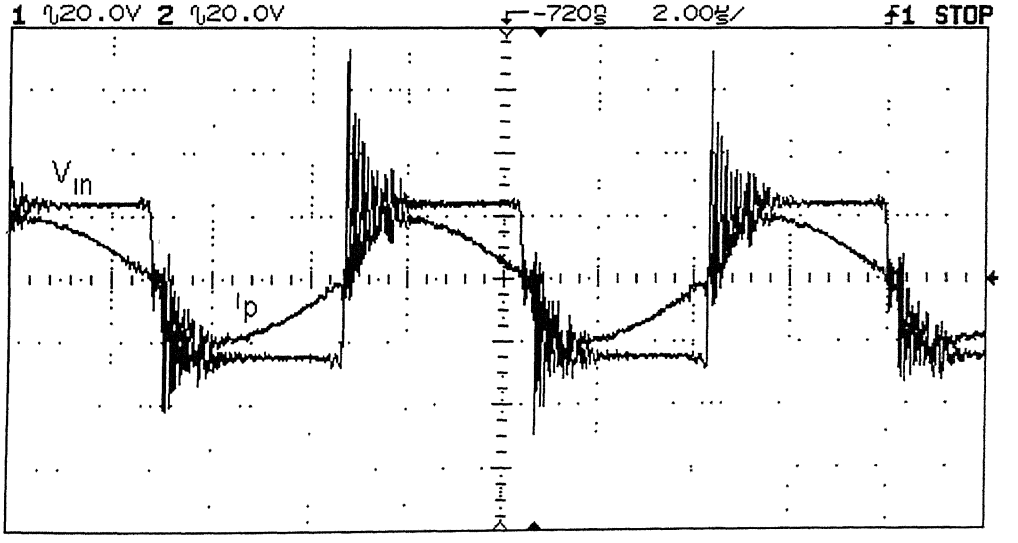

Fig. 5.38 Experimental input voltage and current waveforms to the transformer primary in case4.

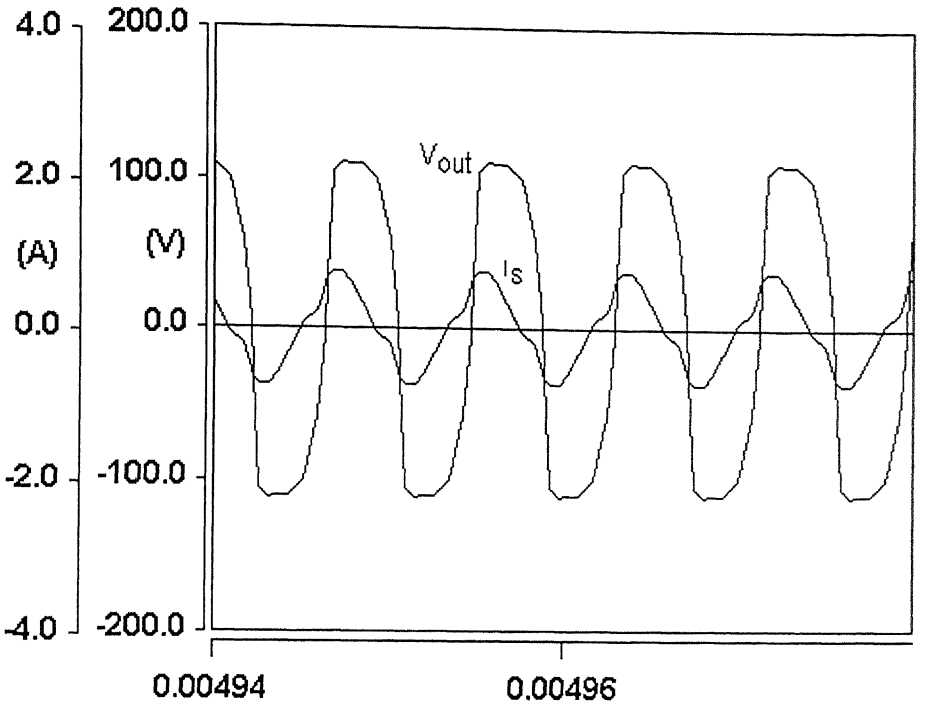

Fig. 5.39 Simulated input voltage and current waveforms to the diode bridge in case4

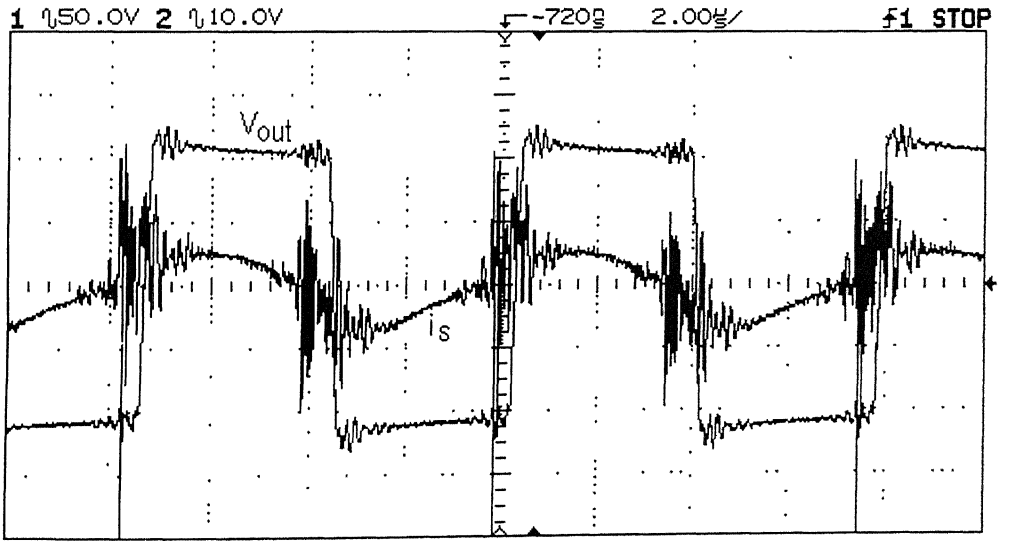

Fig. 5.40 Experimental input voltage and current waveforms to the diode bridge in case4.

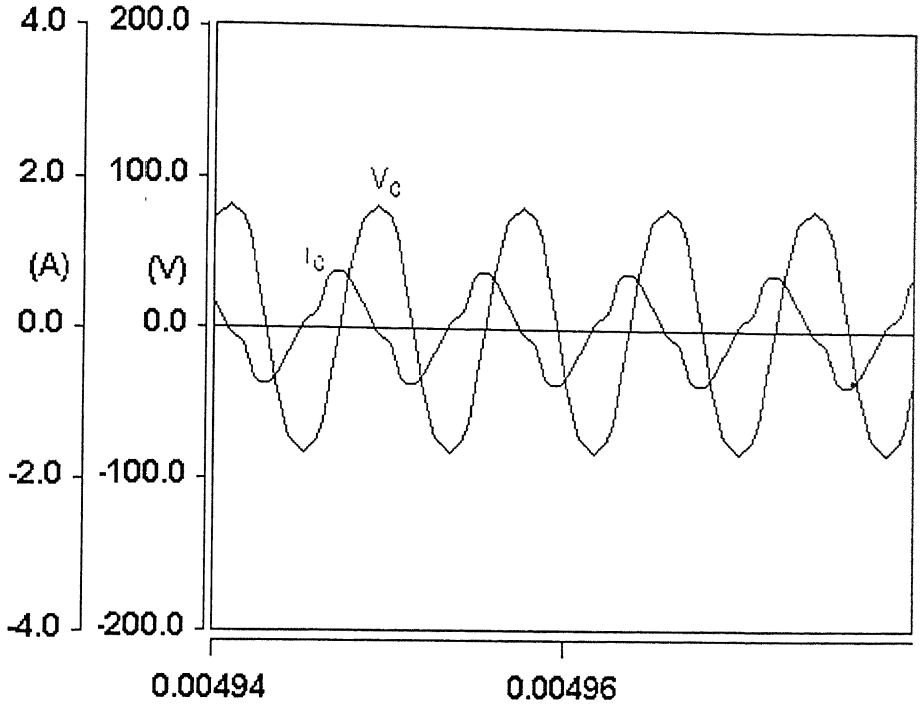

Fig. 5.41 simulated voltage and current waveforms through resonant capacitor, in case4.

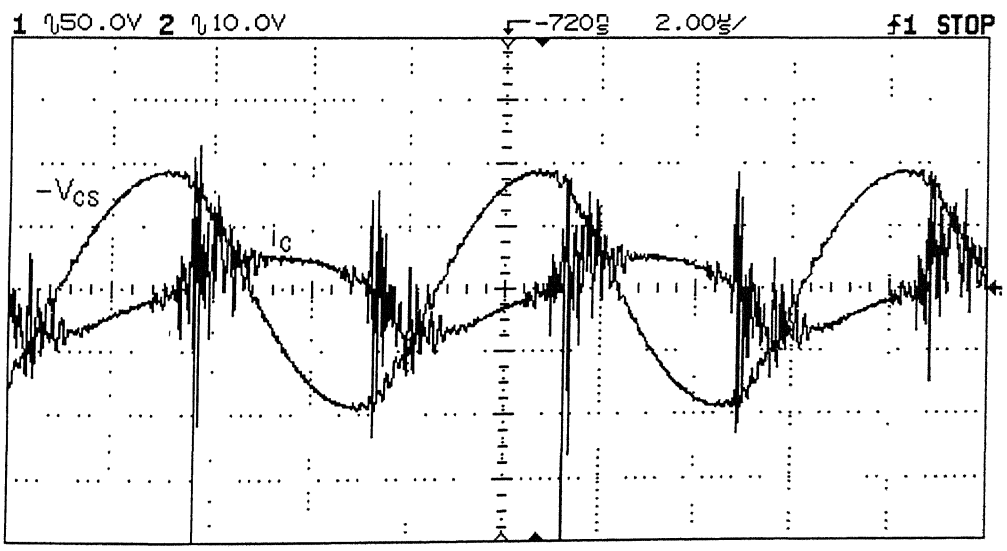

Fig. 5.42 Experimental voltage and current waveforms through resonant capacitor in case4.

CONCLUSION

6.1 CONCLUSION

The general description of the Traveling Wave Tube Amplifier (TWTA), as discussed in chapter 2, shows that it has multiple electrodes (Anodes, collectors and cathode), which are operated at different potentials. An electronic power conditioner (EPC) is usually required to power them up. Two possible configurations have been considered in the present work for the realization of the EPC. The first scheme consists of single-stage high frequency multi-element dc-dc resonant converter. The second approach is a two-stage dc-dc power converter wherein a single pulse width modulated pre-regulator is followed by a high frequency Series Resonant Converter. A multiple secondary high voltage transformer along with multiple diode bridge rectifier and filter stages are used to get multiple dc output voltages from a common input dc source.

In the first method, the effect of transformer leakage inductance and diode bridge junction capacitance are included in the conventional two-element series resonant tank. The resultant topology is a four-element LCLC resonant tank. The operation of the converter above the resonant frequency ensures zero-current and zero-voltage turn-on of all inverter switches. The switches, however, turn off at finite current and finite voltage resulting in turn-off switching losses. The output voltage is controlled by PWM control for load variation and FM control for input voltage variation. The simulation study of closed-loop PWM and FM control with actual multi-output transformer, rectifier and filter units shows that it is possible to maintain the output voltage constant with varying load resistance and varying input voltage. The range of frequency variation is low. The PWM control loop is fast acting while the FM loop is slow acting. Both

controls act to correct for load variation and input voltage variation without sacrificing soft-switching turn-on of inverter switches. It has been shown that the ripple content in the dc output voltage at cathode can be reduced to the specified limit by an active filter proposed in this thesis. This is, however, not possible by a simple capacitor filter since there is restriction in the maximum value of capacitance that can be used. The active filter circuit can also be used for meeting the stringent ripple requirements at any other electrode. Some of the problems associated with the single-stage scheme are high voltage and current stresses in resonant elements and devices, temperature sensitivity, poor efficiency at light loads.

The second scheme explores the best features of Series Resonant Converter (SRC). The only problem associated with the output voltage control is overcome by connecting a buck converter as the first-stage and the SRC as the second-stage. The buck converter is operated at low frequency (10 kHz) under duty ratio control and the SRC is operated exactly at the resonant frequency with the inverter switches turning on and turning off at zero current. The discontinuous mode of current conduction at higher input voltage helps the switch in the buck converter to turn on at zero current.

The design and simulation study of two-stage dc-dc power converter with a single high voltage secondary show that the variation of input voltage is taken care of by the duty ratio control of the buck converter. The SRC is operated on the load independent operating point of the voltage gain versus switching frequency characteristics. The switching frequency is fixed at the resonant frequency and it does not change with the load resistance. A practical prototype of two-stage dc-dc converter shows that the unavoidable parasitics of the high voltage transformer and diode bridge rectifier transforms a simple two-element SRC topology into a multi-element topology. The simulation and implementation results of the practical two-stage converter show that the resonant frequency of the tank slightly depends on the load resistance. The variation of switching

frequency to follow the change in resonant frequency is very low. There is a good agreement between simulation and experimental results.

6.2 SCOPE FOR FUTURE WORK

(i) In two-stage dc-dc power converter, the first-stage (buck-converter) is operated at low frequency due to hard switching. This can be replaced with soft-switched resonant converter, such as ZCS (Zero Current Switch) or ZVS (Zero Voltage Switch).

(ii) The converter is implemented at reduced output voltage. It can be implemented with actual multiple secondary winding high voltage transformer and multiple rectifier and filter units as required in the TWTA.

(iii) The converter analysis is completely based on the sinusoidal steady state approximation. Transient analysis, therefore, can be done to study the behavior of the converter during transients.

6.3 APPLICATIONS

- Electronic Power Conditioner for the Traveling Wave Tube Amplifier (TWTA) used in satellites.
- High voltage power supplies.
- Airborne / space applications.
- Radar applications.

REFERENCES

[1] V.T. Ranganathan, P.D. Ziogas, and V.R. Stefanovic, "A regulated dc-dc voltage source converter using a high-frequency link," *IEEE Trans Industry Applications*, vol. IA-18, no. 3, pp. 279-287, May/June 1982.

[2] H.M. Suryawanshi, S.G. Tarnekar, "Modified LCLC-type series resonant converter with improved performance," *IEE Proc -Electr. Power Appl.*, vol. 143, No. 5, pp. 354-360, September 1996.

[3] Young-Goo Kang, Anand K. Upadhyay, and Dennis L. Stephens, "Analysis and design of a half-bridge parallel resonant converter operating above resonance," *IEEE Trans Industry Applications*, vol. 27, No. 2, pp. 386-395, March/April 1991

[4] G.S.N Raju and Seshagirirao Doradla, "An LCL resonant converter with PWM control-analysis, simulation, and implimentation," *IEEE Trans Power electron.*, vol. 10, No. 2, pp. 164-174, March 1995.

[5] Ashoka K.S.Bhat, "A unified approach for the steady-state analysis of resonant converters," *IEEE Trans Ind. electron*, vol. 38, No. 4, pp. 251-259, August 1991.

[6] M.C. Tsai, "Analysis and implementation of a full-bridge constant-frequency LCC-type parallel resonant converter," *IEE Proc. Electr. Power Appl.*, vol. 141, No. 3, pp. 121-128, May 1994

[7] Ashoka K.S. Bhat and Mahesh M. Swamy, "Analysis and design of a parallel resonant converter including the effect of a high-frequency transformer," *IEEE Trans. Ind electron*, vol. 37, No. 4, pp. 297-306, August 1990.

[8] Rudlof P Severns, "Topologies for three-element resonant converters," *IEEE Trans Power electron.*, vol. 7, No. 1, pp. 89-97, January 1992.

[9] I.Batarseh, "Resonant converter topologies with three and four energy storage elements, " *IEEE Trans. Power electron.*, vol. 9, No. 1, pp. 64-73, January 1994.

[10] Ashoka K.S.Bhat, "A fixed frequency LCL-type series resonant converter," *IEEE Trans. Aerosp Electron. Syst.*, vol. 31, No. 1, pp. 125-137, January 1995.

[11] Allstar Magnetics Inc., *Magnetics (Ferrite cores),* Saugerties, NY 12477, pp. 4.1- 4.19, 1999.

[12] A.K.Sawhney, *A Course In Electrical Machine Design,* Dhanpat Rai and Sons, pp. 894-895, 1987.

APPENDIX A

TABLE-1.

CONTROL CIRCUIT ICs.	DESCRIPTIONS.
74LS04	Hex inverter
74LS08	Quad two input AND gate
74LS53	Expandable 4-wide AND-OR-INVERT gate
74LS74	Dual positive edge triggered D-flip-flops with preset and clear
74LS76	Dual negative edge triggered J-K flip-flops with preset and clear
74LS123	Dual retriggerable monostable multivibrators with clear
74LS124	Dual Voltage controlled oscillators.
74F779	8 Bit UP / DOWN counter.
TLO84	Quad (J-FET) OP-AMPs
LM339	Quad differential comparators
LF353	Dual (JFET) OP-AMPs
MM74C901	Hex inverting TTL buffer
MM74C902	Hex non-inverting TTL buffer
6N137	Opto-isolator
L7805CV	5V, voltage regulator
L7809CV	9V, voltage regulator
L7812CV	12V, voltage regulator
L7815CV	15V, voltage regulator
AD-DAC08 CD	8 Bit digital to analog converter.
NE555N	Digital Timer

TABLE-2.

POWER CIRCUIT ICs.	DESCRIPTIONS.
IRFP150N	44A, 100V, 0.030Ω, N-channel power MOSFET.
IRF840	8A, 500V, 0.85Ω, N-channel power MOSFET.
BUZ21	19A, 100V, 0.1Ω, N-channel power MOSFET.

TABLE-3.

MISCELLANEOUS COMPONENTS.	DESCRIPTIONS.
CL-100	NPN Transistor
CK-100	PNP Transistor
BFW11	N-channel JFET
LHC-50	Current sensor.
LA-55P	Current sensor.

POWER MOSFETs

1. IRFP150N

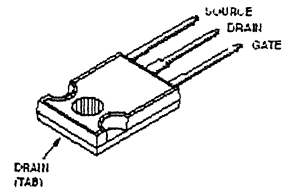

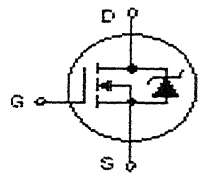

ABSOLUTE MAXIMUM RATINGS		IRFP150N	UNITS
Drain to Source Breakdown Voltage	V_{DSS}	100	V
Drain to gate voltage	V_{DGR}	100	V
Gate to source voltage	V_{GS}	±20	V
Continuous drain current at 25^0C	I_D	44	A
Continuous drain current at 100^0C	I_D	31	A
Drain to Source On Resistance	$R_{DS(on)}$	0.030	Ω
Total Turn-On Time	T_{ON}	130	ns
Total Turn-Off Time	T_{OFF}	150	ns
Source to drain diode break-down voltage	V_{DB}	100	V
Source to drain diode on state voltage	V_{ON}	1.0	V
Reverse recovery time	T_{rr}	105	ns

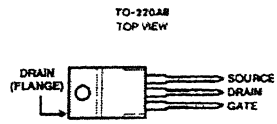

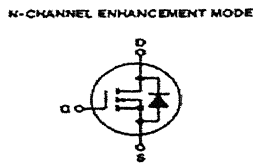

2. BUZ21

ABSOLUTE MAXIMUM RATINGS		BUZ21	UNITS
Drain to Source Breakdown Voltage	V_{DSS}	100	V
Drain to gate voltage	V_{DGR}	100	V
Gate to source voltage	V_{GS}	±20	V
Continuous drain current at 25^{0}C	I_D	19	A
Continuous drain current at 100^{0}C	I_D	7	A
Drain to Source On Resistance	$R_{DS(on)}$	0.1	Ω
Total Turn-On Time	T_{ON}	120	ns
Total Turn-Off Time	T_{OFF}	330	ns
Source to drain diode break-down voltage	V_{DB}	100	V
Source to drain diode on state voltage	V_{ON}	1.5	V
Reverse recovery time	T_{rr}	200	ns

3. IRF840

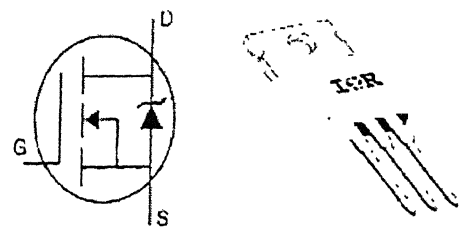

ABSOLUTE MAXIMUM RATINGS		IRFP840N	UNITS
Drain to Source Breakdown Voltage	V_{DSS}	500	V
Drain to gate voltage	V_{DGR}	500	V
Gate to source voltage	V_{GS}	±20	V
Continuous drain current at 25^{0}C	I_D	8	A
Continuous drain current at 100^{0}C	I_D	5.1	A

Drain to Source On Resistance	$R_{DS(on)}$	0.85	Ω
Total Turn-On Time	T_{ON}	37	ns
Total Turn-Off Time	T_{OFF}	69	ns
Source to drain diode break-down voltage	V_{DB}	500	V
Source to drain diode on state voltage	V_{ON}	2.0	V
Reverse recovery time	T_{rr}	460	ns

4. 6N137 OPTOCOUPLER

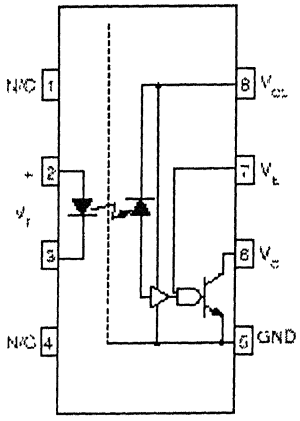

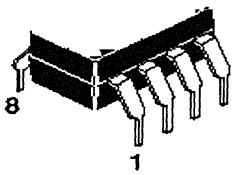

The 6N137 is a single-channel optocoupler consist of a 850 nm AlGaAS LED, optically coupled to a very high-speed integrated photodetector logic gate with a strobable output. This output features an open collector; thereby permitting wired OR outputs. The coupled parameters are guaranteed over the temperature range of -40°C to +85°C. A maximum input signal of 5 mA will provide a minimum output sink current of 13 mA (fan out of 8). An internal noise shield provides superior common mode rejection of typically 10 kV/μs.

Features

- Very high speed-10 MBit/s
- Superior CMR-10 kV/μs
- Double working voltage-480V
- Fan-out of 8 over -40°C to +85°C
- Logic gate output
- Strobable output
- Wired OR-open collector

5.CURRENT SENSOR LA-55P

Current sensor LA-55P is a product of LEM and is useful for the electronic measurement of currents: DC, AC, pulsed, with galvanic isolation between the primary circuit and the secondary circuit. It is capable of carrying up to 50A The closed loop compensated current transducer using hall effect has excellent accuracy, very good linearity, Wide frequency band width, Low temperature drift, optimized response time

APPENDIX B

ELECTRONIC CONTROL CIRCUITS.

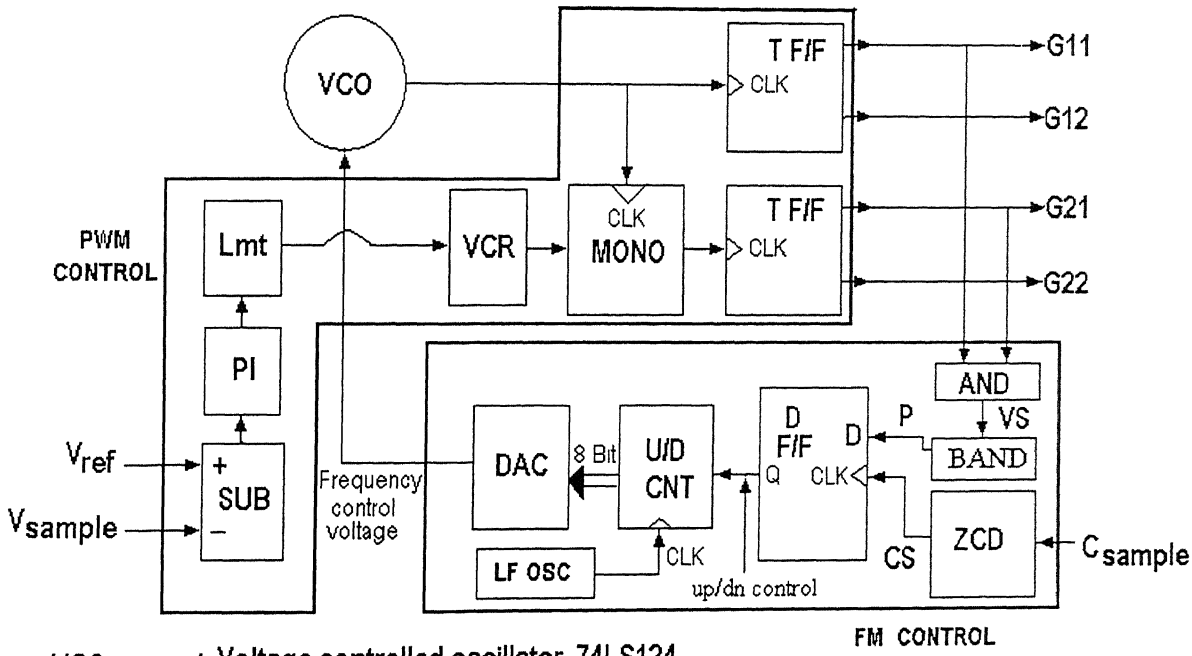

VCO	: Voltage controlled oscillator, 74LS124.
VCR	. Voltage controlled resistor, (BFW10, JFET.)
MONO	: Mono-stable multivibrator, 74LS123.
T F/F	: Toggle flip flop, 74LS76.
ZCD	: Zero Crossing Detector, (LM339)
D F/F	: D Flip-Flop, 74LS74
DAC	: Digital to Analog Converter (DAC AD08 CD and LF353 OP-AMP)
U/D CNT	: 8 Bit digital UP / DOWN counter, 74F779
Vref	: Reference dc output voltage (potentiometer output)
Vsample	: Output load voltage sample (potential divider output)
Csample	: resonant tank input current sample (current sensor LA-55P output)
PI	: Proportional plus integral controller (TL084 OP-AMP)
SUB	: Analog subtractor (TL084 OP-AMP)
Lmt	: Limiter (TL084 OP-AMP)
LF OSC	: Low frequency oscilator (50Hz.), NE555N
AND	: AND gate, 74LS08
BAND	: Narrow band 'A', Fig. 2.10, (Monostable multivibrator, 74LS123)
Vs, Cs	: Voltage signal and current signal respectively.

Fig. 1 Close-loop FM and PWM control circuit for single stage LCLC resonance converter shown in Fig. 2.12.

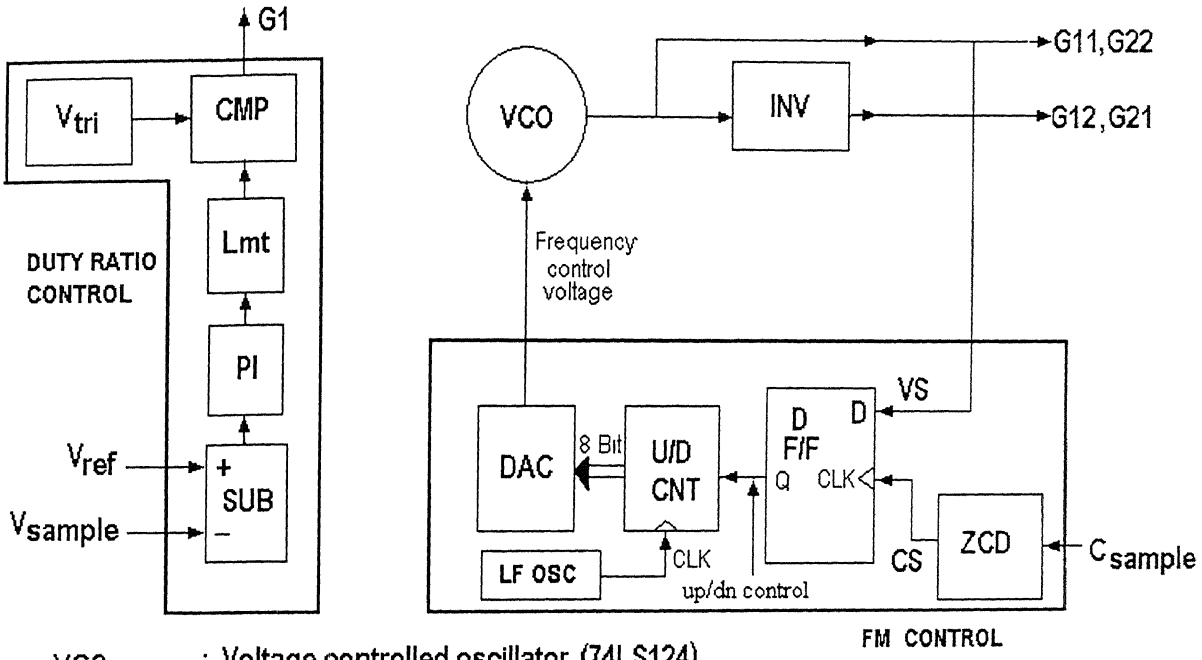

VCO	: Voltage controlled oscillator, (74LS124).
V_{tri}	: 10kHz, triangular wave generator (TL084).
CMP	: Digital comparator, LM339
ZCD	: Zero Crossing Detector, (LM339).
D F/F	: D Flip-Flop, 74LS74
DAC	: Digital to Analog Converter (DAC AD08 CD and LF353 OP-AMP)
U/D CNT	: 8 Bit digital synchronous UP / DOWN counter, 74F779
Vref	: Reference dc output voltage (potentiometer output)
Vsample	: Output load voltage sample (potential divider output)
Csample	: resonant tank input current sample (current sensor LA-55P output)
PI	: Proportional plus integral controller (TL084 OP-AMP)
SUB	: Analog subtractor (TL084 OP-AMP)
Lmt	: Limiter (TL084 OP-AMP)
LF OSC	: Low frequency oscilator (50Hz.), NE555N
INV	: Digital inverter, 74LS04

Fig. 2 Close-loop Duty ratio and FM control circuit for two-stage dc-dc power converter shown in Fig. 3.13.

TRIANGULAR-WAVE GENERATOR CIRCUIT (USING IC. TLO84).

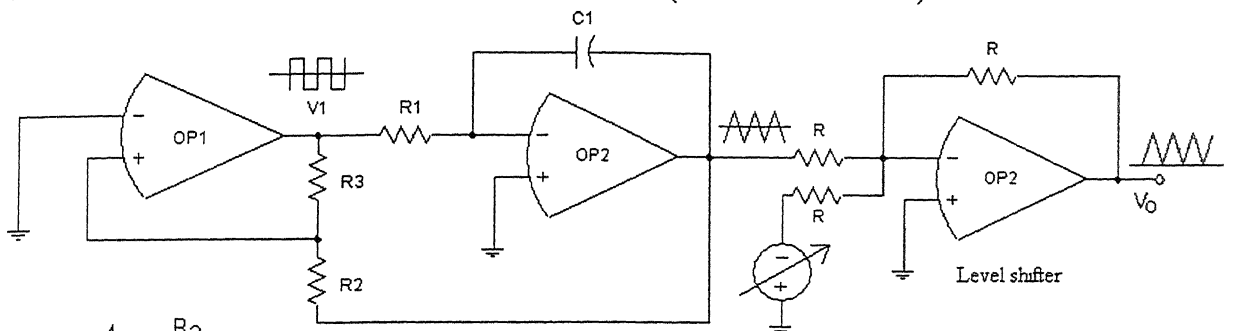

PROPORTIONAL-INTEGRAL CONTROLLER CIRCUIT (USING IC. TLO84).

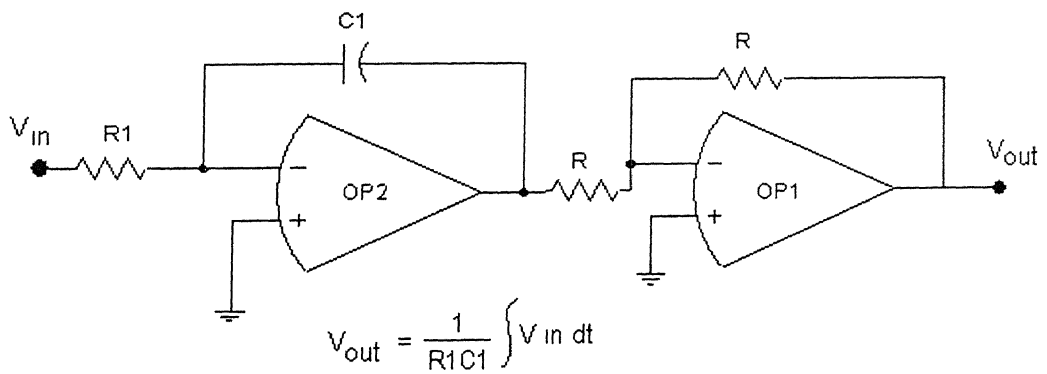

FREQUENCY MODULATION CIRCUIT.

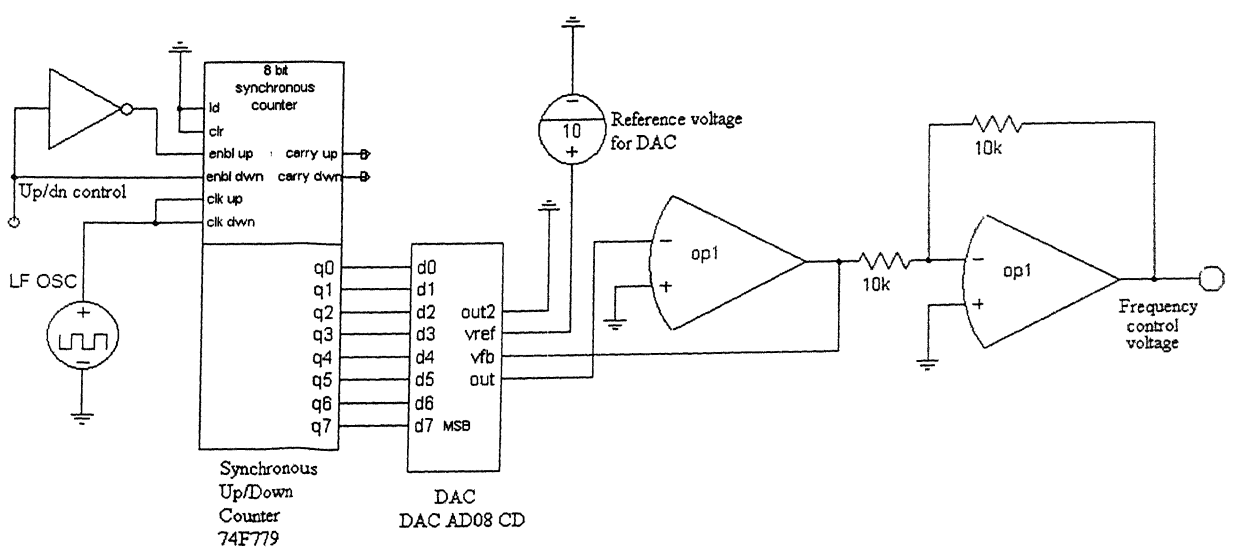

ELECTRONIC CIRCUIT GENERATING NARROW BAND 'A' (as shown in Fig. 2.10).

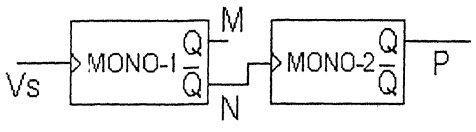

V_{in} Resonant tank input voltage
Vs Resonant tank input voltage signal (Digital)
M Output of Mono-stable multivibrator-1
N Inverted output of Mono-stable multivibrator-1
P Output of Mono-stable multivibrator-2

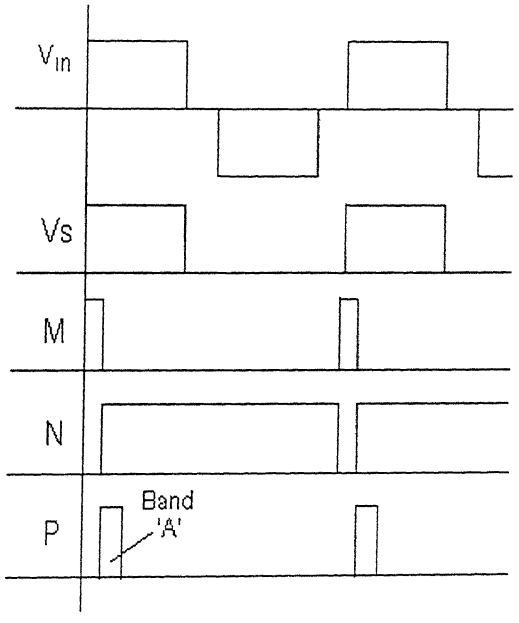

APPENDIX C

DESIGN OF TRANSFORMER USED IN THE EXPERIMENTAL SETUP.

The transformer is designed with following specifications,

300 VA, 100V / 30V, 100kHz, Square wave voltage excitation.

Assuming f = frequency in Hz = 100×10^3 Hz

N_1 = Number of turns of the primary winding

N_2 = Number of turns of the secondary winding.

B_m = maximum core flux density in wb/m^2.

A_{core} = Cross sectional area of the core (middle limb) in m^2.

Φm = maximum core flux = $B_m \times A_{core}$ (wb).

Primary winding self induced e.m.f for square wave excitation,

$V_1 = 4\Phi m\, f N_1$ (V), [11].

$= 4\, B_m\, A_{core}\, f N_1$ (V) = 30V. (1)

The available core has a cross sectional area of 13×12 mm^2 .

Taking Bm = 0.05 wb/ m^2, [11].

$A_{core} = 13\times12\times10^{-6}$ m^2

Substituting these in equation (1) we have,

$N_1 = 9.6 \approx 10$, and $N_2 = \frac{100}{30}\times10 = 33.33 \approx 34$.

Full load Primary current (rms) = $\frac{300}{30}$=10A, and full load secondary current (rms) = $\frac{300}{100}$ = 3A.

Assuming a current density of 6A/mm^2 [11],

The cross sectional area of the primary winding conductors = 1.66 mm^2

Taking 4× 21 SWG [12] copper conductors in parallel (to minimize skin effect) for primary winding. The actual cross sectional area = 4× 0.519 = 2.01 mm^2.

Modified current density for primary winding conductors = 5A/mm^2

The cross sectional area of the secondary winding conductors = 0.5 mm^2.

Taking 4×27 SWG [12] copper conductors in parallel for secondary winding.

The actual cross sectional area = 4×0.136 = 0.544 mm^2

Modified current density for secondary winding conductors = 5.5A/mm^2.

A 137927

Date Slip

The book is to be returned on the date last stamped.